NRC Research and/or Technical Assistance Report

PDR

EGG-LOFT-5529
Project No. P 394
October 1981

COMPARISON OF NUCLEAR AND ELECTRIC HEATER ROD RESPONSES FOR LARGE BREAK PWR LOCA CONDITIONS (SYSTEM 00)

E. L. (Bert) Tolman
W. E. Driskell
M. L. Carboneau

U.S. Department of Energy
Idaho Operations Office • Idaho National Engineering Laboratory

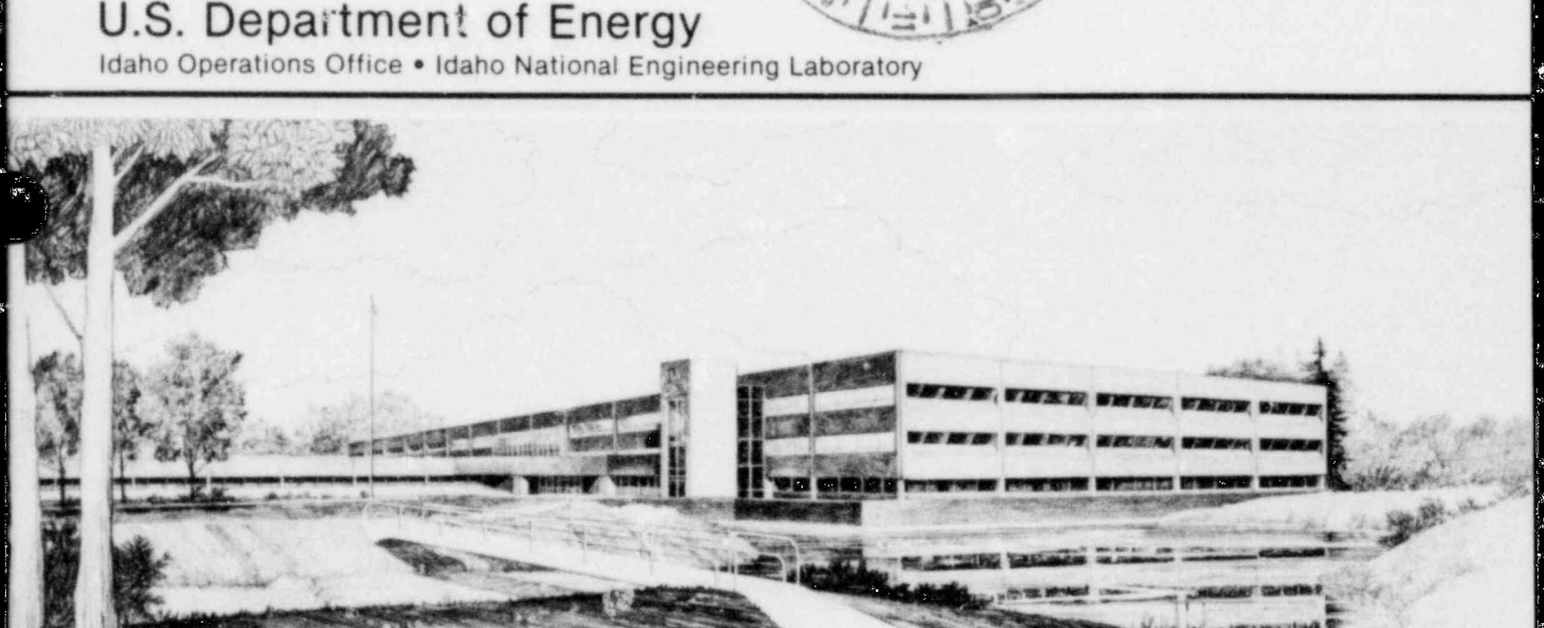

This is an informal report intended for use as a preliminary or working document

Prepared for the
U.S. Nuclear Regulatory Commission
Under DOE Contract No. DE-AC07-76ID01570
FIN No. A6043

EG&G Idaho

EG&G Idaho, Inc.

FORM EG&G 398
(Rev. 11-79)

INTERIM REPORT

Accession No. _____

Report No. EGG-LOFT-5529

Contract Program or Project Title:

LOFT Measurement Division

Subject of this Document:

Comparison of Nuclear and Electric Heater Rod Responses for Large Break PWR LOCA Conditions

Type of Document:

Topical Report

Author(s):

E. L. (Bert) Tolman, W. E. Driskell, M. L. Carboneau

Date of Document:

October 1981

Responsible NRC Individual and NRC Office or Division:

G. D. McPherson, Chief, LOFT Research Branch,
Division of Reactor Safety Research, USNRC

EG&G Idaho, Inc.
Idaho Falls, Idaho **83415**

Prepared for the
U.S. Nuclear Regulatory Commission
Washington, D.C.
Under DOE Contract No. **DE-AC07-76ID01570**
NRC FIN No. A6043

INTERIM REPORT

EG&G Idaho, Inc.

FORM EG&G-229
(Rev. 01-80)

LOFT TECHNICAL REPORT

Title: COMPARISON OF NUCLEAR AND ELECTRIC HEATER ROD RESPONSES FOR LARGE BREAK PWR LOCA CONDITIONS	LTR No. EGG-LOFT-5529
Author: E. L. Tolman, W. E. Driskell, M. L. Carboneau	Released By LOFT CDCS
Performing Organization: LOFT Instrumented Fuels Branch	Date: October 30, 1981
LOFT Review and Approval: D. D. Hamm by [illegible] LMD Mgr.	Project System Engineer: M. L. Russell IFB Mgr.

DISPOSITION OF RECOMMENDATIONS

No disposition required.

ABSTRACT

The applicability of utilizing electric heater rods to duplicate nuclear fuel rod behavior during a large break loss-of-coolant accident (LOCA) is reviewed, and the conservative nature and limiting aspects of the electric rod thermal response are established. Nuclear rod response data are presented from experimental programs being conducted in the Loss-of-Fluid Test (LOFT) facility, Power Burst Facility (PBF), and the Halden research reactor in Norway. The nuclear rod data are compared to nonnuclear electric fuel rod simulator data from the Semiscale, LOFT Test Support Facility (LTSF), and Halden IFA-511 programs. The data comparisons show significant differences between nuclear and electric rod thermal responses during both the blowdown and reflood phases of a large break LOCA. However, the electric and nuclear rod experiments are not yet completed; therefore, the comparison results and conclusions presented here should be interpreted to be preliminary in nature.

SUMMARY

The applicability of utilizing electric heater rods to duplicate nuclear fuel rod behavior during a large break loss-of-coolant accident (LOCA) is reviewed, and the conservative nature and limiting aspects of the electric rod thermal response are established. Nuclear rod response data are presented from experimental programs being conducted in the Loss-of-Fluid Test (LOFT) facility, Power Burst Facility (PBF), and the Halden research reactor in Norway. The nuclear rod data are compared to nonnuclear electric fuel rod simulator data from the Semiscale, LOFT Test Support Facility (LTSF), and Halden IFA-511 programs.

General conclusions regarding electric heater rod capability to simulate nuclear fuel rod response based on the analysis of available experimental data are:

1. The electric heater rod response showed conservatively high rod cladding temperatures and lower cooling rates compared with a nuclear rod for both the blowdown and reflood phases of a large break LOCA.

2. A solid internal heater rod cannot simulate (a) the initial stored energy of a nuclear rod, (b) the transient energy equilibration of the nuclear rod during the first 10 to 15 s of the LOCA, and (c) the rapid quench that is possible on a nuclear rod.

3. Small-scale electric rod experiments are generally adequate for separate effects studies; however, because electric heater rods cannot simulate the nuclear rod initial stored energy or the transient thermal and mechanical responses during the first 10 to 20 s of the LOCA, small-scale electrically heated experiments cannot provide the necessary data for assessing the thermal and hydraulic response of a nuclear core. Nuclear experiments are necessary to confirm the important phenomena that control the nuclear rod thermal and mechanical responses.

4. Additional experiments are necessary to better represent film-to-nucleate transition heat transfer and quench behavior.

The data comparisons show significant differences between nuclear and electric rod thermal responses during both the blowdown and reflood phases of a large break LOCA. However, the electric and nuclear rod experiments are not yet completed; therefore, the comparison results and conclusions presented here should be interpreted to be preliminary in nature

Pertinent nuclear experiments which will provide necessary data to quantify important nuclear rod response phenomena are LOFT large break LOCEs L2-5 and L2-6, PBF Experiment Series TC-4, and NRU cladding deformation experiments. These experimental results will provide a wide range of model assessment data, and efforts will be specifically directed at evaluating model capabilities to predict the important nuclear response.

CONTENTS

FIGURES

TABLES

COMPARISON OF NUCLEAR AND ELECTRIC HEATER ROD RESPONSES FOR LARGE BREAK PWR LOCA CONDITIONS

1. INTRODUCTION

The capability of electric fuel rod simulators to duplicate the response of nuclear fuel rods is reviewed, and comparisons between nuclear fuel rods and electric heater rods for a variety of cooling conditions that simulate large break loss-of-coolant accident (LOCA) conditions in a pressurized water reactor (PWR) are presented. The nuclear rod response data were obtained from ongoing experimental programs in the Loss-of-Fluid Test (LOFT) facility, Power Burst Facility (PBF), and the Halden research reactor in Norway from 1978 through 1980. The nuclear rod data are compared with electric heater rod data from the Semiscale, LOFT Test Support Facility (LTSF), and Halden IFA-511 programs. The electric and nuclear rod experiments are not yet completed; therefore, the comparison results and conclusions presented here should be interpreted to be preliminary in nature.

The designs for electric fuel rod simulators differ for blowdown heat transfer experiments, reflood heat transfer experiments, and cladding deformation (ballooning) experiments. A review of the limitations of electric heater rod designs to duplicate the nuclear rod response is presented in Section 2 and provides the background for interpreting the electric and nuclear rod response data. Comparisons of electric and nuclear rod thermal responses during reactor system simulation experiments and separate effects experiments to investigate blowdown and reflood heat transfer are included in Section 3. Section 4 states conclusions from this investigation. Recommendations are presented in Section 5 regarding additional work required to integrate the experimental results from these programs and to assess licensing conservatisms. Section 6 discusses future experiments that will provide data to quantify important differences between electric and nuclear rods.

2. LIMITATIONS OF ELECTRIC FUEL ROD SIMULATORS

To assure that the coupling between the rod heat transfer and local hydraulics for an electric heater rod is identical to the nuclear fuel rod, it is necessary for the heater rod response to exactly duplicate the nuclear fuel rod cladding temperature, surface heat flux, and cladding deformation along the entire length of the rod. There is no heater rod capable of exactly simulating these parameters during all phases of a LOCA, and in general, heater rod designs differ for blowdown and reflood heat transfer experiments. The simulation limitations related to each of these experiment categories are discussed in the following subsections.

2.1 Blowdown Heat Transfer

Electric heater rods used for blowdown heat transfer experiments do not achieve the initial steady state stored energy typical of nuclear rods, because electric heater elements cannot operate at the high temperatures characteristic of the nuclear fuel. To compensate for the lower initial stored energy, the electric power to the rods during the blowdown transient must be specified to produce the nuclear rod cladding temperature and surface heat transfer. In order to specify the electric power to the heater rods, either of two methods are used: (a) the preprogrammed-power method requiring the nuclear rod response to be estimated prior to the experiment, and (b) the online-power control method requiring real-time modeling of both the electric and nuclear rod thermal response during the transient with an automatic feedback control on the electric rod power. In either method, the simulation of the nuclear rod is dependent on a priori knowledge of the nuclear fuel rod response. Thus, the electric rod simulation using either method simulates only the cladding temperature response of the calculated nuclear rod response.

Another important limitation related to blowdown heat transfer simulation is the cladding quenching characteristics of a nuclear rod. It is shown in this report that solid heater rods of the Semiscale and FLECHT types cannot physically duplicate the rapid cladding quenches that have been observed on nuclear rods in both LOFT and the PBF experiments. In order

for an electric heater rod to duplicate quench characteristics of a nuclear rod, it would require power densities and thermal properties much closer to those of a nuclear rod.

2.2 Reflood Heat Transfer

The ability of electric heater rods to duplicate nuclear rod thermal response during reflood has been questioned because of the large differences in electric and nuclear rod thermal properties. The rod thermal diffusivity controls the rod heat release rate which, in turn, influences the hydraulic conditions and heat transfer environment along the rod. Furthermore, electric rods do not exactly simulate the nuclear rod stored energy because of differences in heat capacity between electric and nuclear rod materials. Another limitation of most electric rod designs for reflood experiments is the inability of the electric rods to simulate cladding deformation and resulting flow channel blockage. These limitations are all coupled in their affect on the system hydraulics and rod thermal-mechanical response.

2.3 Reactor System Simulation Experiments

Reactor system simulation experiments are intended to provide thermal-hydraulic response data representative of a reactor system and to quantify the cladding temperature response during the complete LOCA sequence, that is, blowdown, refill, and reflood. The limitations of the electric heater rods for these experiments are as discussed in the previous sections for blowdown and reflood heat transfer. However, the limitations of the electric heater rods are even more important for the system simulation experiments because they may atypically affect the reactor vessel hydraulics and rod cooling. Thus, both rod simulation limitations and resulting atypical hydraulic response could obscure the true cladding temperature response for a nuclear rod. Another important factor related to the system simulation experiments is the ability to properly duplicate nuclear system hydraulic response in the smaller scale experiments. As is shown in Section 3, these limitations in simulating rod behavior and differences in system hydraulic response can result in large differences in peak rod cladding temperature.

3. EXPERIMENT COMPARISONS

The first data comparisons discussed herein focus on the importance of blowdown heat transfer and the differences observed between nuclear and electric rod experiments. Comparisons are presented for the LOFT and Semiscale large break loss-of-coolant experiments (LOCEs), which utilize nearly identical system configurations to simulate a four-loop PWR. These experiment comparisons show large differences in the peak cladding temperatures that are attributed, at least in part, to the different behavior of electric and nuclear rods. Supporting analysis is presented to more fully understand these important experiments.

Results of separate effects experiments to study the quench behavior of electric and nuclear rods are also presented. These experiments have shown large differences in rod cooling and quench characteristics. Supporting analysis results are presented which yield additional insight into the quench behavior of nuclear and electric rods and the capability of analytical models to predict the observed differences.

Preliminary comparisons between reflood experiments performed in the Halden reactor on identical bundles of nuclear and electric rods are presented and discussed. These experiments indicate that the nuclear rods cool faster than the solid electric heater rods.

3.1 Blowdown Heat Transfer for Reactor System Simulation Experiments--LOFT Versus Semiscale

Experiments to simulate the large break LOCA response of a PWR have been conducted in the LOFT and Semiscale facilities. The experiments used for this comparison are LOFT LOCEs L2-2[1] and L2-3[2] and LOFT counterpart Tests S-06-2,[3] S-06-3,[4] and S-06-4[5] conducted in the Semiscale facility. Conflicting results have been obtained from these experiments regarding the important mode of fuel rod energy removal during the LOCE. The LOFT nuclear experiments suggest that the important energy removal mechanism is related to blowdown heat transfer during the first 0 to 15 s, as indicated by the measured core-wide quench during this period. Details of the core thermal response during the LOFT experiments are summarized in Appendix A, and the

measured LOFT system response data are presented in References 1 and 2. Semiscale experiments, intended to duplicate the LOFT experiments, did not show the early core quenches and indicate that the important heat transfer takes place during final core reflood between 80 and 180 s. The Semiscale data are presented in References 3 through 5 for the LOFT counterpart experiments. An example of the differences in cladding temperature for experiments initiated at peak rod powers of 39.4 kW/m are shown in Figure 1. Note in Figure 1 that the LOFT cladding temperatures are represented as an uncertainty envelope due to the potential perturbation influences of the LOFT surface thermocouples. The cooling influences of the LOFT surface thermocouples have been extensively evaluated experimentally, and the results show that during a high-pressure cooling transient, the cladding surface thermocouples experience some selective cooling, but do not significantly affect the thermal response of a nuclear rod. The separate effects experiments to investigate the influence of LOFT thermocouples are documented in Reference 6, and a summary of this work is presented in Appendix A.

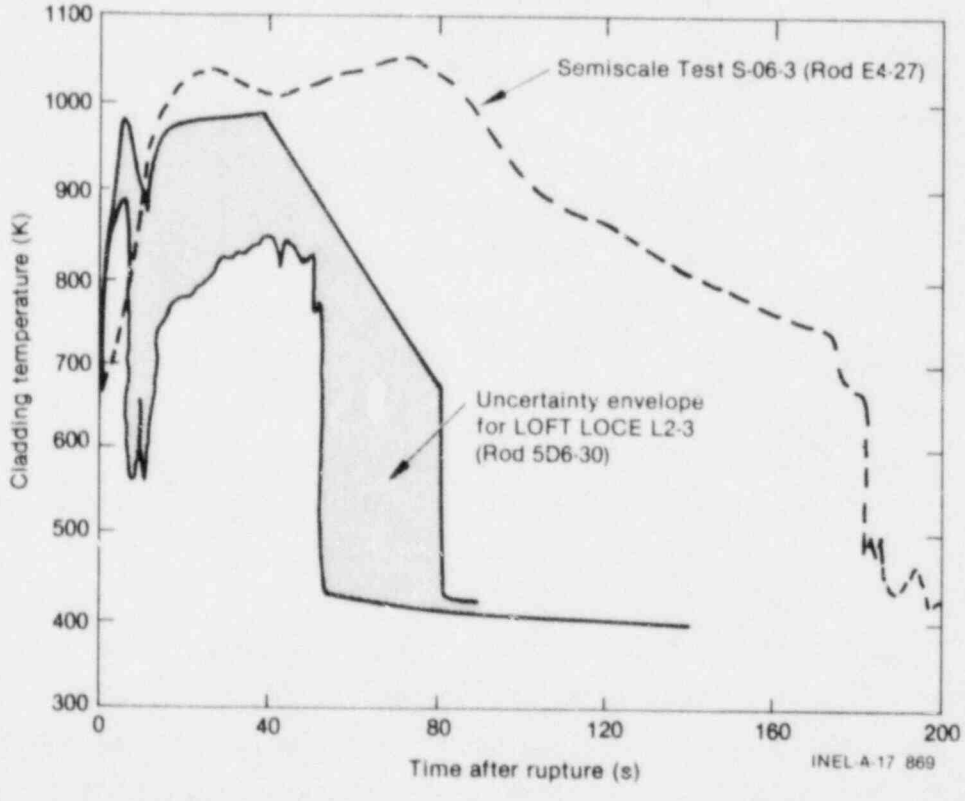

Figure 1. Comparison of peak cladding temperatures for LOFT LOCE L2-3 and Semiscale Test S-06-3 (39 kW/m).

As discussed in Section 2.1, two important limiting aspects of electric heater rods during blowdown are (a) inability to simulate the initial steady state stored energy of the nuclear fuel, and (b) inability to simulate the rod thermal response during a rapid cladding quench. The fuel rod cladding temperature during the first 10 to 20 s of a large break LOCA is driven by the initial steady state stored energy in the rod prior to the transient. The inability of the Semiscale heater rod to simulate the nuclear rod stored energy is shown graphically in Figure 2, which compares the temperature profiles of a LOFT and Semiscale rod at steady state conditions of 36 kW/m. Because of the deficient steady state stored energy, power must be delivered to the Semiscale rods during the first few seconds of the transient so that the resulting cladding temperature and heat flux for the Semiscale and LOFT rods are identical. Since the Semiscale experiments were performed prior to the LOFT experiments, the rod power was estimated based on pretest calculations using the RELAP4/MOD5 computer code.[7] The calculated LOFT peak cladding temperature and the resulting heater rod power history necessary to simulate the pretest LOCE L2-3 transient (39 kW/m) are shown in Figure 3. Because the pretest predicted cladding temperature was much different from the actual LOFT experimental results (compare Figures 1 and 3), the transient Semiscale power history resulted in a larger energy delivery to the cladding than required to simulate the LOFT nuclear response. Note also, that the heater rod power increase occurred during the same time that LOFT experienced the initial cladding quench (5 to 6 s). The higher rod power is hypothesized to have caused the differences between LOFT and Semiscale cladding temperatures. The increased power between 3 and 10 s would have resulted in a near impossible cladding quench condition on the Semiscale heater rod. Appendix B discusses the capability of a Semiscale-type heater rod to duplicate the nuclear rod quench characteristics and shows that, for the Semiscale rod to simulate a rapid cladding quench, negative power must be applied to the rod during the quench period.

Although the Semiscale rod transient power would have precluded the rod quench, it is evident from the Semiscale cladding temperature of Figure 3 that no significant cooling occurred in Semiscale over the first 20 s (the change in cladding temperature slope is largely a result of the decreasing rod power). This suggests a significant difference in core flows (during blowdown) between Semiscale and LOFT.

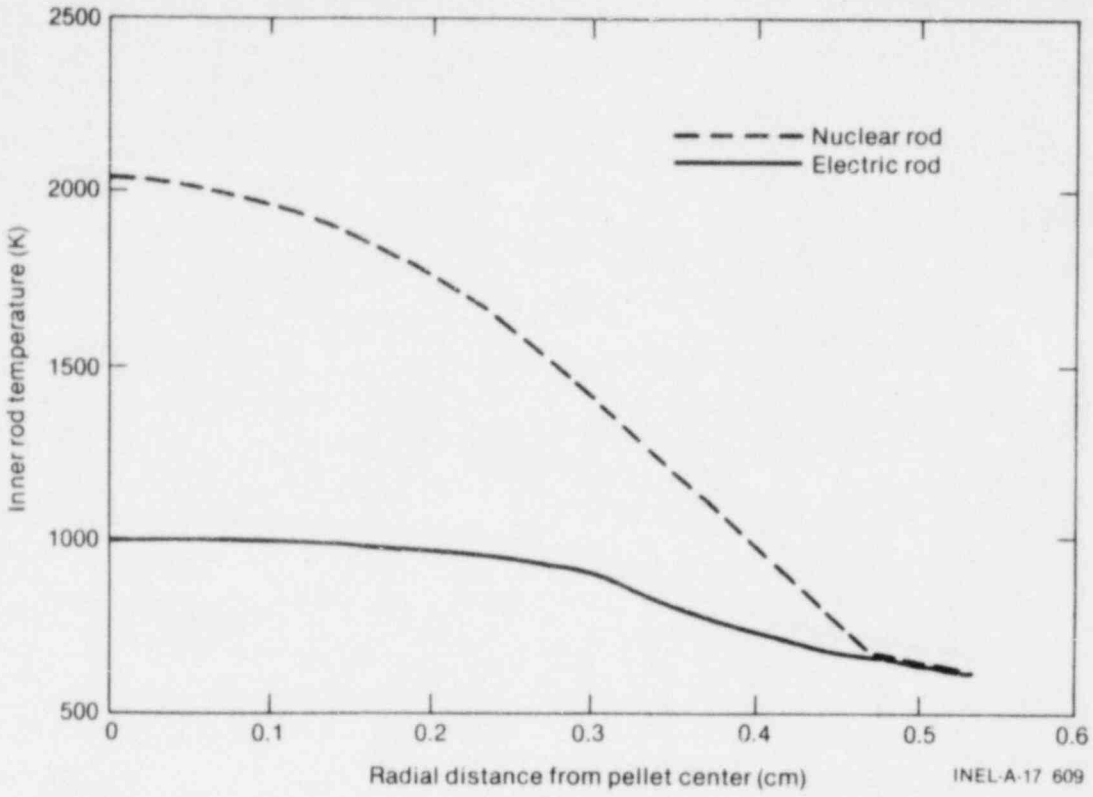

Figure 2. Comparison of radial temperatures for LOFT and Semiscale rods at a steady state power of 39 kW/m.

Comparisons of the measured hydraulic responses for LOFT and Semiscale are shown in Appendix C and indicate that the volumetrically scaled flows are similar in both systems, except in the intact and broken loop hot legs. Figure 4 compares the measured Semiscale core inlet mass flux with the best-estimate prediction for LOFT LOCE L2-3[a,8] using the RELAP4/MOD6 computer code.[9] Figure 4 indicates the positive core flows in LOFT to be initiated sooner than in Semiscale and to extend longer. These relative core flows are consistent with the measured cladding temperatures from the two systems. The core flows are a result of small pressure differences across the core

---

a. The core inlet flow measurement for LOFT was not made. Thus, the only way to estimate the LOFT core flow was to normalize RELAP4/MOD6 with the measured reactor vessel inlet and outlet flows and utilize the resulting calculated core flow. The reactor vessel inlet and outlet flows were well predicted, giving confidence in the estimated core flow. See Appendix C for additional details.

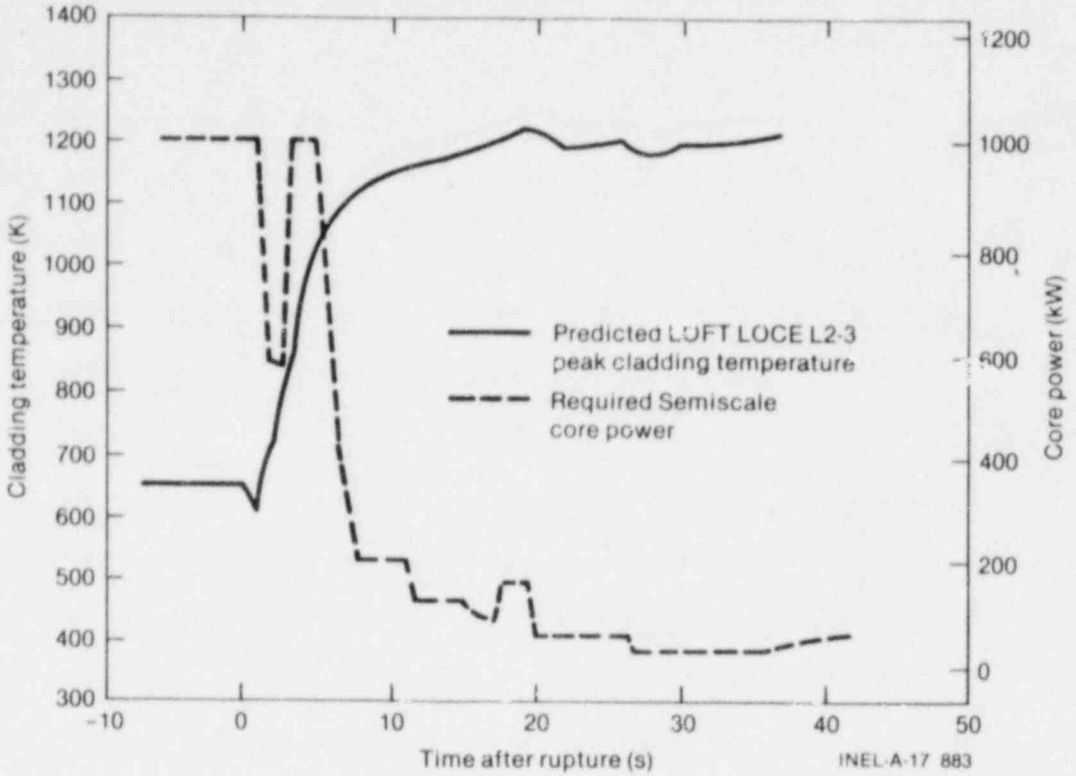

Figure 3. Predicted LOFT LOCE L2-3 peak cladding temperature and Semiscale core power required to simulate the LOFT response (prior to conducting the LOFT experiment).

and it is conceivable that differences in heat transfer between electric and nuclear rods could influence pressure differentials in the reactor vessel and produce differing core flows.

The LOFT and Semiscale experiments clearly show that the electric rods yield higher peak cladding temperatures and are thus conservative. It is not certain from the measurements if differences in the system hydraulics or differences between nuclear and electric rods cause the observed differences in measured cladding temperature. It is likely that both of these effects could be important, and calculations are being performed to determine if either is a controlling influence. The differences between the two systems, however, confirm the need for nuclear system data to identify the important phenomena that influence the nuclear fuel rod response.

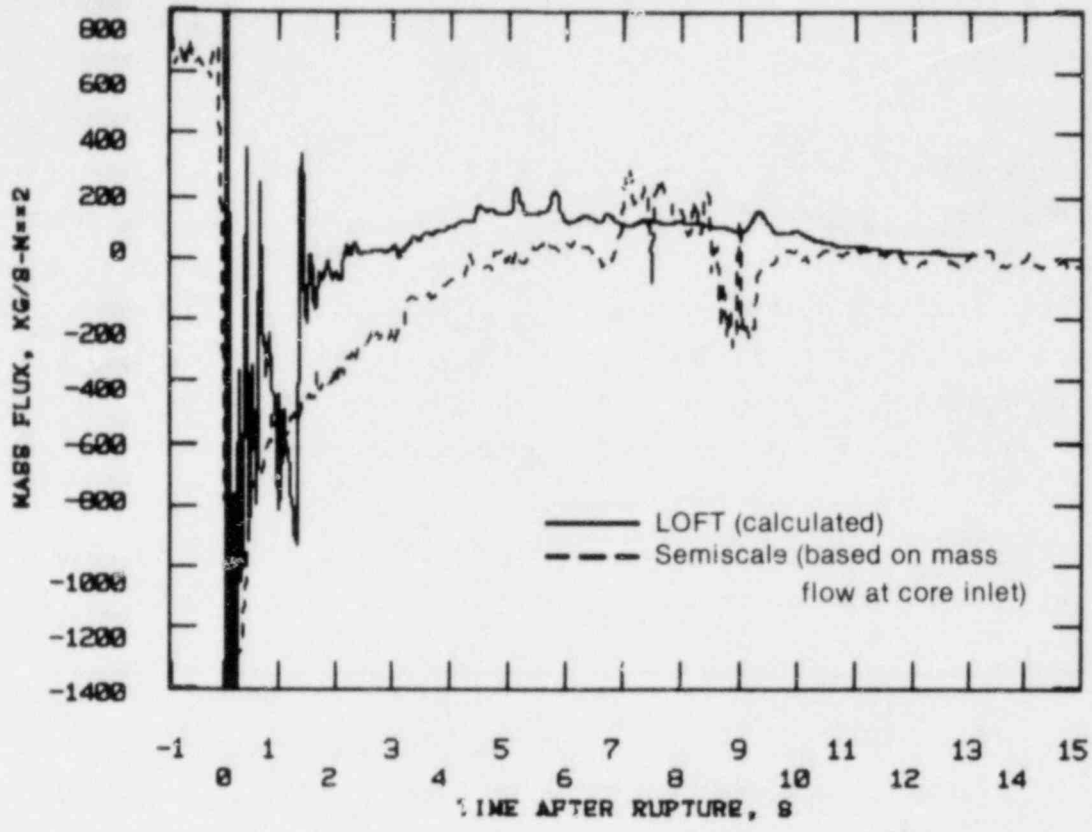

Figure 4. Comparison of core mass fluxes near core inlet as calculated for LOFT and measured (based on mass flow measured at core inlet) for Semiscale.

3.2 Blowdown Heat Transfer for LTSF and PBF Quench Experiments

After the LOFT experiments showed a major cladding quench, experiments were conducted in the LTSF to study the influence of cladding surface thermocouples on cladding quench behavior of a single Semiscale heater rod over a wide range of inlet hydraulic conditions. Quench experiments in the PBF using LOFT nuclear rods were also performed. Initial test results from these programs have provided insight into the effects of external cladding thermocouples on cladding quench behavior, the important characteristics of cladding cooldown and quench on both electric and nuclear rods, and the ability of best-estimate thermal-hydraulic models to predict the cladding quench characteristics of both electric and nuclear rods. The LTSF experiments, PBF experiments, and the capability of analytical models to predict these experiments are discussed in the following subsections.

3.2.1 LTSF Experiments

The initial series of LTSF experiments used a single, Semiscale heater rod enclosed in a flow shroud. A cross section of the Semiscale heater rod and the geometry of the rod in the LTSF flow shroud is shown in Figure 5. The rod was slowly heated (~1.6 kW/m) in a near adiabatic nitrogen environment until the desired cladding temperature was attained; a valve was then opened at the bottom of the test section, resulting in rapid flooding of the rod and flow shroud.

For the initial experiment series, experiments were run on rods with and without surface thermocouples over a range of inlet flow velocities and qualities, system pressure, and initial cladding temperatures, as summarized in Table 1. Reference 10 summarizes the data and discusses the results obtained from these experiments. The cladding temperature response for the quench experiments most representative of flow conditions for the LOFT quench (inlet flow at 1.8 m/s velocity and zero quality) are shown in Figure 6. These results show initial cladding cooling rates ranging from 17 to 42 K/s, depending upon the initial rod temperatures.

The LTSF rod quench experiments show that the cladding quench on the Semiscale rod does not occur as rapidly as measured in the LOFT LOCEs L2-2 and L2-3 and is consistent with the earlier Semiscale experiments. It is shown in Appendix B that a solid-type heater rod of the Semiscale design cannot duplicate a rapid nuclear rod cooldown, or quench, because the electric rod energy is transferred too rapidly to the cladding, thus maintaining the high cladding temperature that inhibits liquid rewetting of the cladding surface.

3.2.2 PBF Quench Tests

Several LOCEs have been conducted in the PBF to evaluate the cooling effects of surface thermocouples during blowdown and reflood conditions. The primary objective of the experiments was to simulate the fuel rod response during the rapid cooling conditions observed during the first 10 s of the LOFT experiments. For each PBF experiment, four individually shrouded test fuel rods were used, as shown in Figure 7: two of the fuel

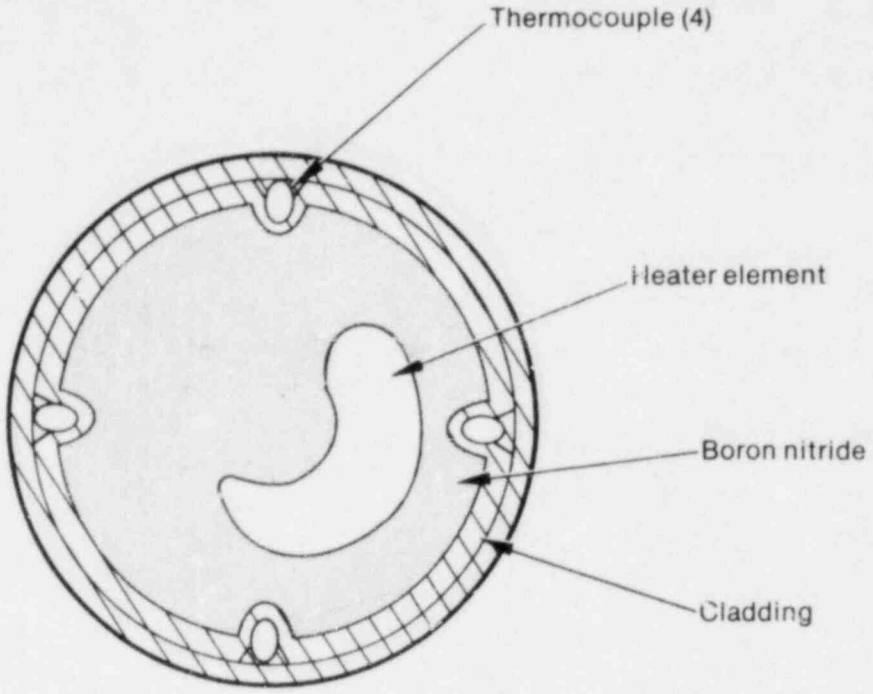

Semiscale electric rod geometry

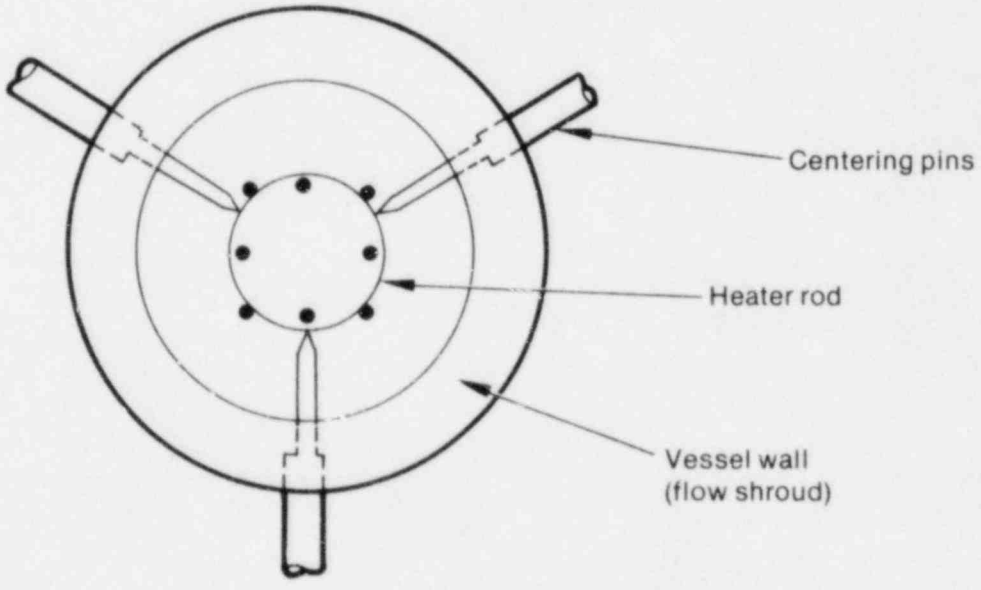

LTSF flow shroud configuration

Figure 5. Semiscale electric rod geometry and LTSF flow shroud configuration for LTSF quench experiments.

TABLE 1. NOMINAL TEST CONDITIONS FOR LTSF HIGH PRESSURE (7.0 MPa) QUENCH TESTS

Run	Test Section Inlet Quality (%)	Average Test Section Inlet Fluid Velocity (m/s)	Rod Hot Spot Initial Temperature (K)	Test Section Mass Flow Rate (kg/s)
6	0	0.4	775	0.11
7	0	0.4	1025	0.11
8	11	1.3	1025	0.11
10	0	1.8	775	0.5
11	0	1.8	1025	0.5
11A	0	1.8	1025	0.5
11B	0	1.8	1025	0.5
24	0	1.8	1025	0.5
12	5	3.5	1025	0.5
13	15	7.5	1025	0.5
14	0	1.8	1175	0.5
15	0	3.0	1025	0.83
17	15	11.0	1025	0.83
20	15	11.0	1175	0.83
21	0	6.0	1025	1.66
23	0	6.0	1175	1.66

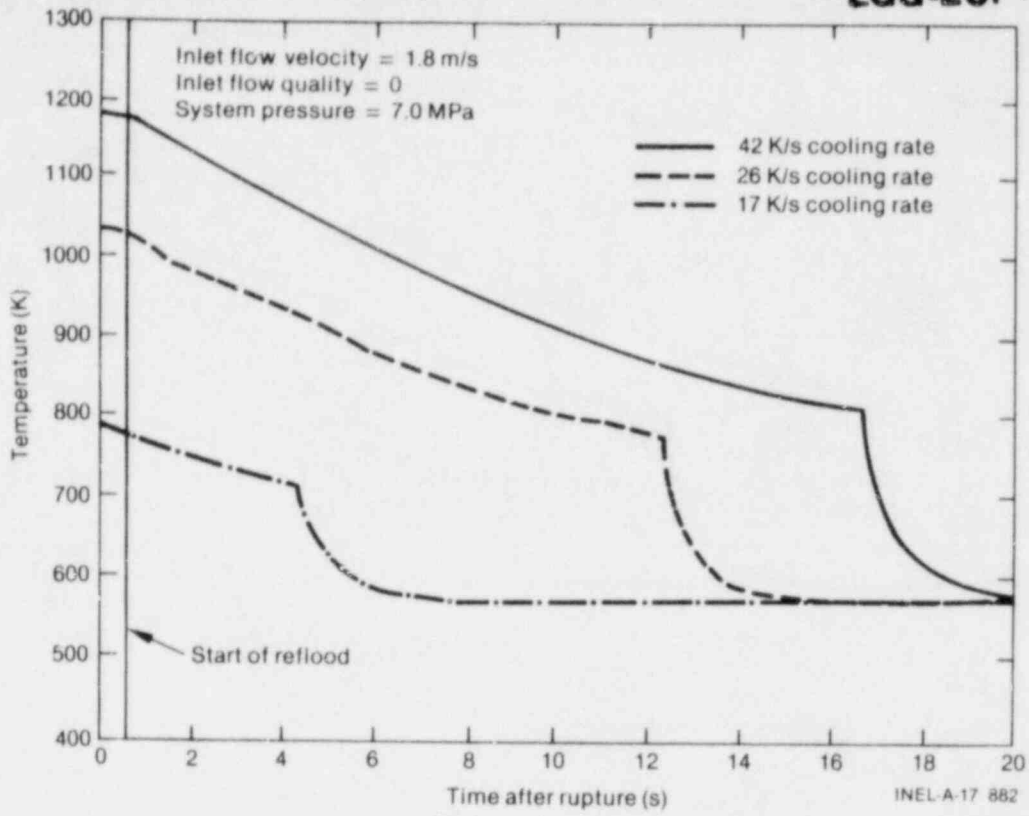

Figure 6. Cladding temperature for LTSF quench experiments.

rods were instrumented with both cladding surface and internal thermocouples and internal fuel pellet thermocouples, while the other two fuel rods were instrumented with only the internal cladding and fuel pellet thermocouples. Figure 8 gives the details for type and placement of these thermocouples. In this manner, both the influence of cladding surface thermocouples and the cladding quench characteristics were determined.

Hydraulic conditions simulating the LOFT blowdown core flow were achieved by cycling the blowdown system isolation valves and the hot and cold leg blowdown valves which produced a rapid, low-quality flow through the test section. After simulating the early (5 to 10 s) cladding quench, the rods were powered for approximately 100 s to increase the cladding temperature to approximately 1200 K. The test section was then reflooded at a flow rate similar to that (10 cm/s) experienced for LOFT experiments.

The first PBF thermocouple evaluation experiment series, designated TC-1, was completed during 1980; however, during these initial experiments, the blowdown system isolation valves were not cycled to allow low-quality

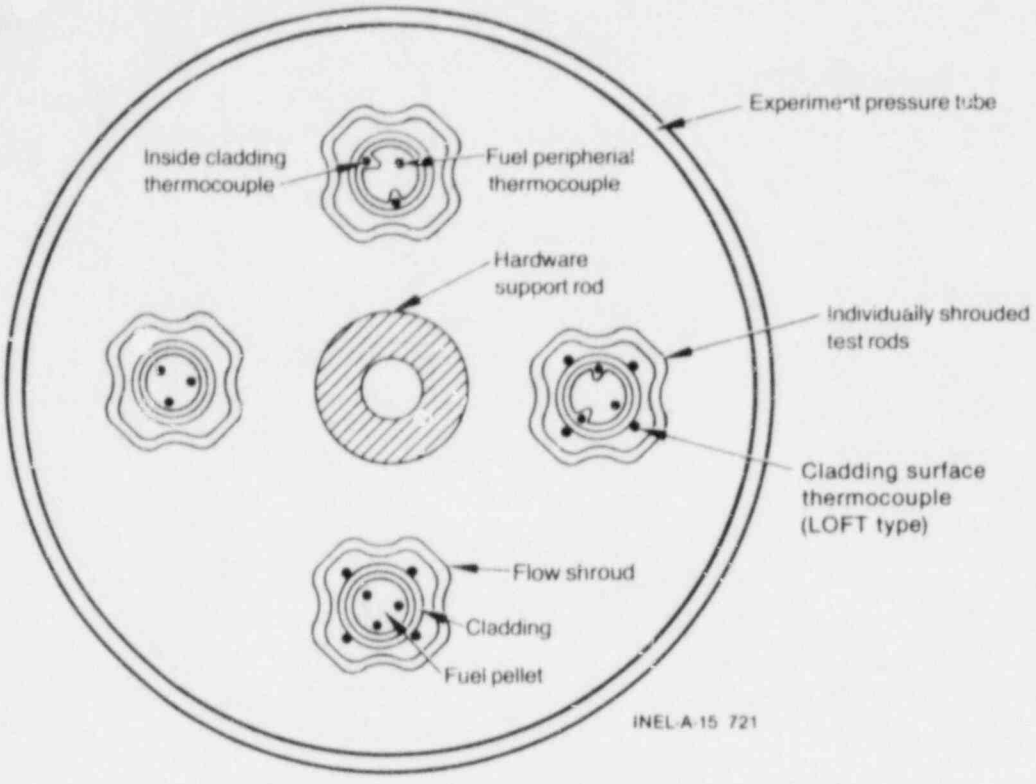

Figure 7. PBF test fuel rod configuration for Experiment Series TC-1.

fluid into the test section, and the desired hydraulic conditions for cladding quench were not achieved.[11] Subsequently, the blowdown system valve sequence was changed to result in more low-quality cooling of the rods, and Experiment Series TC-3 was conducted. One of these experiments produced nuclear cladding quenches with coolant flow velocity and quality similar to that experienced in LOFT.[12] Figure 9 shows the measured response from internal thermocouples for a bare rod (no surface thermocouples). The cladding cooling rates (inferred from the measured fuel temperatures) are shown to be greater than 100 K/s (see Appendix D for additional details) which is much higher than observed on the single-rod quench tests in the LTSF. Thus, the PBF TC-3 experiments show that nuclear fuel rods can be cooled rapidly which is consistant with the early core-wide quench measured during the LOFT experiments.

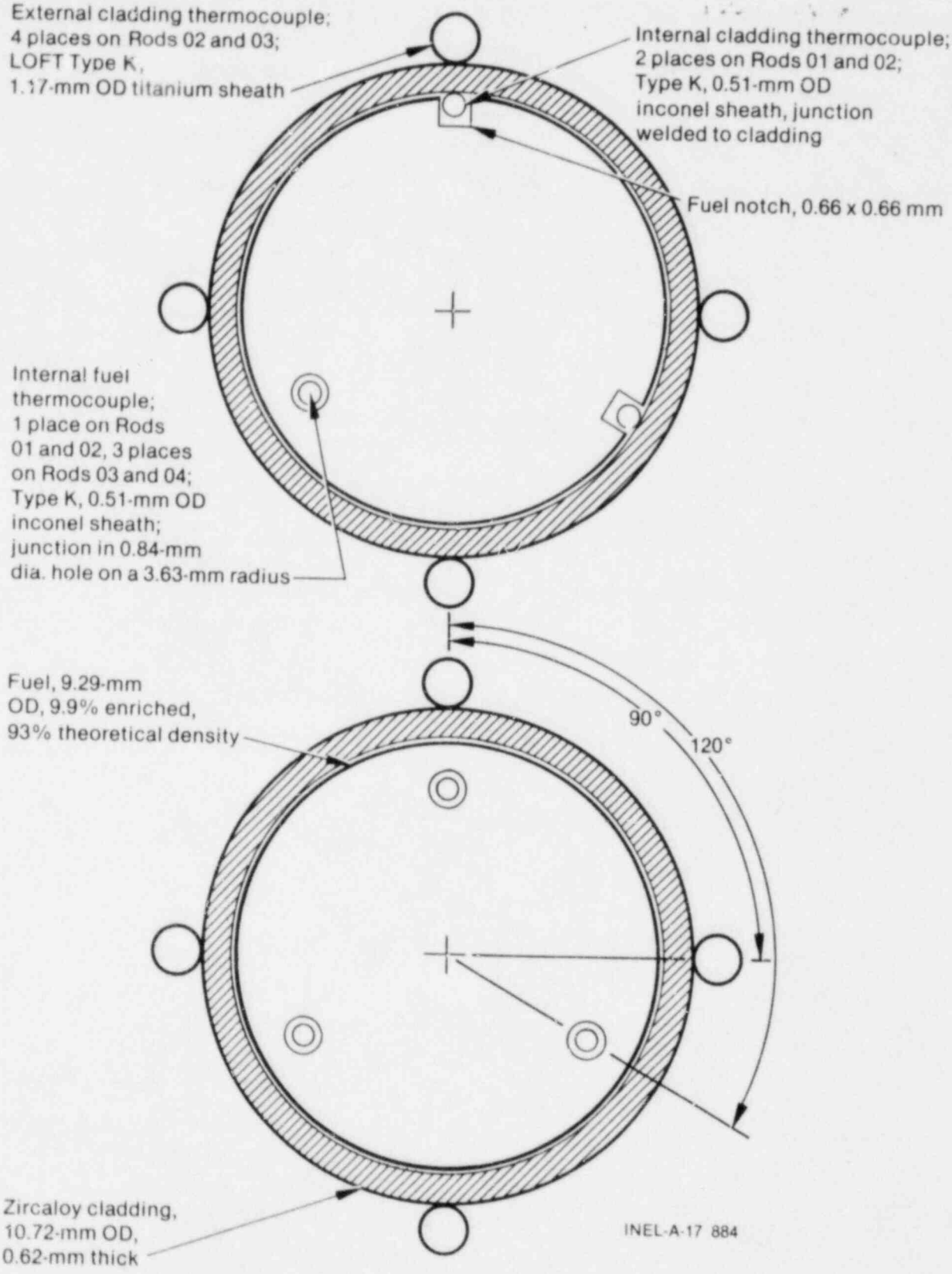

Figure 8. PBF test fuel rod dimensions for Experiment Series TC-1.

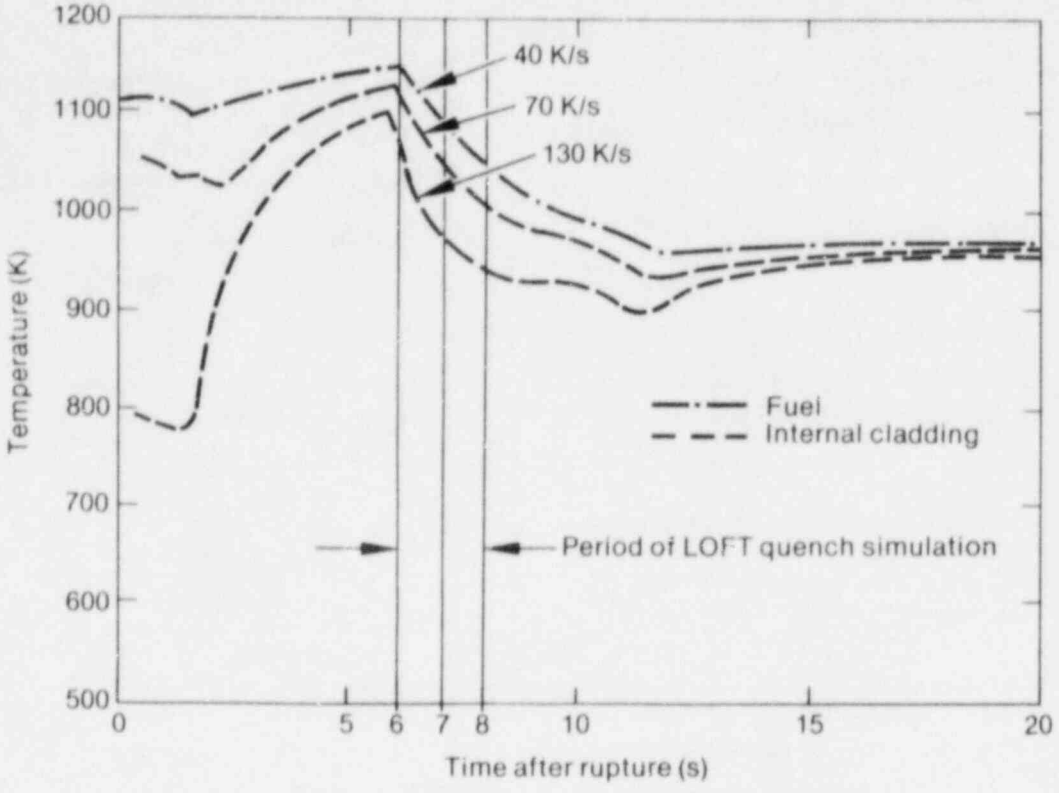

a. Fuel rod internal temperatures

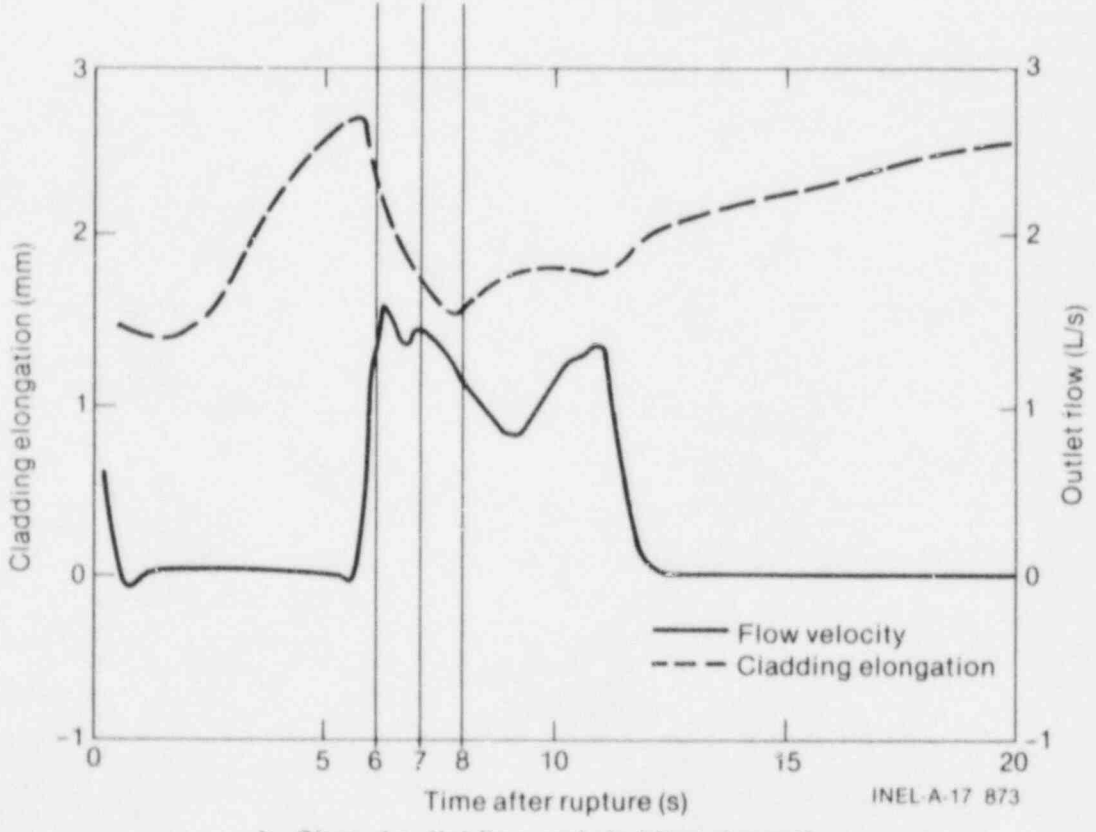

b. Shroud outlet flow and cladding elongation

Figure 9. Internal temperature, shroud outlet flow, and cladding elongation responses for test Fuel Rod 1 without surface thermocouples during Experiment TC-3.

3.2.3 Analytical Capability to Predict Cladding Quench

Because of the large differences in quench cooling rates between the LTSF-Semiscale electric heater rod and the PBF nuclear rods, a study was undertaken to investigate the current modeling capability of the RELAP4/MOD6 computer code to predict cladding cooling rates and quench times. The LTSF experiments were modeled, since these experiments offer a simple geometry and the flow shroud inlet hydraulic conditions are accurately measured. The Groenveld 5.9 film boiling correlation was used in conjunction with the RELAP4/MOD6 standard blowdown heat transfer package. The calculational results are compared to the experimental data in Figure 10 for the LTSF test which best simulated the LOFT LOCE L2-3 quench conditions. The calculated data show a reasonable comparison with the data for this test. Similar comparisons were achieved for experiments with inlet flow rates ranging from 0.4 to 7 m/s.

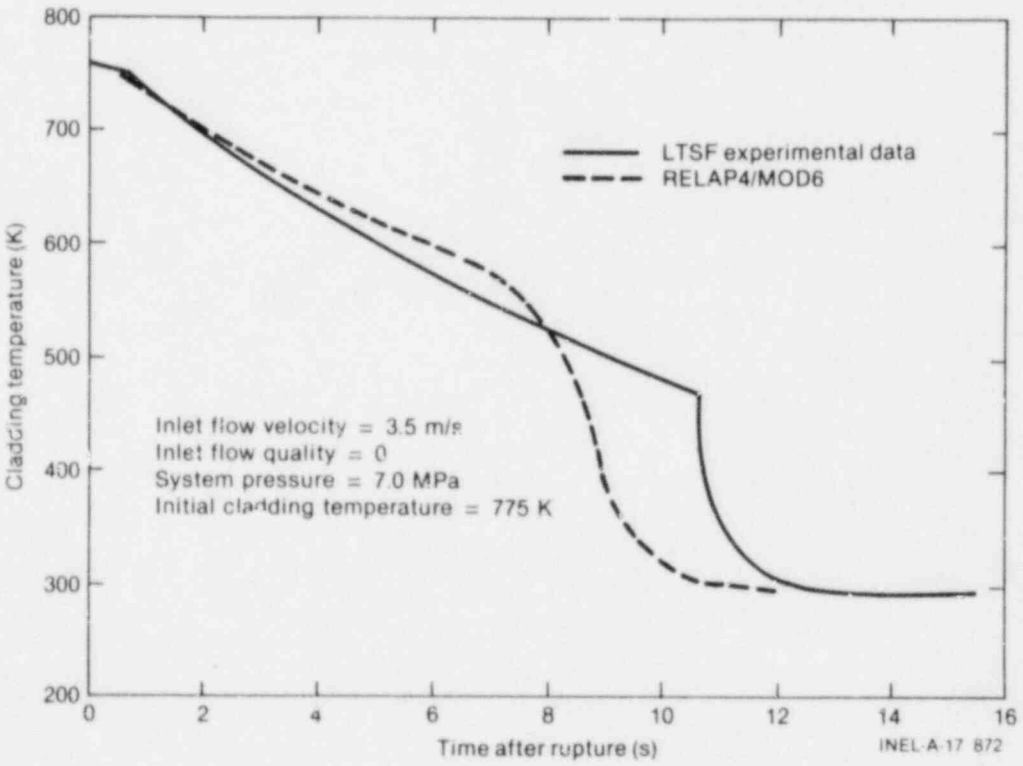

Figure 10. Comparison of quench data measured in LTSF and calculated by RELAP4/MOD6.

A nuclear rod was substituted in the RELAP4/MOD6 LTSF model, and several calculations were performed for comparison with the Semiscale rod cladding temperature response. Calculations were performed for the nuclear rod with stainless steel and zircaloy cladding and assuming very large and very small fuel-cladding gap conductance values. The results of these calculations (see Figure 11) show (a) the important influence of the UO_2 thermal conductivity in limiting heat flow to the cladding, (b) a zircaloy-clad nuclear rod (no gap resistance) cools more rapidly than a similar stainless-steel-clad rod, and (c) the zircaloy-clad fuel rod with a fuel-cladding gap conductance (0.31 W/cm^2 K) has an initial cooling rate approximately five times faster and quenches nearly 8 s earlier than the Semiscale rod.

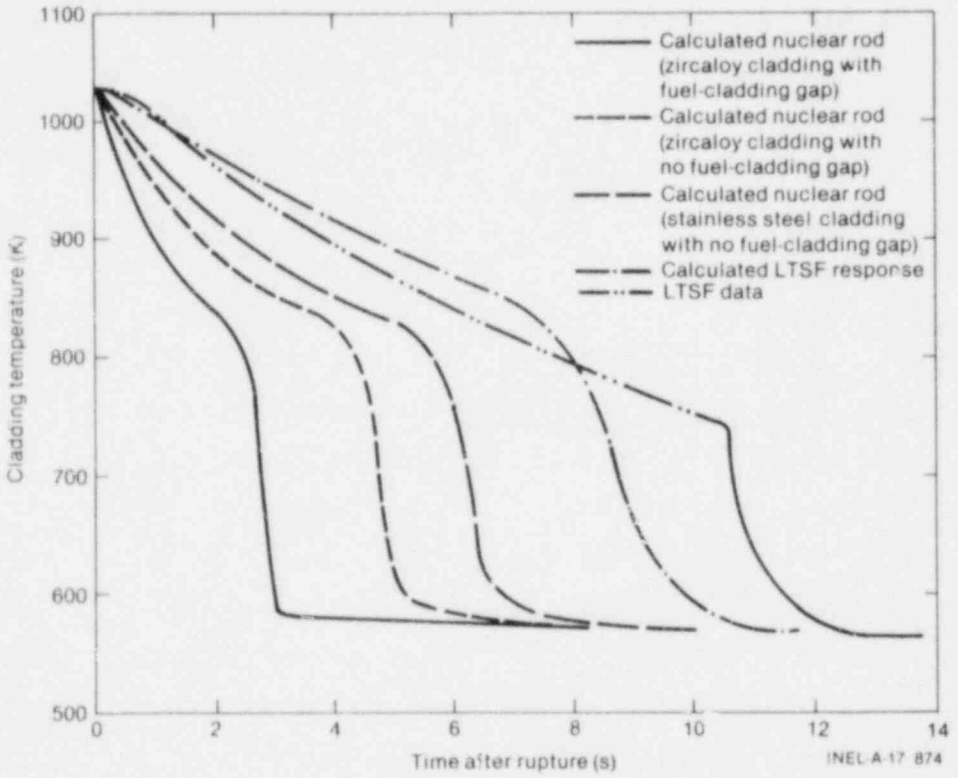

Figure 11. RELAP4/MOD6 calculations showing sensitivity of fuel rod thermal parameters.

Calculations were also made for nuclear rods at different inlet flow conditions tested in the LTSF. The results of these predictions comparing the initial cooling rates for nuclear and electric rods are summarized in Figure 12. Also shown in Figure 12 is the initial cladding cooling rate as measured from the PBF TC-3 experiment. These results suggest that current

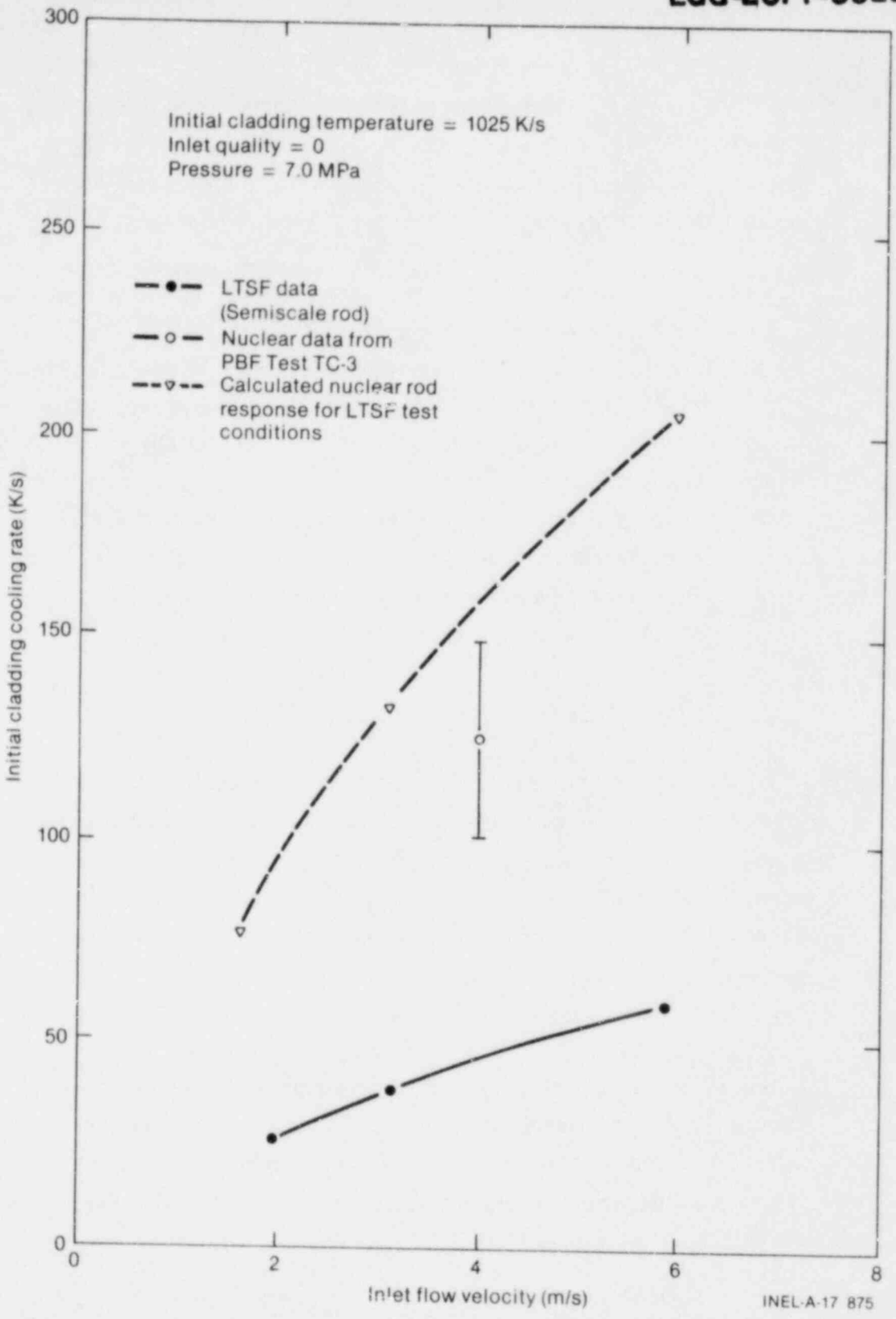

Figure 12. Comparison of measured Semiscale rod cooling rate and calculated nuclear rod cooling rate from LTSF quench experiments and nuclear rod cooling rate from PBF Test TC-3.

thermal-hydraulic models can predict the relative differences observed experimentally between the initial cooling rates of electric heater rods and nuclear fuel rods; however, these results are based upon data from only one nuclear experiment. More nuclear data are required over a wider range of hydraulic conditions for assessment of computer models.

It is noted that solid, internally-heated, electric rods cannot duplicate nuclear rod response during rapid cooling transients because of the relative high thermal diffusivity of the electric heaters. Because the UO_2 conductivity and fuel-cladding gap limit the energy delivery to the cladding, the nuclear rod cladding can be quenched by removing only the energy in the cladding; for the solid, electric heater rod, not only the cladding energy but also a significant portion of the rod internal energy must be transferred before cladding quench can occur. This basic limitation of a solid, electric heater rod was identified shortly after LOFT LOCE L2-2[13] and is discussed in detail in Appendix B.

3.3 Reflood Heat Transfer for Halden IFA-511 Experiments

The IFA-511 experiments,[14] performed in the Halden research reactor in Norway, exposed nuclear- and electric-heater-rod bundles to nearly identical heatup and reflood conditions. The experiments consisted of a series with nuclear rods (IFA-511.2) and a series with electric heater rods (IFA-511.3). The experiments for each series were performed with a seven-rod bundle consisting of six peripheral rods symmetrically surrounding the center rod, as shown in Figure 13. The heated length was 1.5 m. Both the nuclear- and electric-rod bundles were instrumented identically with both external and internal cladding thermocouples. Five of the rods were instrumented with internal cladding thermocouples, and one peripheral rod was instrumented with LOFT-type external thermocouples. The cladding thermocouples were positioned at various azimuthal orientations and at five different axial elevations.

Parameters varied during each test series included rod power, peak cladding temperature prior to reflood initiation, and reflood rate. The rod average linear heat generation rate ranged from about 1.0 to 3.0 kW/m. Measured peak cladding temperatures ranged from 580 to 1100 K, and the

TC#	Elevation from rod bottom (m)
TOC1	0.15
TOC2	0.90
TOC3	1.35
TOC4	0.60
TIC3	0.60
TIC4	0.15
TIC5	0.40
TIC6	0.60
TIC10	0.60
TIC11	0.40
TIC12	0.15
TIC13	1.35
TIC14	0.73
TIC15	0.90
TIC16	0.60
TIC20	0.73
TIC21	1.35
TIC26	0.73
TIC27	0.90

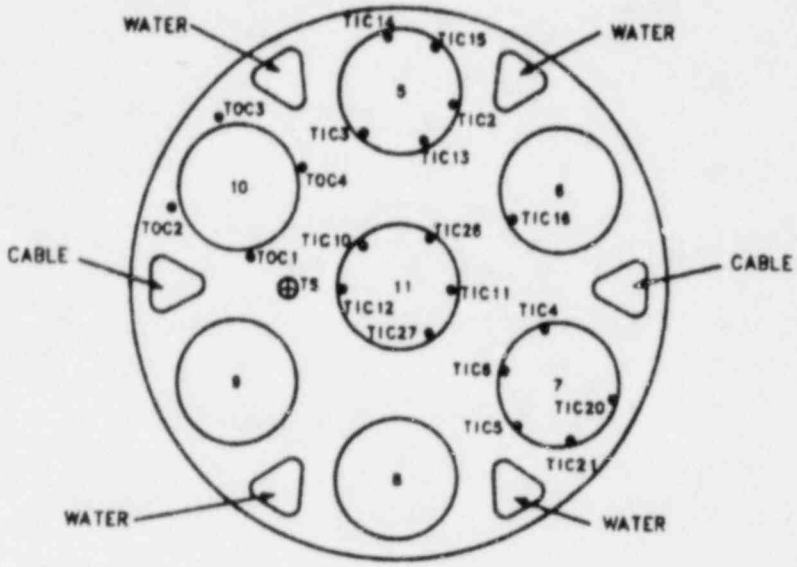

a. Nuclear rod test bundle

SXX-281-2

TC#	Elevation above rod bottom (m)
TOC1	0.13
TOC2	0.88
TOC3	1.33
TOC4	0.58
TIC4	0.13
TIC5	0.38
TIC6	0.60
TIC7	0.15
TIC8	0.40
TIC9	0.60
TIC20	0.72
TIC21	1.34
TIC24	0.90

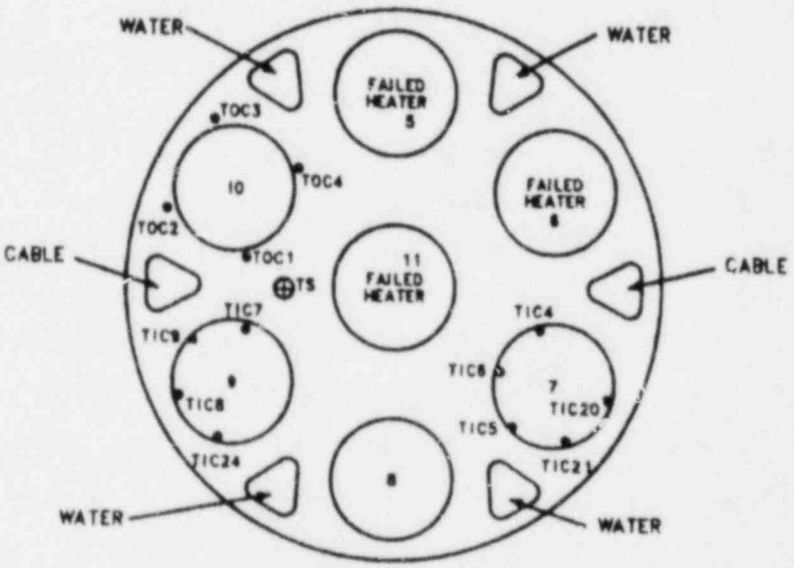

b. Electric rod test bundle

SXX-281-1

Figure 13. Schematics of electric and nuclear rod test bundles for Halden IFA-511 experiments.

reflood rate was systematically varied from approximately 2 to 10 cm/s. The peak cladding temperature, just prior to reflood, was varied by controlling the time to reflood. The test conditions for the IFA-511.2 and -511.3 experiment series are summarized in Table 2.

The experiments were initiated by first isolating the primary coolant system, then activating the test section blowdown valves to deplete the test section coolant. The rods were allowed to heat up in a nearly adiabatic environment until the desired cladding temperatures were achieved, after which reflood was initiated. Appendix E reviews the experiment sequence and summarizes the data trends from the nuclear and initial electric rod experiments. Several nuclear- and electric-rod bundle experiments were replicated, showing excellent experiment repeatability.

The data from the nuclear experiments are documented and discussed in Reference 15. In general, there was no well defined cladding quench, but rather, the cooling rates continually increased after reflood initiation until the cladding was cooled to the fluid saturation temperature. Figure 14 shows the center rod cladding temperatures for an experiment with high initial cladding temperatures. The nuclear experiments indicated that increasing the rod power and increasing the initial cladding temperature had little influence on the peak cladding temperatures and quench times. This behavior suggests that the thermal properties of the UO_2 and fuel-cladding gap effectively decouple the cooling and quench behavior of the cladding from the fuel pellet. Decreasing the reflood rates resulted in higher cladding temperatures and decreased the measured rod cooling rates. These trends are consistent with experiments performed in Semiscale[16] and FLECHT.[17,18]

The Halden electric-rod bundle experiments (IFA-511.3) were performed using a Semiscale-type heater rod. Eleven experiments were conducted to duplicate the previous nuclear-rod bundle experiments. However, during the electric rod experiments, three of the seven electric heater rods failed (produced no power); therefore, direct comparison between the nuclear and electric rods cannot be used to quantify differences between rod responses or experiment hydraulic behavior. Nevertheless, comparison of the electric and nuclear rod responses are qualitative, and as shown in Figure 15, the

TABLE 2. EXPERIMENTS IFA-511.2 AND IFA-511.3 TEST MATRIX

Run	Average Linear Heat Generation Rate (kW/m)	Reflood Rate (g/s)	Time to Reflood (s)
IFA-511.2 (Nuclear Fuel Rod)			
4693	1.05	61	58
4694	1.07	59	58
4695	1.06	61	58
4696	1.99	60	58
4697	1.93	54	58
4698	1.95	14/54	58
4719	2.82	66	58
4712	2.88	66	44
4714	2.92	64	44
5236	1.87	55	58
5237	1.91	55	58
5238	1.91	43	58
5239	1.90	33	58
5240	1.89	12	58
5241	1.89	43	82
5242	1.89	42	92
5243	1.90	42	92
5244	1.89	43	103
5245	1.92	42	113
5246	1.92	41	113
5247	1.92	42	113
IFA-511.3 (Semiscale Electric Heater Rod)			
5257	1.85	53	58
5258	1.87	55	58
5259	1.91	55	58
5260	1.91	40	58
5261	1.90	34	58
5262	1.89	12/30	58
5263	1.92	44	113
5264	1.92	44	113
5265	1.92	44	113
5266	2.0	12	11
5267	3.0	14	58

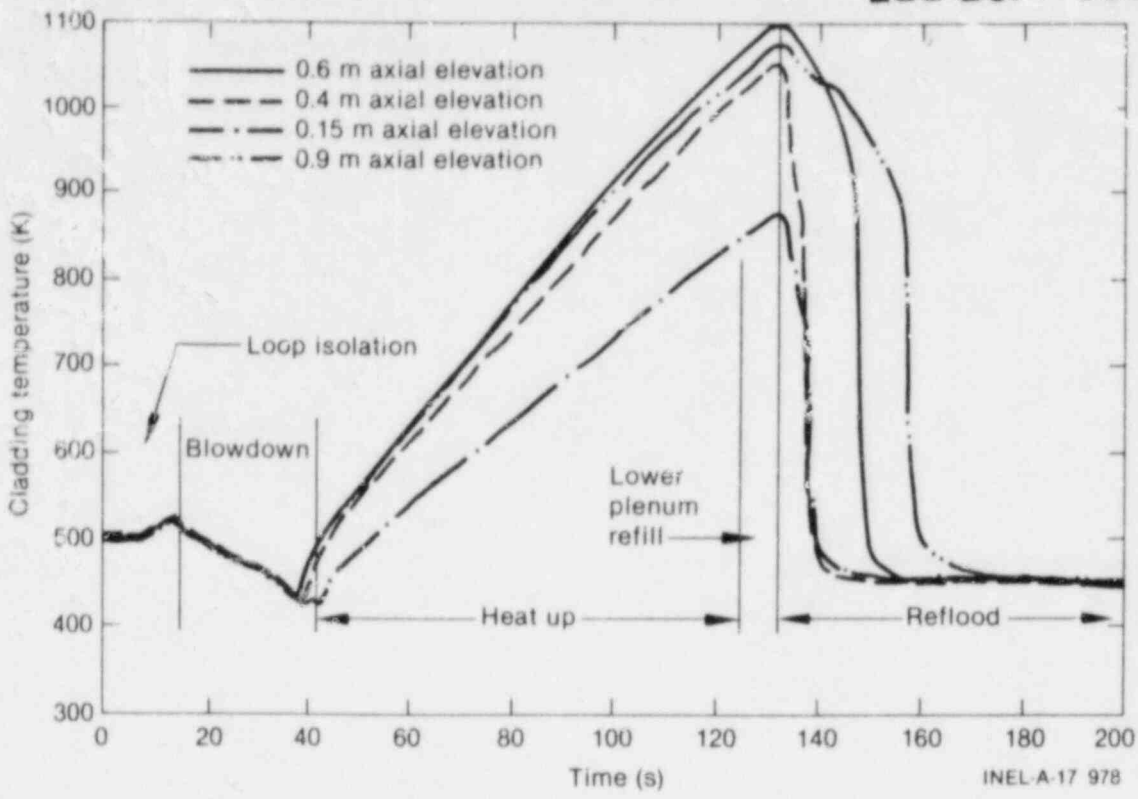

Figure 14. Thermal response of a center nuclear rod during Halden Experiment IFA-511.2, Run 5246.

nuclear rod cools approximately four times faster than the electric rod. Also, it is observed that the electric rod, unlike the nuclear rod, is characterized by a well defined quench.

If the three electric heater rods had not failed, the electric rod power generation would have been greater, resulting in more liquid entrainment and enhanced cooling above the quench front than was observed. Therefore, if the electric rods had not failed, the heater rod cooling rates, prior to quench, may have been higher and in closer agreement with the nuclear data. In Appendix E, the experiments are compared in such a manner as to estimate the influence that the failed rods may have had on the heater rod response. These comparisons suggest, as do the data in Figure 15, that significant differences in the cooldown rates of nuclear and electric rods may be experienced.

Additional experiments will confirm this trend and provide data for assessing code capability to model the important surface heat transfer and

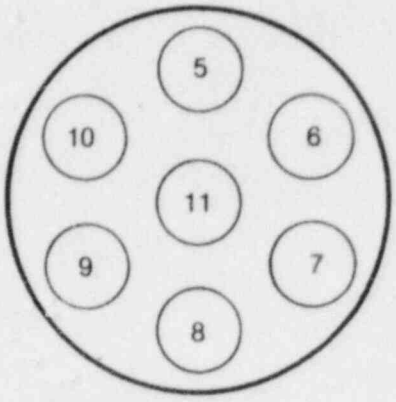

IFA-511 test
rod configuration

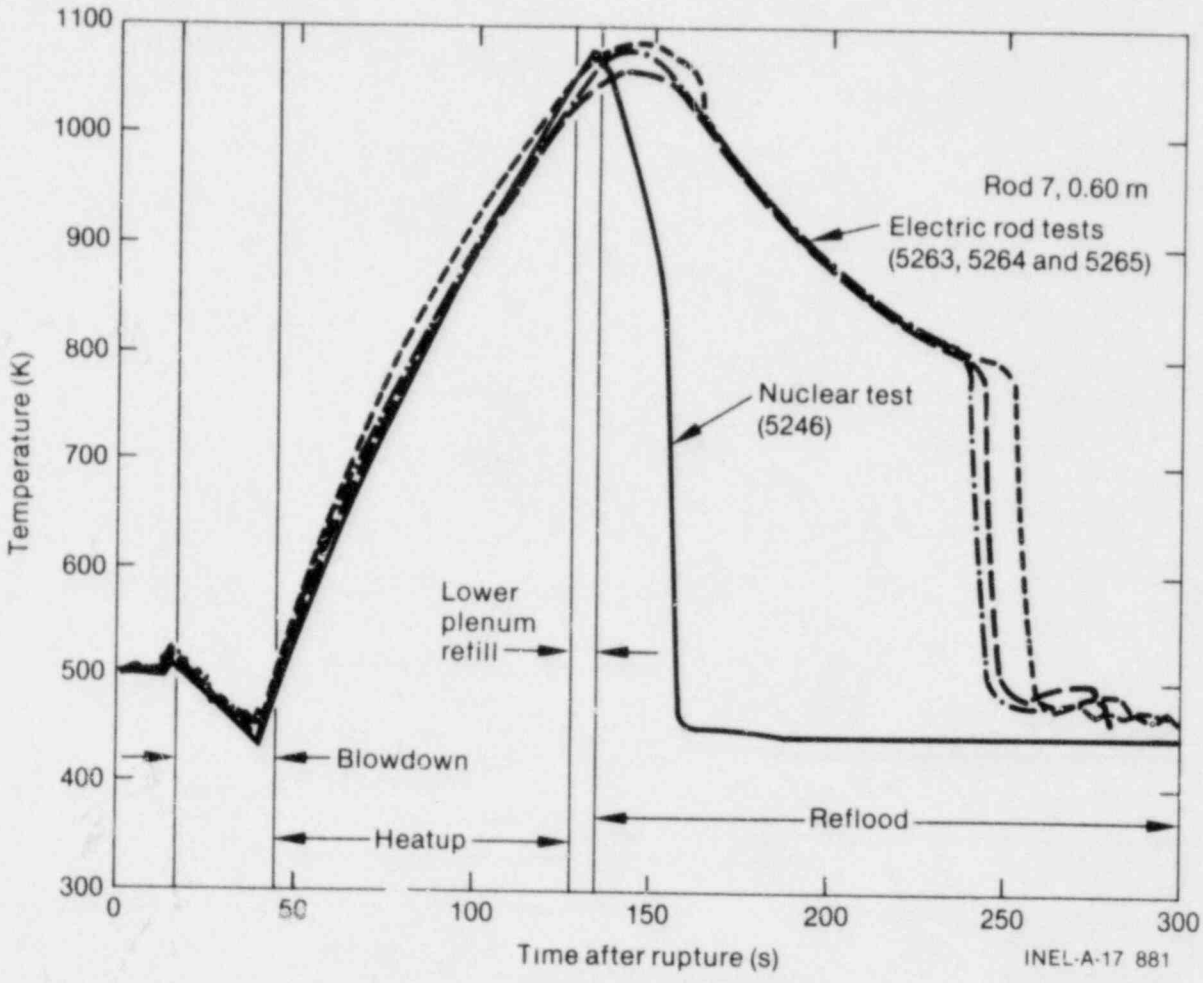

Figure 15. Comparison of nuclear and electric rod thermal responses for similar Halden reflood experiments.

rod thermal responses. The observed differences are consistent with trends observed in the high-pressure quench experiments in LOFT and PBF, showing the more rapid cooling and quench of nuclear rods.

4. OBSERVATIONS AND CONCLUSIONS

Significant differences between nuclear and electric rod thermal responses were observed during both the blowdown and reflood phases of the LOCA experiments and are summarized as follows:

1. Blowdown heat transfer:

   a. The hydraulic system responses of comparable LOFT and Semiscale experiments were similar during the first 10 to 15 s, although differences in the core flows were observed which contributed to the 100 to 200 K higher cladding temperature observed in Semiscale.

      The LOFT experiments indicate that most of the nuclear stored energy was removed as a result of a cladding quench during the first 10 s (blowdown). In contrast, the Semiscale experiments show that most of the heater rod energy was removed during the final core reflood (after 50 s).

   b. Separate effects quench experiments in the PBF using LOFT nuclear rods also show that nuclear rods can be quenched in the same time period as measured in LOFT (1 to 3 s). However, separate effects quench experiments in the LTSF using a Semiscale heater rod shows that the electric heater rod is much more difficult to quench than a nuclear rod under the same cooling influence.

2. Reflood heat transfer: Halden Experiments IFA-511.2 and IFA-511.3 showed large differences in nuclear and electric rod cooling rates; however, quantification of the differences between the rod responses was not possible because of electric rod failures which precluded direct comparison.

General conclusions regarding electric heater rod capability to simulate nuclear rod response based on analysis of the available experimental data are:

1. The electric heater rod response yielded conservatively high cladding temperatures and lower cooling rates compared to a nuclear rod for both the blowdown and reflood phases of a large break LOCA.

2. A solid, internal heater rod cannot simulate (a) the initial stored energy of a nuclear rod, (b) the transient energy equilibration of the nuclear rod during the first 10 to 15 s of the LOCA, and (c) the rapid quench that is possible on a nuclear rod.

3. Small-scale electric rod experiments are generally adequate for separate effects studies; however, because electric heater rods cannot simulate the nuclear rod initial stored energy or the transient thermal and mechanical response during the first 10 to 20 s of the LOCA, small-scale electrically heated experiments cannot provide the necessary data for assessing the thermal and hydraulic response of a nuclear core. Nuclear experiments are necessary to confirm the important phenomena that control the nuclear rod thermal and mechanical response.

4. Additional experiments are necessary to better represent film-to-nucleate transition heat transfer and quench behavior.

5. RECOMMENDATIONS

Identification of the limiting aspects of electric fuel rod simulators is necessary to assess the conservative margin of licensing models and the capability of best-estimate codes to predict fuel rod behavior during a LOCA.

To evaluate the capability of electric rods to simulate nuclear fuel rod response requires a nuclear data base for identifying the important limitations of electric heater rods. In addition it is necessary for the analytical models to be able to predict the differences in rod responses to provide the confidence required for best-estimate codes and to provide the understanding to quantify conservatism in the licensing models. Only in this manner can any unwarranted conservatisms be addressed. From this viewpoint, the following recommendations are made:

1. The ongoing nuclear programs must be completed to gain a better understanding of the nuclear system response and nuclear fuel rod behavior during the design bases LOCA as follows:

   a. Additional experiments in LOFT large break Experiment Series L2 will lead to a better understanding of the conditions necessary for core flow stagnation. In addition, the experiments will also investigate cladding deformation and core flow blockage characteristics that can occur in a nuclear core.

   b. PBF Experiment Series TC-4 will provide additional information concerning the rapid cooling and quench of a nuclear rod and will provide information relating to improved fuel rod instrumentation.

   c. Completion of nuclear reflood experiments sponsored by the U.S. Nuclear Regulatory Commission in the Canadian NRU reactor will provide comparison data with recently completed electric rod experiments for a similar configuration in FLECHT. These experiments will allow assessment of cladding

deformation influences on this reflood thermal-hydraulic behavior. Preliminary nuclear experiments have been completed, but a complete analysis of the data has not been possible at this time.

d. Additional experiments in Halden Experiment Series IFA-511 will indentify the differences in reflood responses between nuclear and electric rods and will provide the data base for assessing the capability of computer codes to predict nuclear and electric rod behavior.

2. Analysis work is necessary to assess computer code capability in the following specific areas:

a. Resolution of differences in core thermal-hydraulic responses between Semiscale and LOFT large break LOCEs. These studies will provide insight into the influence of the electrically heated core on the hydraulic response inside the reactor vessel.

b. Further evaluation of the Halden IFA-511 data will provide a basis for establishing the conservatism of electric rod reflood data and the capability of reflood models to predict the nuclear rod response. Similar experimental and analytical comparisons of the NRU reflood experiments with FLECHT data will provide an independent basis for reflood evaluation.

6. FUTURE EXPERIMENTS FOR EVALUATION

Pertinent nuclear experiments which will provide necessary data to quantify important differences between electric and nuclear rods are:

1. LOFT large break LOCEs L2-5 and L2-6

2. PBF Experiment Series TC-4

3. NRU cladding deformation experiments.

Coordination and completion of the Halden IFA-511 experiments are also anticipated in the future.

The experimental results will provide a wide range of model assessment data, and efforts will be specifically directed at evaluating model capabilities to predict the important nuclear response.

7. REFERENCES

1. M. McCormick-Barger, Experiment Data Report for LOFT Power Ascension Test L2-2, NUREG/CR-0492, TREE-1322, February 1979.

2. P. G. Prassinos et al., Experiment Data Report for LOFT Power Ascension Experiment L2-3, NUREG/CR-0792, TREE-1326, July 1979.

3. M. Patton et al., Experiment Data Report for Semiscale Mod-1 Test S-06-2 (LOFT Counterpart Test), TREE-NUREG-1122, August 1977.

4. B. Collins et al., Experiment Data Report for Semiscale Mod-1 Test S-06-3 (LOFT Counterpart Test), NUREG/CR-0251, TREE-1123, July 1978.

5. R. Gillins et al., Experiment Data Report for Semiscale Mod-1 Test S-06-4 (LOFT Counterpart Test), TREE-NUREG-1124, December 1977.

6. E. L. Tolman and E. W. Coryell, Review of LOFT Cladding Temperature Response for L2-2 and L2-3: Recommendations for Improved LOFT Fuel Rod Measurements, EGG-LOFT-5244, October 1980.

7. K. R. Katsma et al., RELAP4/MOD5 - A Computer Program for Transient Thermal-Hydraulic Analysis of Nuclear Reactors and Related Systems - User's Manual, ANCR-NUREG-1335, September 1976.

8. E. J. Kee and W. H. Grush, Best Estimate Prediction for LOFT Nuclear Experiment L2-3, EP-L2-3, April 1979.

9. EG&G Idaho, Inc., RELAP4/MOD6 - A Computer Program for Transient Thermal-Hydraulic Analysis of Nuclear Reactors and Related Systems - User's Manual, CDAP-TR-003, January 1978.

10. R. C. Gottula and J. A. Good, The Effect of Cladding Surface Thermocouples on the Quench Behavior of an Electrical Heater Rod, EG&G Idaho Inc., Internal Report LO-00-80-115, March 5, 1980.

11. T. Yackle et al., Loss-of-Coolant Accident Test Series--Test TC-1 Test Results Report, EGG-TFBP-5068, May 1980.

12. T. Yackle, "An Assessment of the Influence of Surface Thermocouples on the Behavior of Nuclear Fuel Rods During Large Break LOCE," Eighth U.S. NRC Water Reactor Safety Research Information Meeting, Gaithersburg, Maryland, October 27-30, 1980.

13. R. Hagor, "Problems in Simulating the Response of Nuclear Fuel Pins Using Electrical-Heated Pins," USNRC Sponsored Workshop on Rewet Phenomena, Denver, Colorado, April 11-12, 1979.

14. R. A. Cushman et al., Proposed Test Specifications for Halden Instrumented Fuel Assembly IFA-511 Light Water Flow Starvation Test Series, TFBP-TR-316, Revision 1, December 1979.

15. C. Vitanza et al., Results of Blowdown/Reflood Tests with Nuclear Heated Rods (IFA-511.2), HPR-248, May 1980.

16. A. C. Peterson et al., Thermal and Hydraulic Response of the Semiscale MOD-1 Core During Forced Feed Reflood Tests, TREE-NUREG-1001, October 1976.

17. F. F. Cadek et al., PWR-FLECHT Final Report Supplement, WCAP-7931, October 1972.

18. J. A. Blaisdell et al., PWR-FLECHT-SET Phase A Report, WCAP-8238, December 1973.

BLANK

APPENDIX A

SUMMARY OF MEASURED CORE THERMAL RESPONSE DURING LOFT EXPERIMENTS L2-2 AND L2-3 AND ACCURACY OF CLADDING SURFACE THERMOCOUPLES

BLANK

APPENDIX A
SUMMARY OF MEASURED CORE THERMAL RESPONSE DURING LOFT EXPERIMENTS L2-2 AND L2-3 AND ACCURACY OF CLADDING SURFACE THERMOCOUPLES

1. SUMMARY OF MEASURED CORE THERMAL RESPONSE DURING LOFT EXPERIMENTS L2-2 AND L2-3

Large-break nuclear loss-of-coolant experiments (LOCEs) L2-2 and L2-3 have been completed in the Loss-of-Fluid Test (LOFT) facility. The only operating condition specified to be different for these experiments was the linear fuel rod power generation rate. The initial conditions for these experiments are summarized in Table A-1.

The measured transient cladding temperature response of the fuel rods, near the axial peak power zone for the two experiments are compared in Figure A-1. Initial departure from nucleate boiling (DNB) occurred between 1 and 2 s and coincided with a general flow stagnation; after which, the measured cladding temperature rapidly increased for 1 to 2 s. At approximately 3 s, however, measured upward core flow was established which cooled the core and reduced the rate of cladding temperature increase. At about 4 s, the flow into the reactor vessel increased as a result of the flow reduction (choking) in the cold leg break. This flow redistribution resulted in peak flow velocities through the reactor core from 150 to 200 cm/s and caused a core-wide quench from approximately 5.5 to 7.5 s. The cladding quench was maintained for several seconds, but eventually, as the reactor vessel coolant was depleted, a second DNB or dryout occurred at about 10 to 18 s. After this time, the cladding temperatures in the peak power location increased slowly until emergency core coolant (ECC) rapidly reflooded the core. Details of the measured cladding temperature response for LOCEs L2-2 and L2-3 are presented in References A-1 and A-2, respectively.

In LOCEs L2-2 and L2-3, the peak cladding temperatures were achieved during the first 6 s, just prior to the measured cladding quench. The cladding temperatures measured in the center fuel module on several instrumented fuel rods were consistent at each axial location, but varied axially

TABLE A-1. PLANT OPERATING CONDITIONS AT EXPERIMENT INITIATION

Parameter	LOCE L2-2	LOCE L2-3
Primary system:		
Pressure (MPa)	15.64	15.06
Temperature (K)	570	573
Mass flow (kg/s)	194.2	299.8
Boron (ppm)	838	697
ECC accumulator:		
Pressure (MPa)	4.11	4.18
Temperature (K)	300	307
Boron (ppm)	3301	3281
Injected volume (m^3)	1.05	0.96
Reactor core:		
Power [MW(t)]	24.9	36.7
Average linear heat generation rate (kW/m)	10.9	16.0
Maximum linear heat generation rate (kW/m)	26.37	39.4
Coolant temperature rise (K)	22.7	32.2

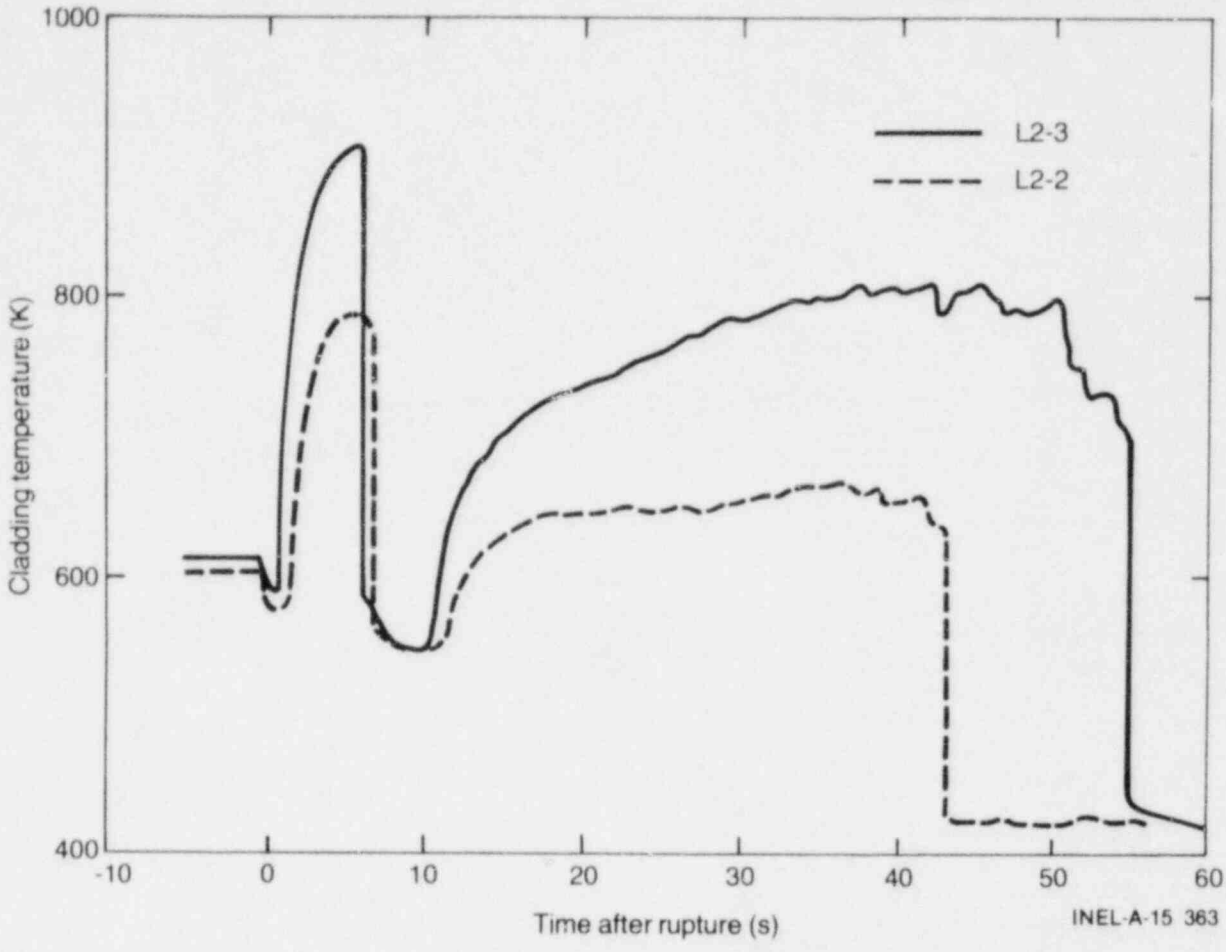

Figure A-1. Peak cladding temperatures for LOFT LOCEs L2-2 and L2-3.

as a result of the axial power distribution and changing coolant conditions. The measured cladding temperatures versus time at the 8-in. axial elevation during the first 10 s of LOCE L2-3 are shown in Figure A-2. Notice the uniformity in response from the three separate fuel rods, the very sharp initiation of the cooling transient at about 6.0 s, and the rapid quench to the saturation temperature.

Figure A-3 shows the center fuel assembly temperature response at the 15-in. axial elevation during LOCE L2-3. The initial time-to-DNB varied by approximately 0.75 s, but the post-DNB temperature was similar for all rods and the peak cladding temperatures correlated to the time-to-DNB. The initiation of the quench cooling is well defined, occurring at about 6.0 s on all rods at the 15-in. axial elevation. The cladding quench at this axial

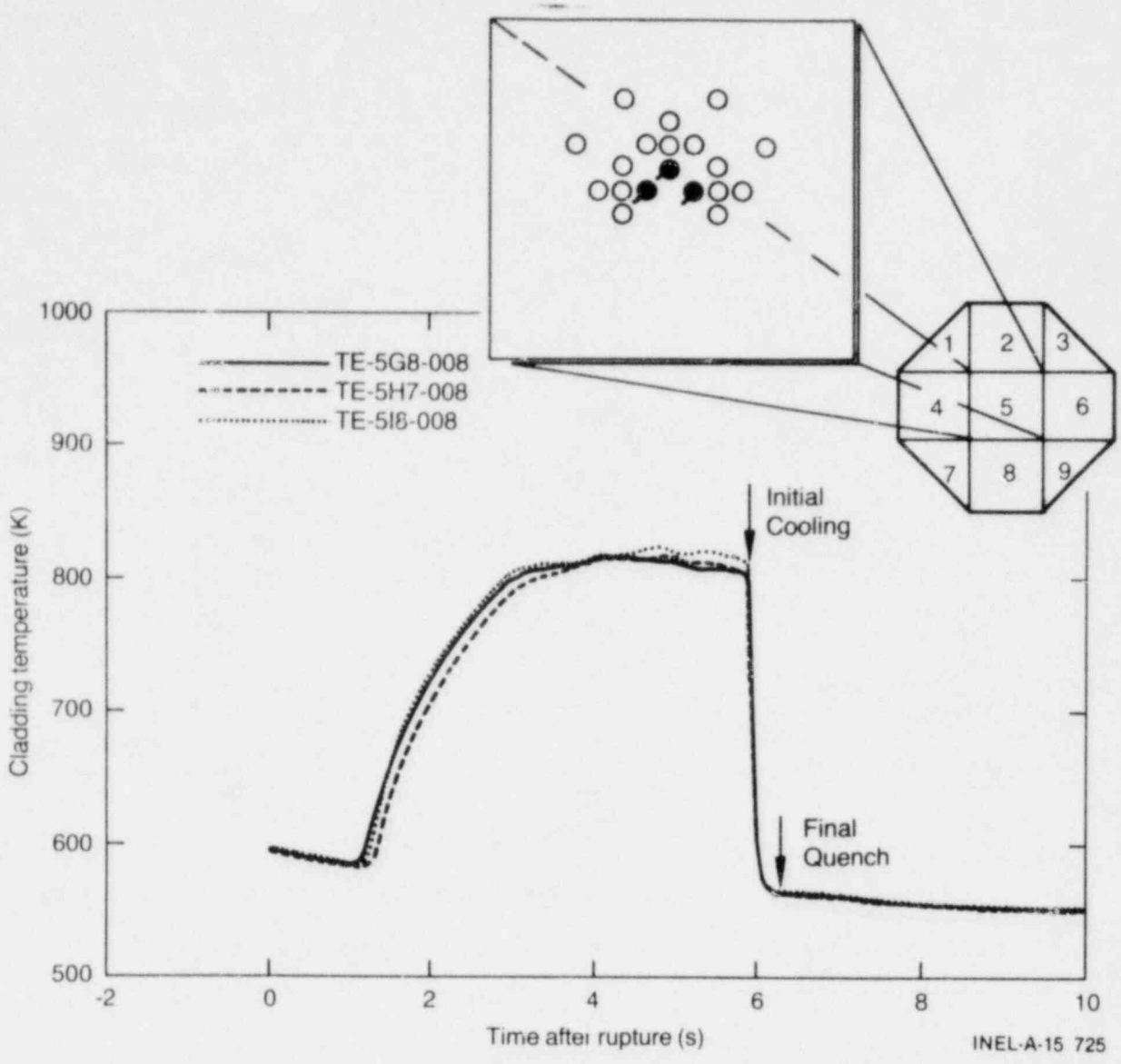

Figure A-2. Center fuel module cladding temperature response at 8-in. axial elevation for LOFT LOCE L2-2.

location occurred rapidly, in less than 0.3 s for most thermocouples; however, two of the five thermocouples showed small temperature oscillations for approximately 1 s before reaching the coolant saturation temperature. The final quench is defined as the point at which the thermocouples indicated stable coolant saturation conditions, as shown in Figure A-3.

Figure A-4 shows the measured cladding temperature at the peak power axial position (26-in. axial elevation), which was similar to the lower axial elevation response up to the time of the cladding quench. The quench

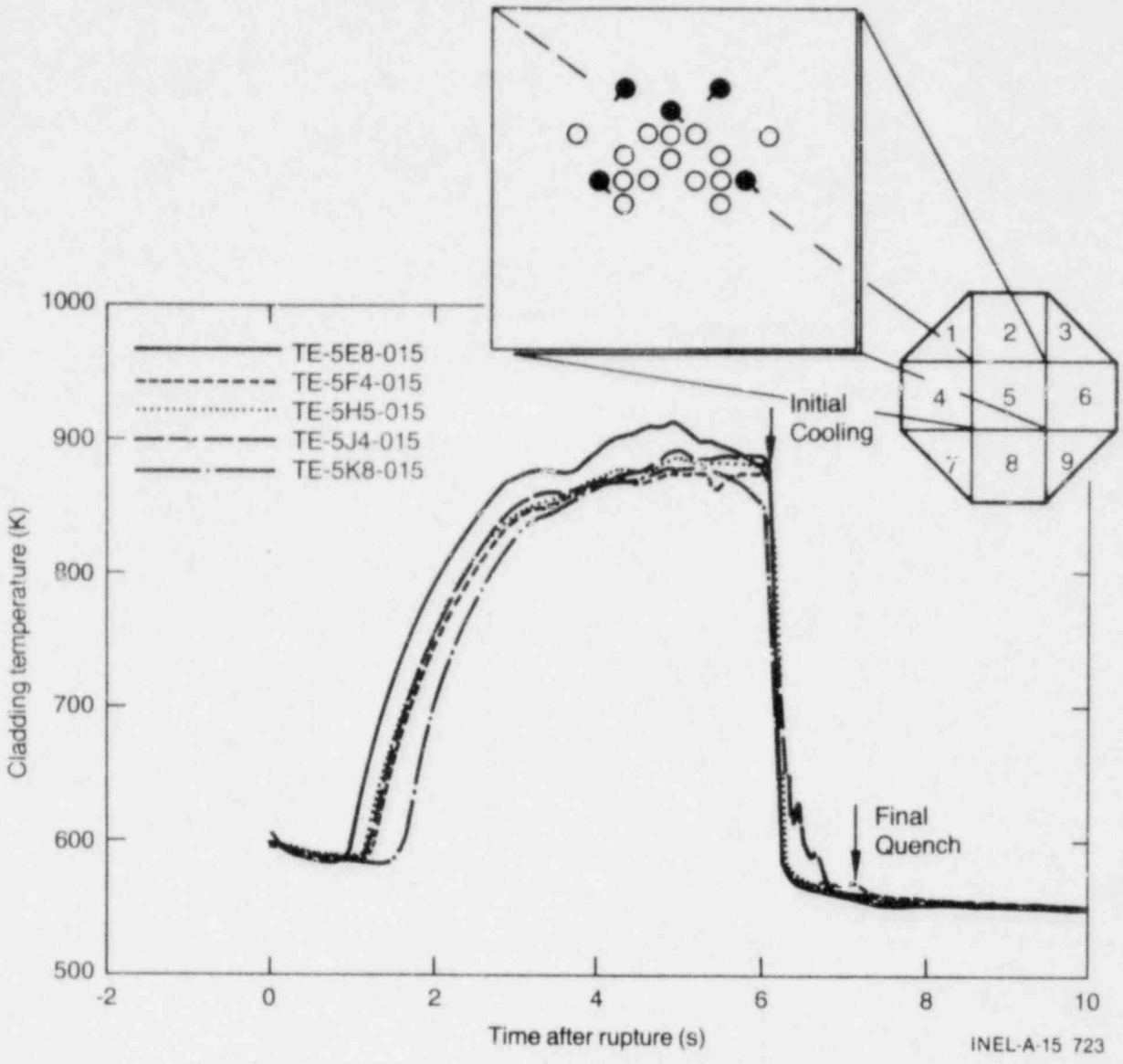

Figure A-3. Center fuel module cladding temperature response at 15-in. axial elevation for LOFT LOCE L2-3.

initiation times measured by all five thermocouples were identical; however, the time of measured cooldown to coolant saturation differed, ranging from 0.8 to 1.4 s.

Figure A-5 shows the measured thermocouple response at the 32-in. axial elevation which is similar to the response at the 26-in. elevation. However, notice that even longer times (~1.0 to 2.5 s) were required to quench the cladding. Figure A-6 shows a similar unstable cooling period at the 45-in. axial elevation, even though the local power at this location was a

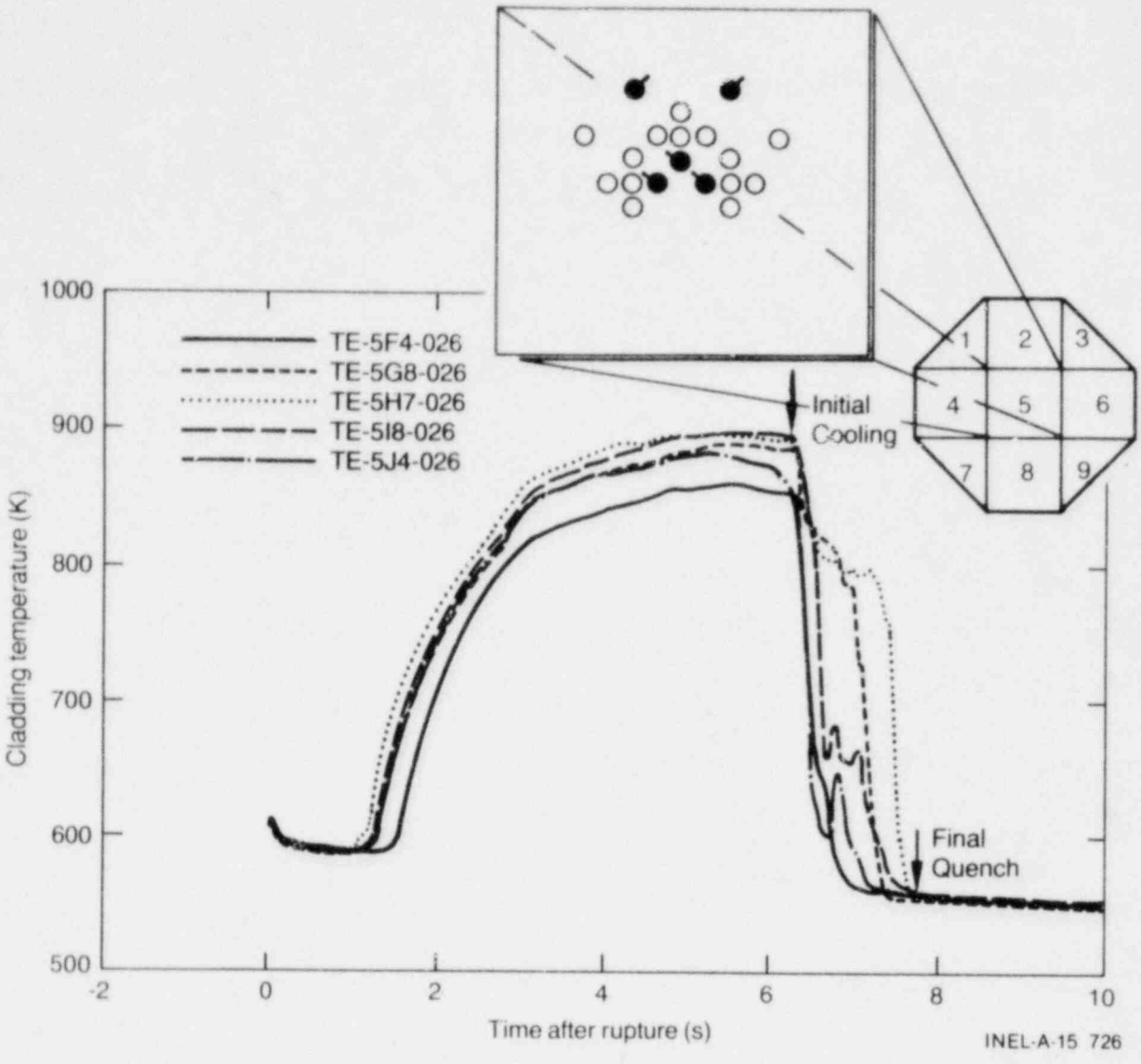

Figure A-4. Center fuel module cladding temperature response at 26-in. axial elevation for LOFT LOCE L2-3.

factor of two lower than the peak rod power. The difference in quench characteristics at the same power zones at the bottom and top of the core (rapid versus unstable quench) suggests changing local hydraulic conditions along the axial length of the rod.

Figure A-7 summarizes the measured cladding quench characteristic for LOCE L2-3, showing the times for the initiation and completion of quench as a function of rod axial elevation. Notice that the initial cooling of the rod as a function of axial position was nearly linear with time. The final cladding quench was clearly a function of the axial power profile and was

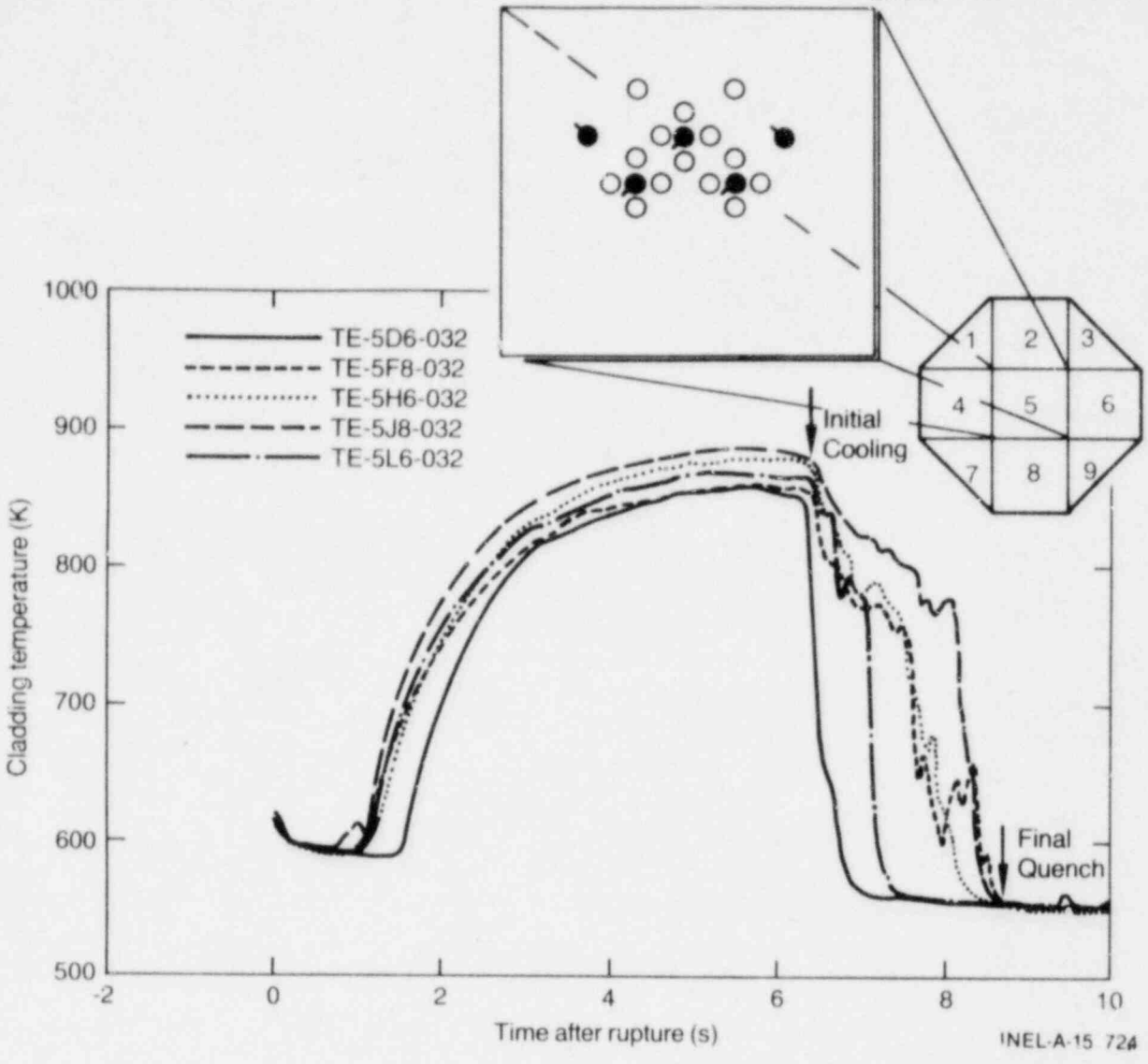

Figure A-5. Center fuel module cladding temperature response at 32-in. axial elevation for LOFT LOCE L2-3.

significantly influenced by the fuel rod grid spacers, suggesting that changing coolant conditions along the rod affected the rod heat transfer and cladding quench characteristics.

The measured cladding quench characteristic during LOCE L2-2 are shown in Figure A-8 and are much the same as for LOCE L2-3; although, in general the cladding quench required less time--1.0 to 1.5 s compared to 2.0 to 2.5 s for LOCE L2-3. The more rapid cladding quench for LOCE L2-2 was a result of lower initial fuel rod power and resulting transient cladding temperatures.

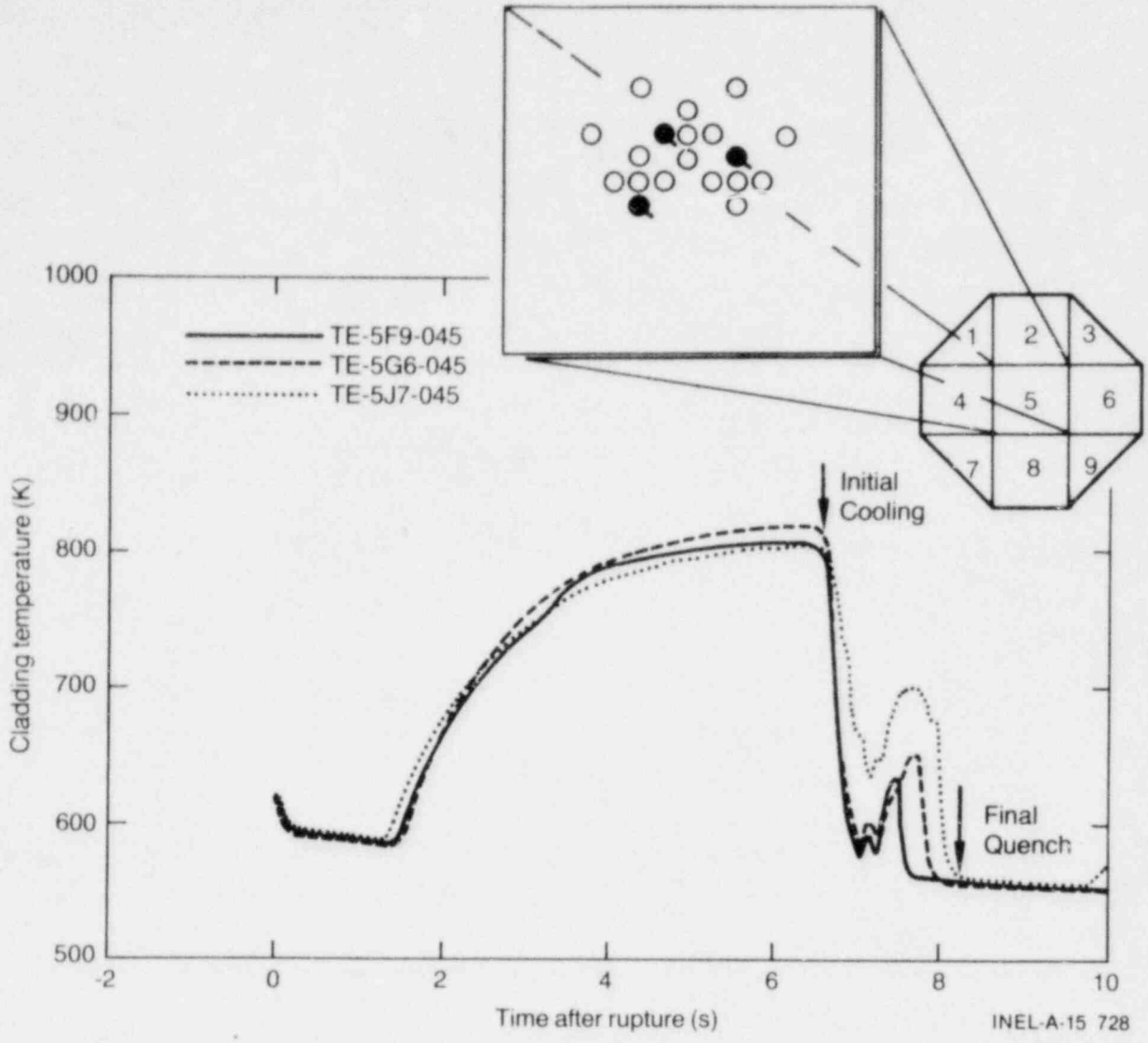

Figure A-6. Center fuel module cladding temperature response at 45-in. axial elevation for LOFT LOCE L2-3.

Two additional measurements indicated a changing coolant flow through the core that was coincident with the cladding temperature quenches. The first is the self-powered neutron detector (SPND) located at the 24-in. axial position and which is sensitive to coolant quality changes. Figure A-9 compares the response of the SPND and the cladding thermocouples located at the 24-in. axial elevation. The rapid cooling of the thermocouples and the noticeable change in the SPND response from 6.2 to 6.6 s indicate a low quality coolant influence during this period. The second indication of low quality flow upward through the core was obtained from

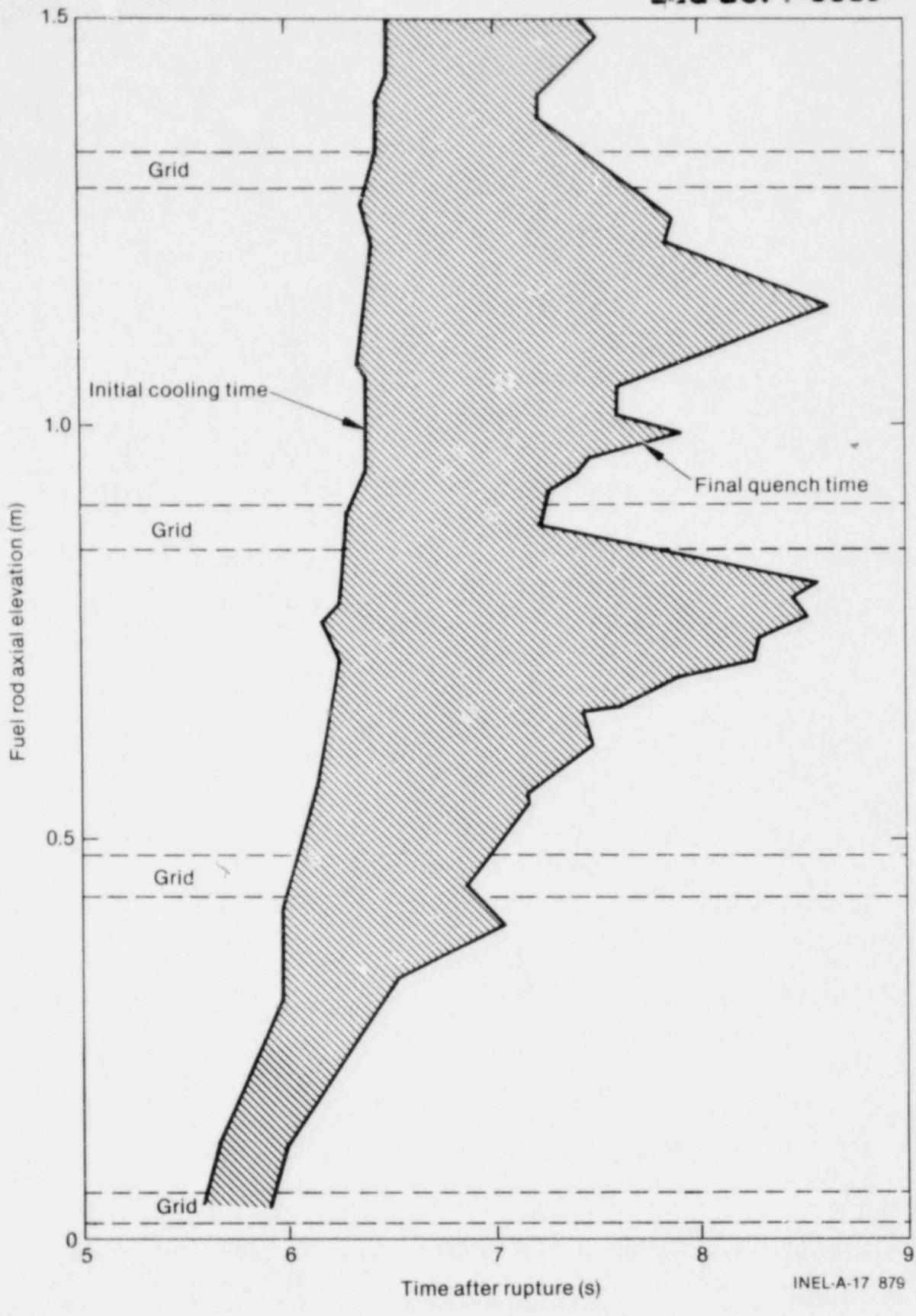

Figure A-7. Quench characteristics versus axial elevation for LOFT LOCE L2-3.

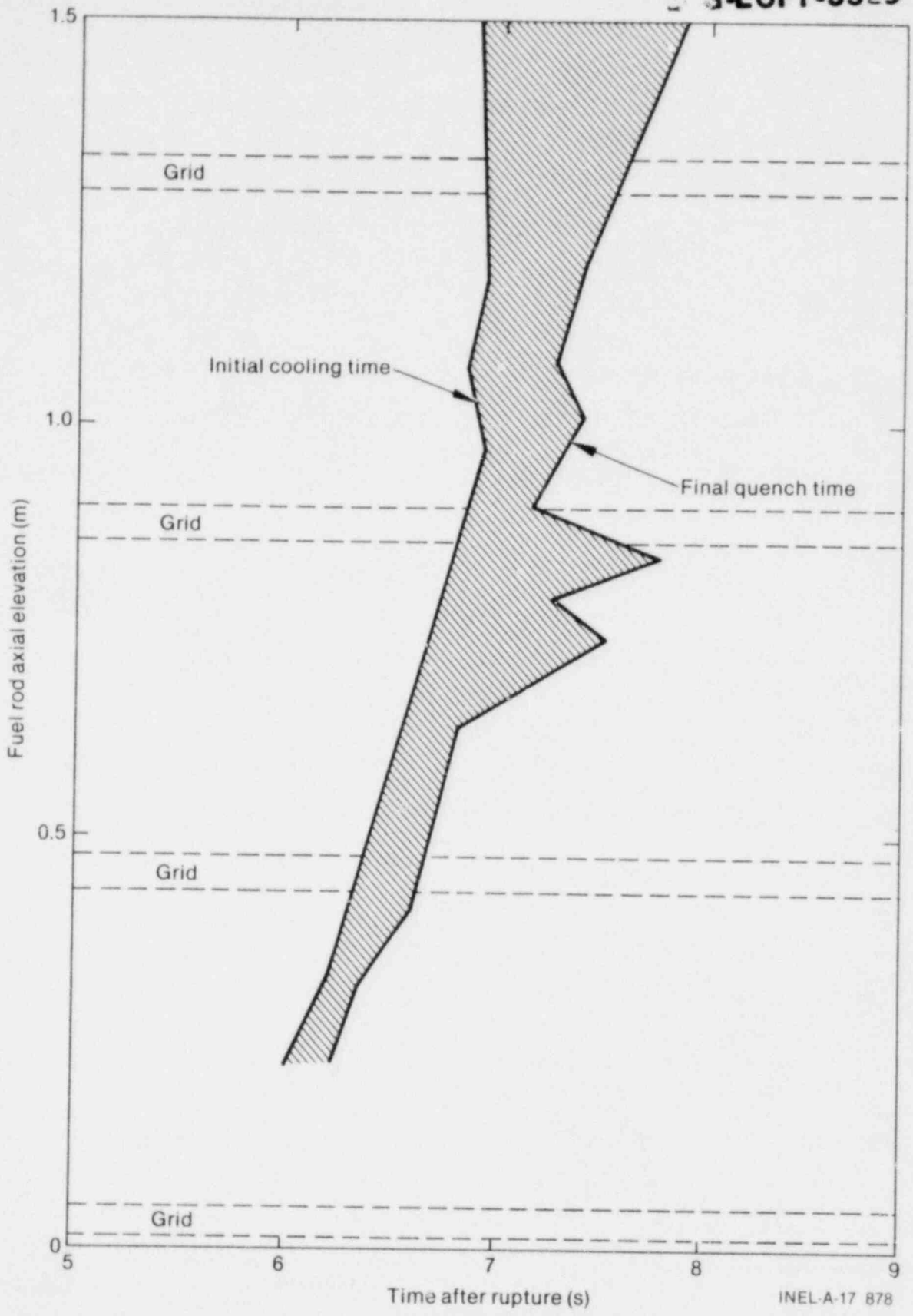

Figure A-8. Quench characteristics versus axial elevation for LOFT LOCE L2-2.

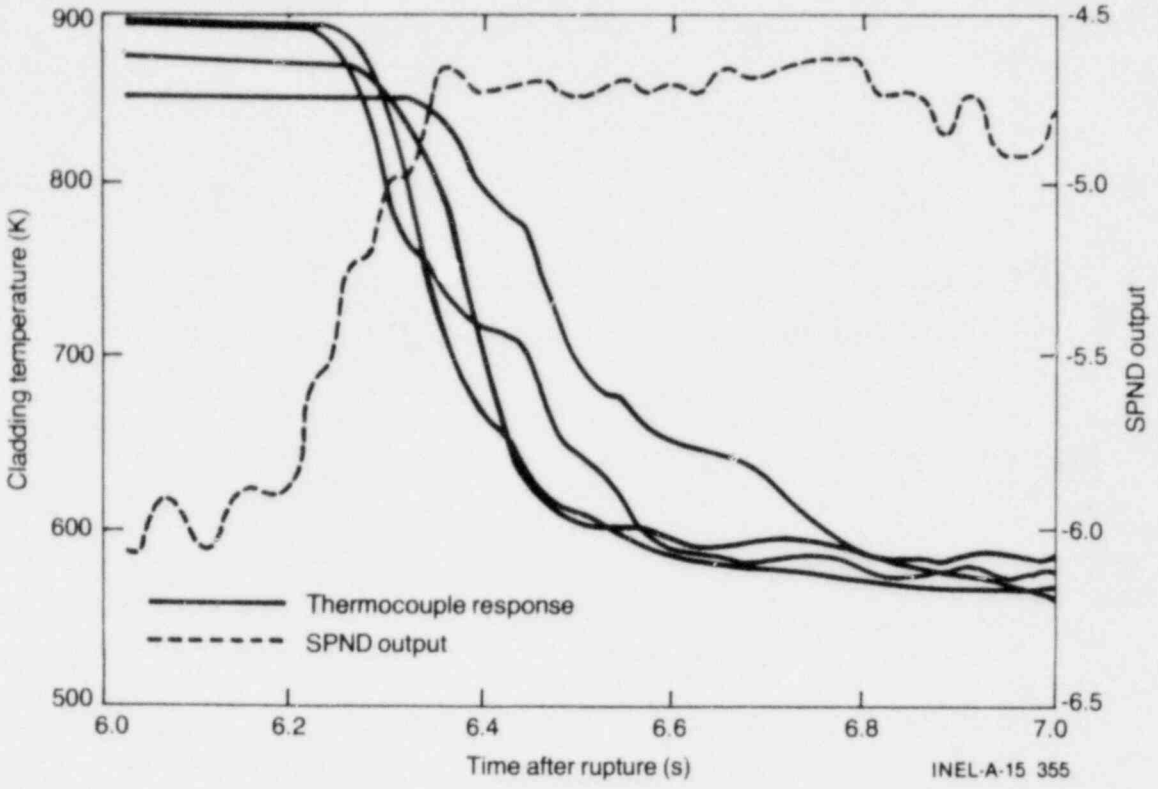

Figure A-9. Cladding temperature and SPND response at 24-in. axial elevation for LOFT LOCE L2-3.

the upper plenum thermocouples which measure coolant temperatures directly above the core. Figure A-10 shows that from approximately 3 to 6 s, the coolant in the upper plenum nearest the core was superheated vapor. However, at approximately 6 s, the upper plenum coolant temperature was rapidly reduced to the saturation temperature. The time of coolant temperature reduction is consistent with the axial position versus time for initial cladding cooling, as shown in Figure A-11. The upper plenum coolant thermocouple quench occurred just after the highest elevation cladding thermocouples began to quench. Assuming the initial, rapid cladding cooling versus axial position represents the coolant velocity through the core, flow velocities of 150 to 200 cm/s were achieved.

Figure A-12 shows the peak cladding temperatures for each of the axial cladding measurement locations compared to the fuel rod axial power profile. Notice the peak cladding temperatures do not reflect the axial power profile, being relatively higher at the higher axial elevations. This behavior

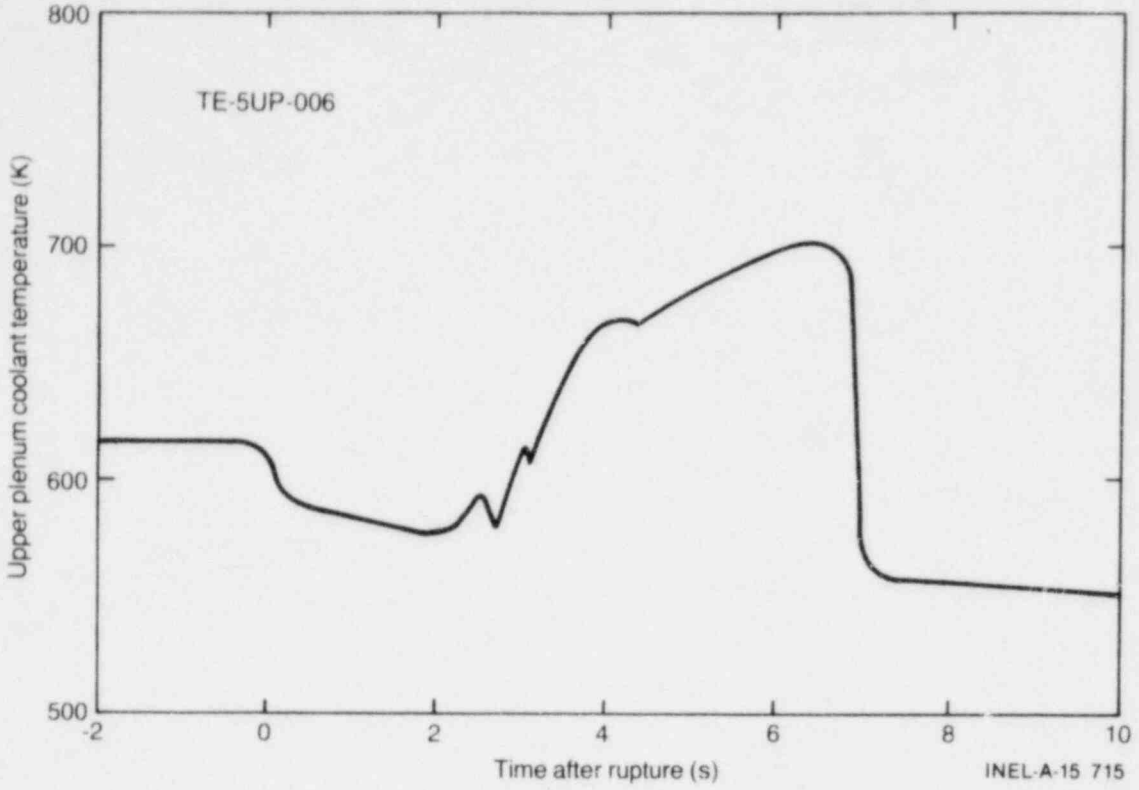

Figure A-10. Coolant temperature in reactor vessel upper plenum for LOFT LOCE L2-3.

is consistent with the measured low upward core flow for 1 to 2 s prior to quench and the increased coolant quality and degraded rod cooling at higher elevations.

The fuel rod stored energy during LOCE L2-3 was estimated from FRAP-T5 calculations. The initial, steady state fuel rod thermal conditions just prior to the transient were obtained from FRAPCON-1 calculations and are summarized in Table A-2. Estimates of the initial, steady state fuel rod stored energy can only be made from calculations, since no direct UO_2 pellet temperatures were measured during the LOFT experiments.

The calculated transient fuel rod power utilized in the FRAP-T5 calculations was obtained from RELAP4/MOD6 predictions which model the effects of the rapidly changing coolant conditions on the core neutronics; the American Nuclear Society standard decay power was utilized. The measured transient cladding surface temperature was input to the code as a cladding temperature boundary condition.

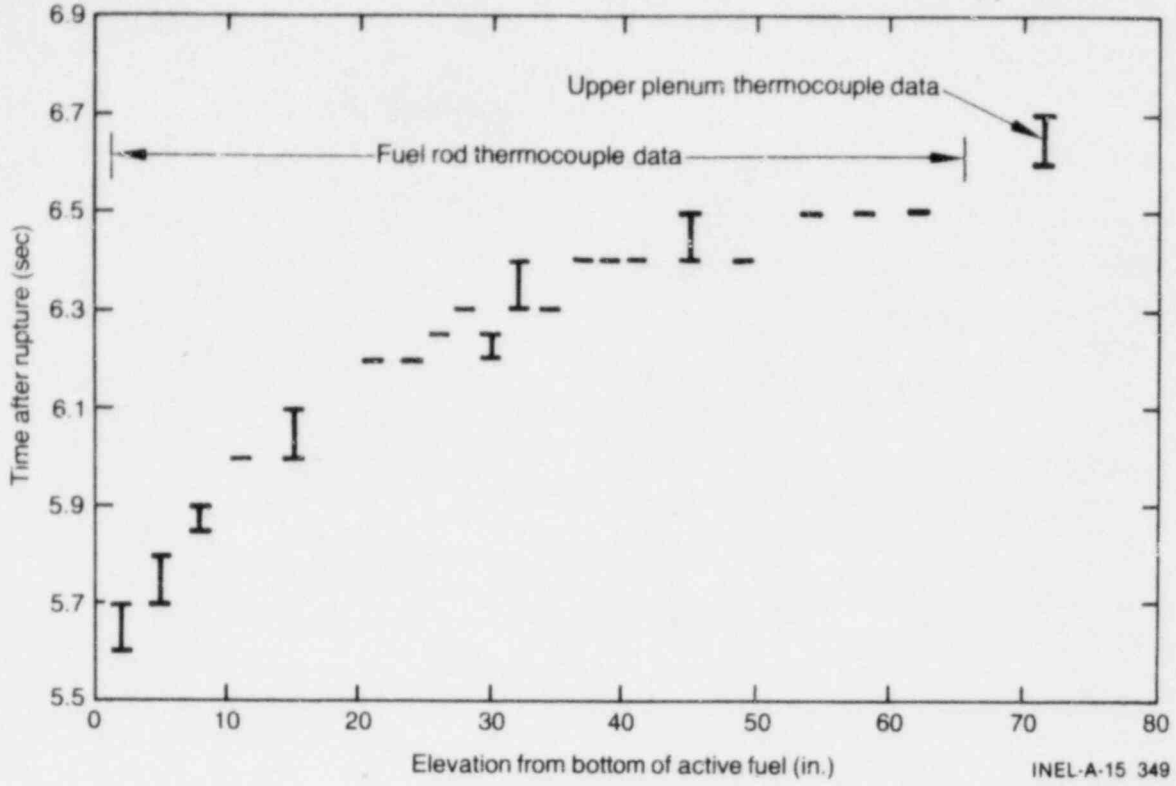

Figure A-11. Comparison of initial quench cooling of fuel rod cladding and upper plenum fluid thermocouples showing the quench front movement through the core region.

The calculated fuel pellet energy versus time (volumetric average) is shown in Figure A-13. In general, the response can be classified into three time periods--prequench, quench, and postquench. During the prequench period (0 to 5.5 s), approximately 20 to 25% of the initial fuel rod energy is transferred from the rod. During the quench period (5.5 to 12 s), approximately 30 to 40% of the rod energy is lost. The postquench period is characterized by very low heat transfer, and during LOCE L2-3, the cladding temperature increased slowly until just before final core reflood (38 to 55 s). The cladding surface heat transfer coefficients for LOCEs L2-2 and L2-3 are shown in Figure A-14 based on the fuel rod thermocouple measurements and best estimate FRAPCON-1 calculation of the initial fuel rod energy.

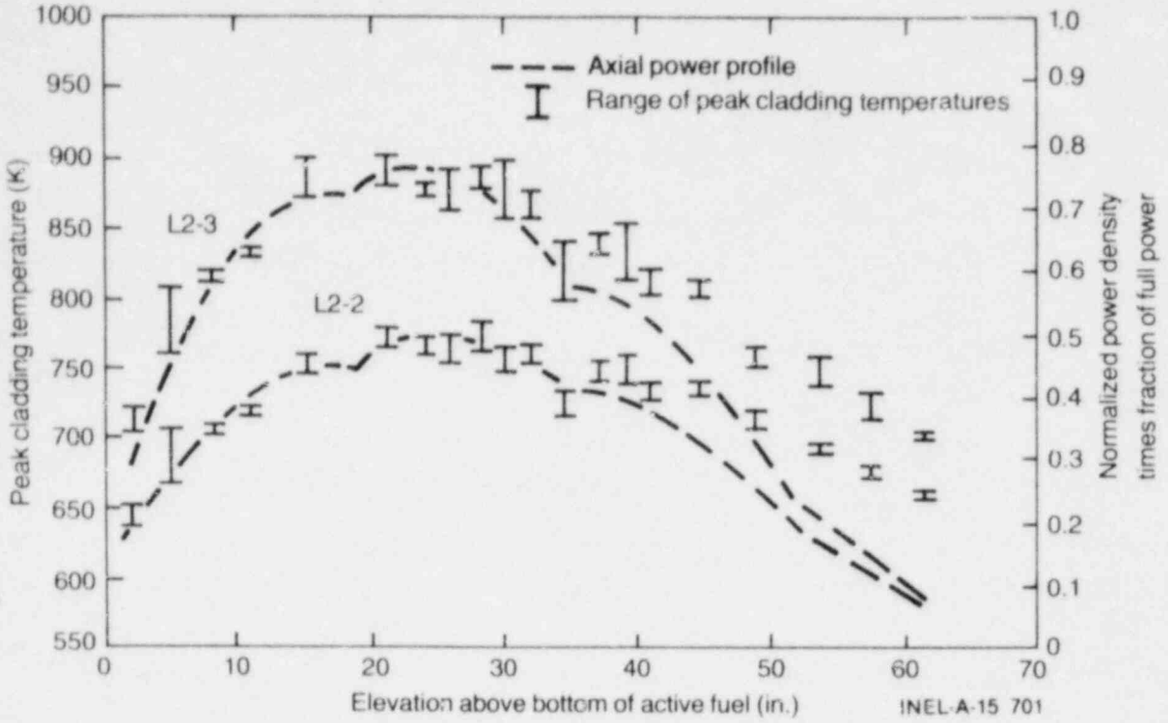

Figure A-12. Comparison of peak cladding temperature and axial power versus axial position for LOFT LOCEs L2-2 and L2-3.

TABLE A-2. CALCULATED STEADY STATE FUEL ROD THERMAL DATA FOR LOFT EXPERIMENTS L2-2 AND L2-3 USING FRAPCON-1

	LOCE	
Parameter	L2-2	L2-3
Peak core power (kW/m)	26.25	39.38
Peak core burnup (MWd/MtU)	834.3	996.6
Fuel centerline temperature (K)	1590.7	2041.1
Fuel pellet ΔT (K)	915.2	1341.3
Pellet-cladding gap ΔT (K)	24.9	33.8
Gap conductance (kW/m^2 - K)	36.7	40.06
Cladding ΔT (K)	30.3	45.1
Fuel stored energy (enthalpy) (J/g)	240.4	317.0

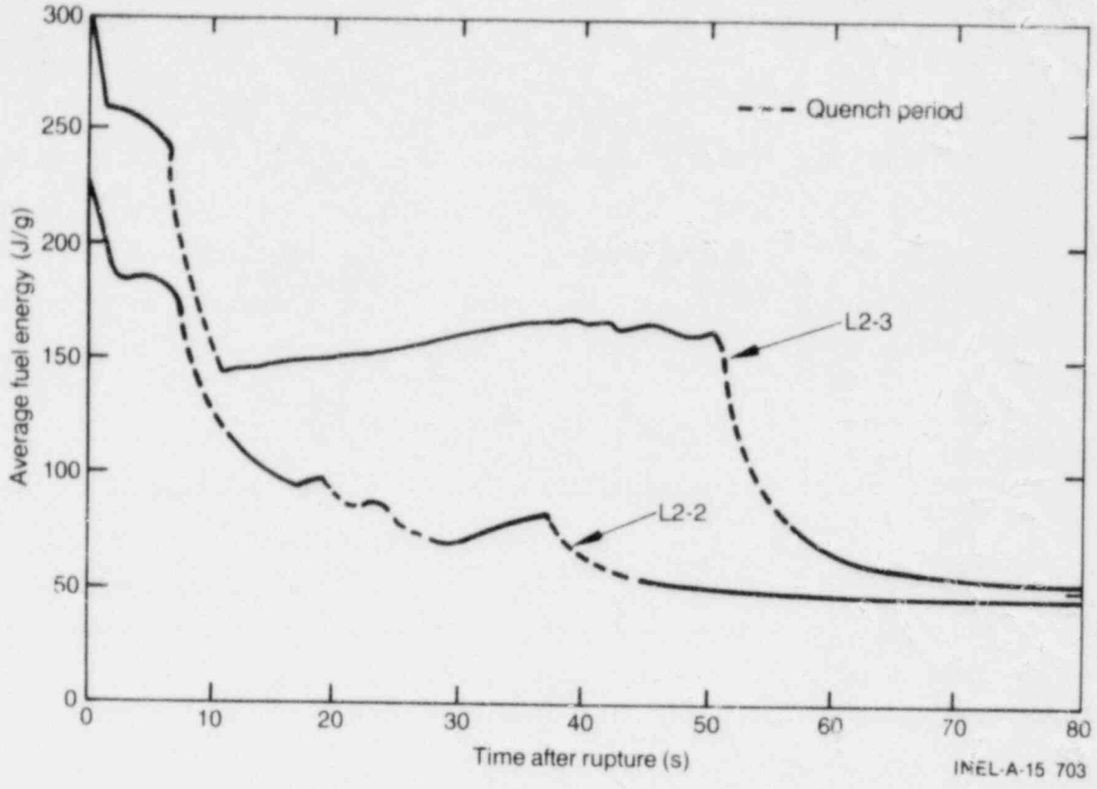

Figure A-13. Calculated fuel rod energy during LOFT LOCEs L2-2 and L2-3.

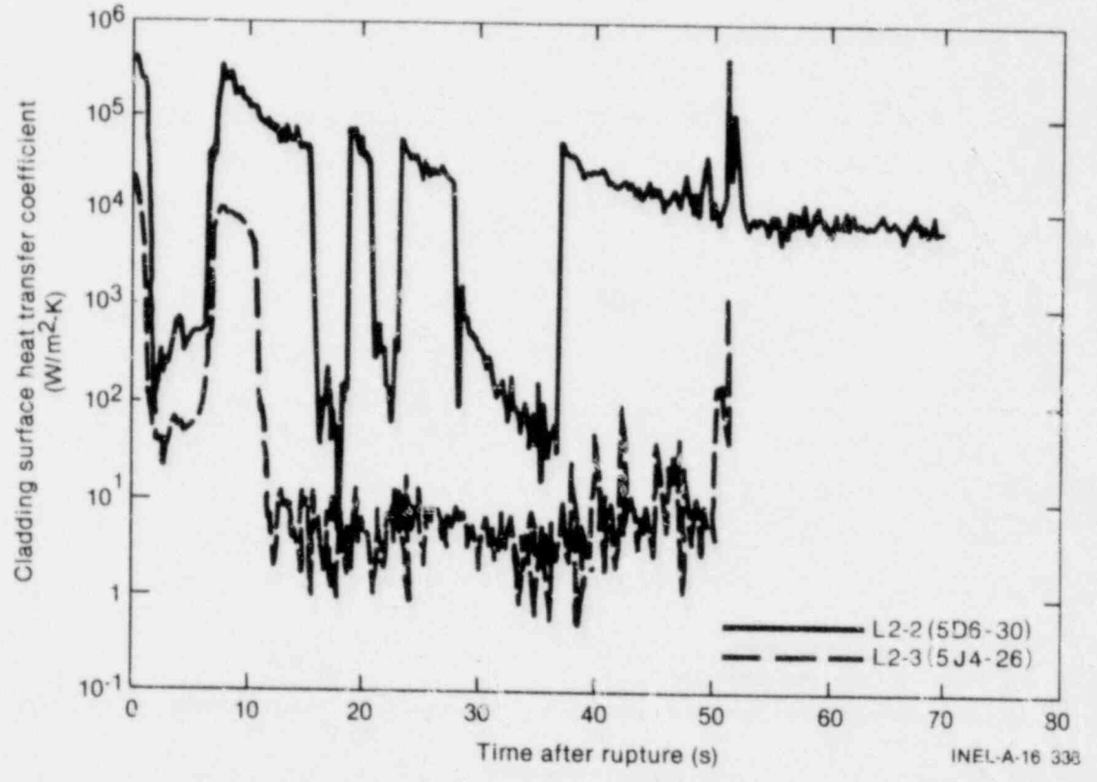

Figure A-14. Nominal cladding surface heat transfer coefficient during LOFT LOCEs L2-2 and L2-3.

2. ACCURACY OF THE LOFT CLADDING THERMOCOUPLES

The accuracy of the cladding thermocouples becomes important in understanding the core heat transfer and thermal-hydraulic behavior, particularly for assessing computer code capability. Several test programs have been carried out or are now underway to evaluate the accuracy and perturbation effects of the LOFT cladding thermocouples. These experiments have provided a basis for estimating the influence of the LOFT thermocouples during LOCE L2-3.

Because the cladding surface thermocouples enhance cooling of the rod, the measured data represent a lower bound for the cladding temperature. The upper bound temperature response for LOFT LOCE L2-3 is estimated based on the cooling influences characterized by the separate effects experiments. The following boundary conditions were established to estimate the upper bound cladding temperature for LOCE L2-3:[a]

1. Initial DNB occurred 0.5 s earlier than measured by the thermocouples, based on the LOFT transient DNB tests.[A-4]

2. From the time of DNB to the initiation of the early quench, the heat transfer from the instrumented rods was assumed to be increased by 30% due to the increased surface area for heat transfer which aids in cooling the rod (fin effect).[A-5,A-6]

3. During the quench period, as indicated by the surface thermocouples, the cladding thermocouples were assumed to be measuring coolant temperature. The cladding temperature decrease during this time was assumed to be 26 K/s as determined from the LOFT Test Support Facility high-pressure quench test data.[A-7]

---

a. Reference A-3 provides an in-depth discussion of the experiments to evaluate the perturbation influence and accuracy of the LOFT thermocouples.

4. The early part of the secondary heat-up phase of the experiment was also assumed to be characterized by thermocouple selective cooling. Therefore, the heat transfer from the time of secondary DNB initiation to the onset of final core flooding was represented by the average heat transfer during the 25- to 35-s time interval which is characterized by nearly adiabatic heat transfer.

5. During final reflood cooling, the measured LOFT precursory cooling rates (5.5 K/s) were assumed to represent the cooling rate of the uninstrumented rods, based on the data from Test Series TC-1 performed in the Power Burst Facility.[A-6] The upper bound cladding temperature was assumed to cool at this rate until a cladding temperature of 750 K was reached, after which a rapid quench was assumed.

The estimated upper bound temperature response calculated under these assumptions is compared to the measured data in Figure A-15. An uncertainty in peak cladding temperature of 100 K exists, as reflected by the estimated upper bound temperature envelope. Also a difference of approximately 25 s exists in the final reflood temperature quench. The upper bound estimate is compared to the RELAP4/MOD6 pretest predictions in Figure A-16 and shows the calculated cladding temperature cooldown during the period from 6 to 12 s is similar to the estimated upper bound. The fuel rod stored energy for the bounding cases are shown in Figure A-17, which shows the importance of the heat transfer during the first 10 s of the transient.

Further resolution of the peak cladding temperatures from the LOFT experiments will not likely be achieved from metallographic examination of the fuel rods, since for a peak cladding temperature of less than 1100 K, accurate determination of cladding temperatures from zircaloy microstructures or oxidation characteristics is not possible. Evaluation of the cladding temperature from posttest cladding deformation will also be marginal, since, for the LOCE L2-3 bounding cladding temperatures, little or no cladding deformation is expected, based on out-of-reactor cladding deformation experiments[A-8] as shown in Figure A-18.

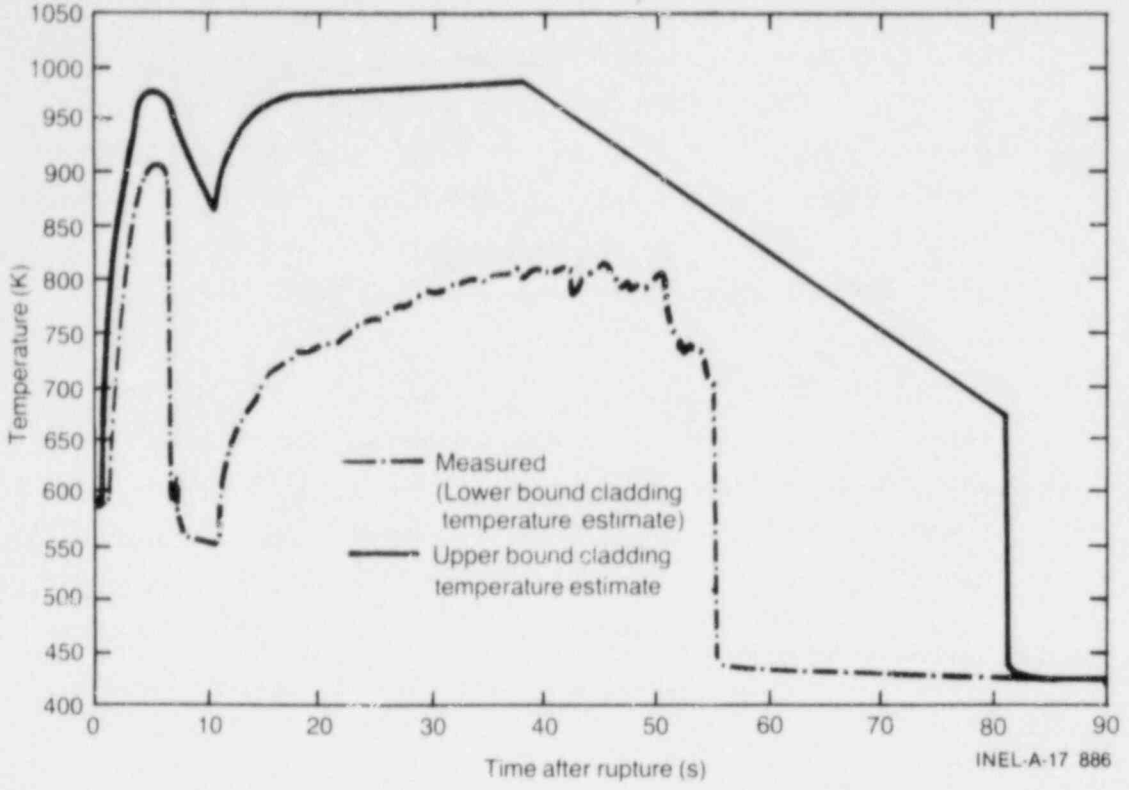

Figure A-15. Estimated upper bound cladding temperature data for LOFT LOCE L2-3 based on assumed maximum perturbation influences of LOFT surface thermocouples.

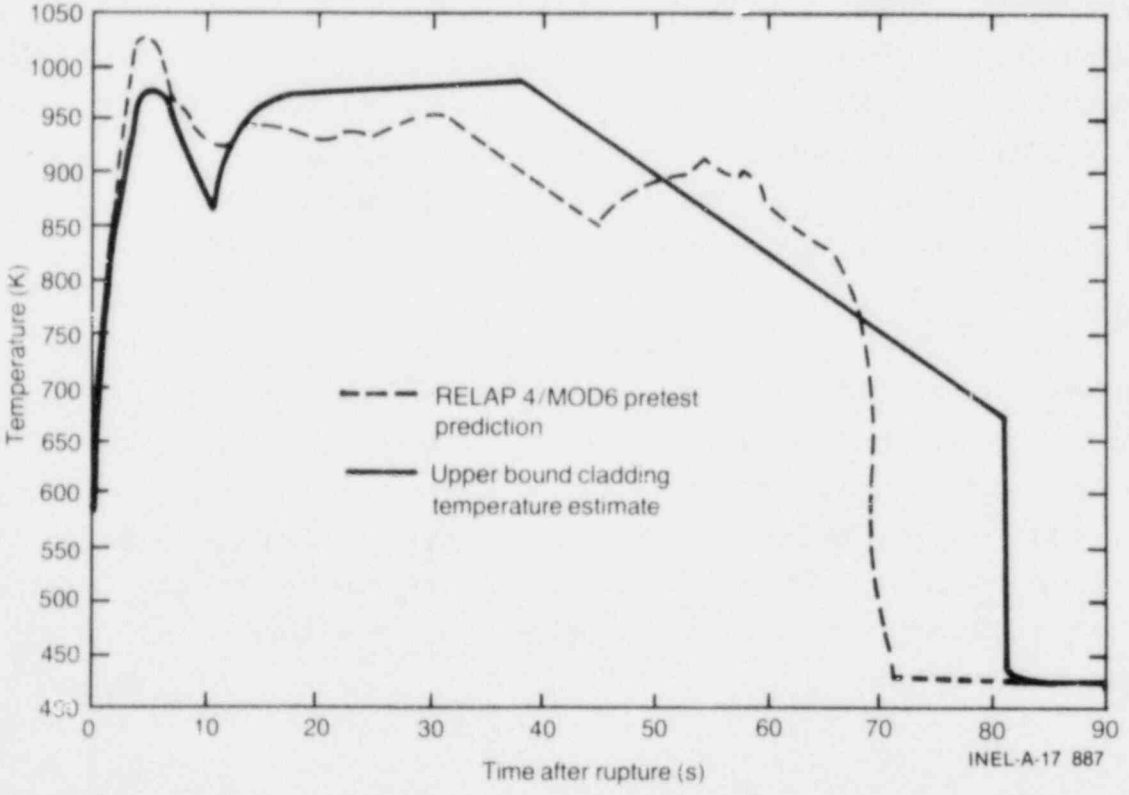

Figure A-16. Comparison of upper bound cladding temperatures during LOFT LOCE L2-3 and pretest predicted RELAP4/MOD6 cladding temperature (best estimate code version).

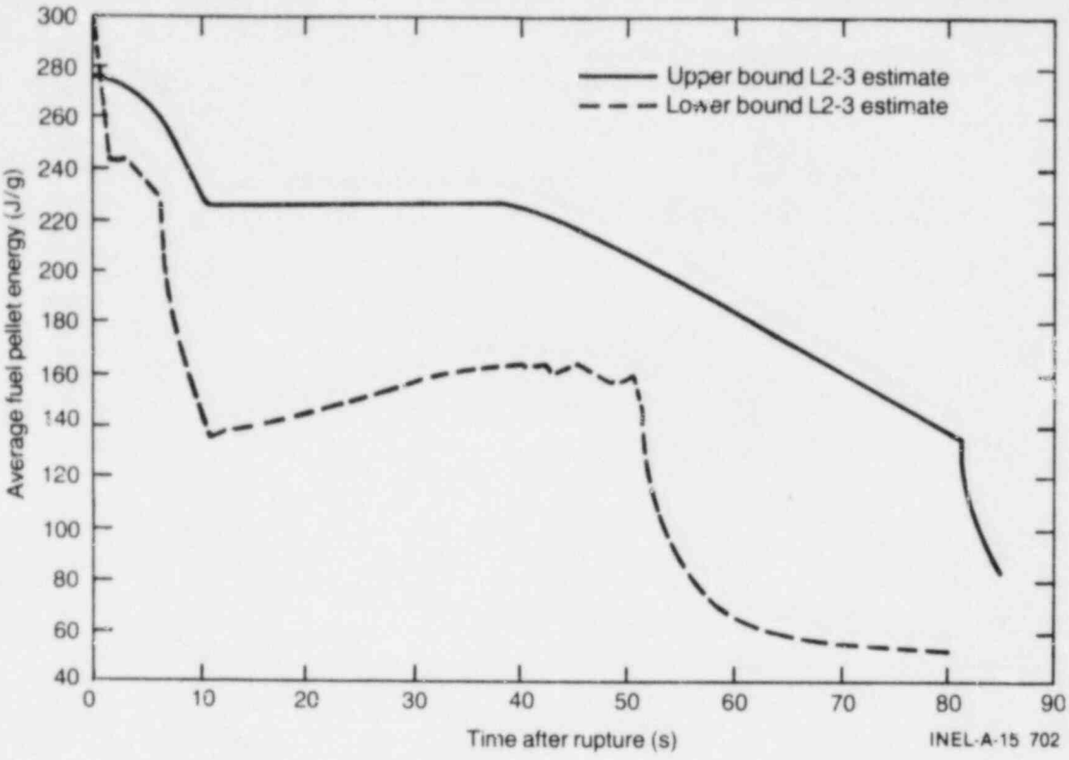

Figure A-17. Fuel rod stored energy envelope for LOFT LOCE L2-3.

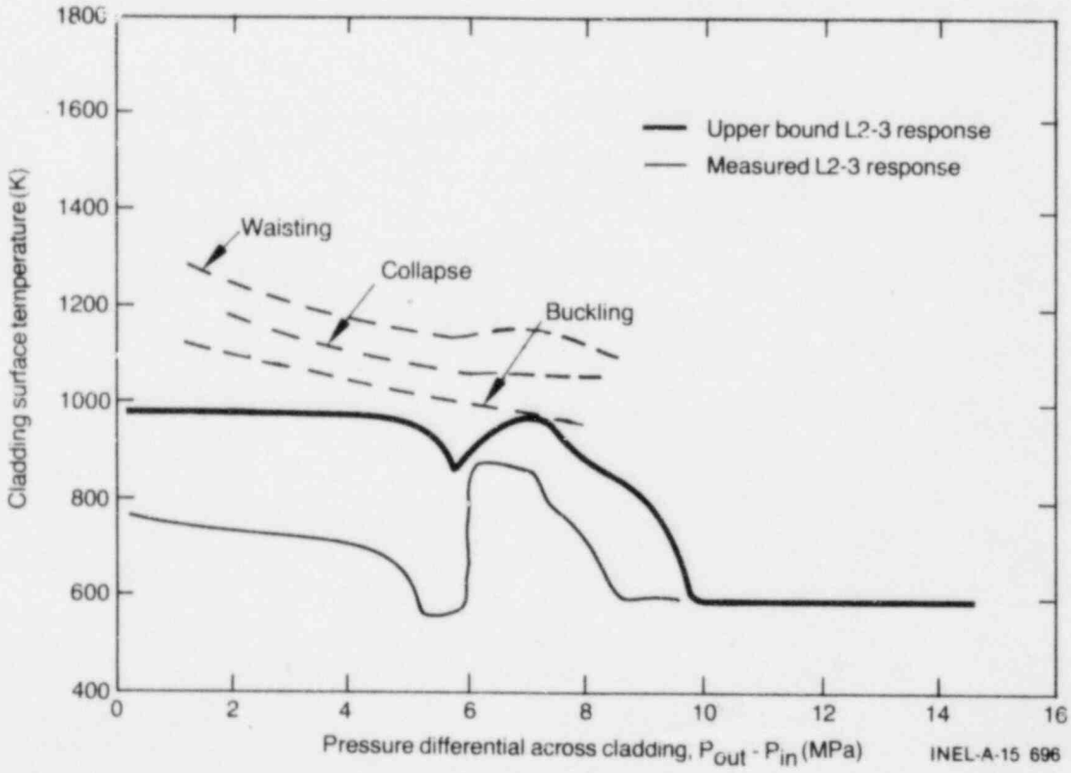

Figure A-18. Cladding deformation expected for upper bound fuel rod response during LOFT LOCE L2-3.

Resolution of the true cladding temperature response is likely to require replication of either, or both, LOCEs L2-2 and L2-3 with instruments installed specifically designed to measure the cladding temperature during rapid cooling transients. An improved cladding temperature measurement is being developed for future LOFT experiments and will consist of a small thermocouple embedded on the cladding inside surface as shown in Figures A-19 and A-20.

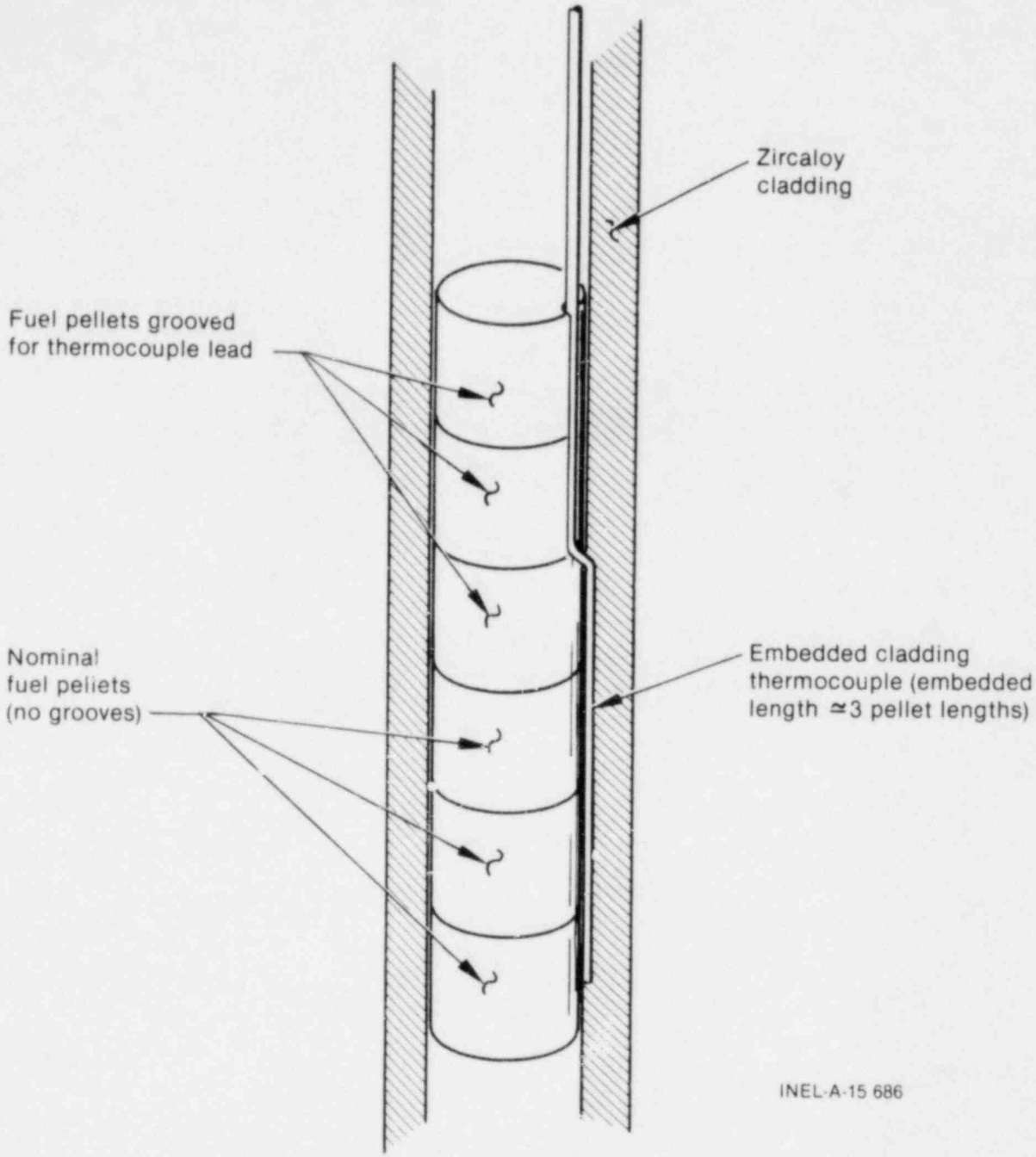

Figure A-19. Proposed geometry of LOFT internal, embedded cladding thermocouple.

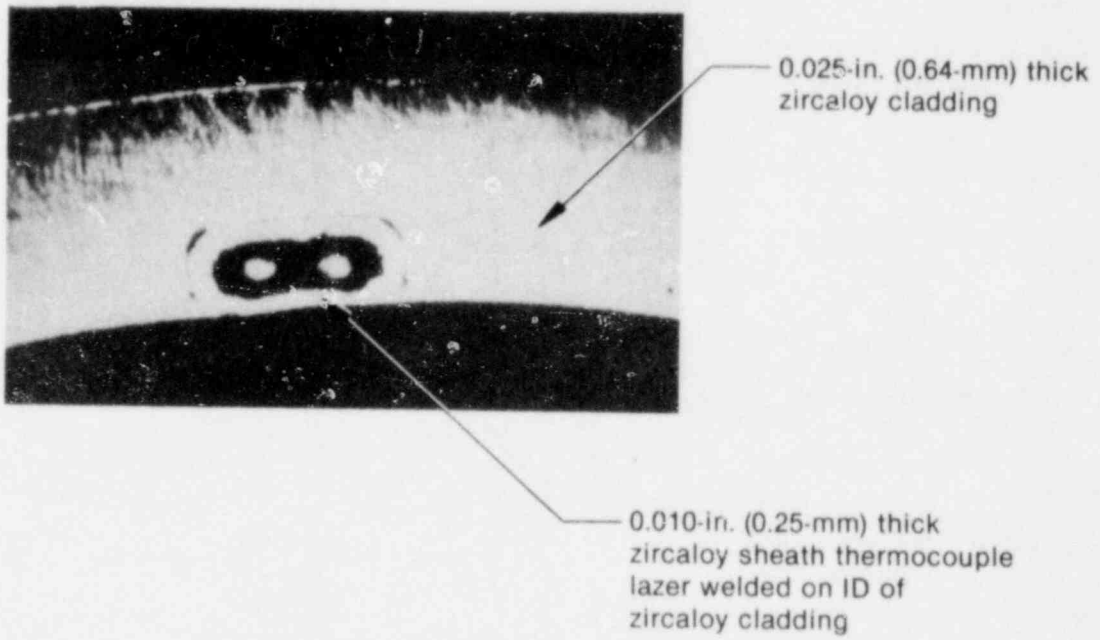

Figure A-20. Cross-sectional view of 0.25-mm thick embedded thermocouple proposed for LOFT fuel rods.

3. REFERENCES

A-1. M. McCormick-Barger, Experiment Data Report for LOFT Power Ascension Test L2-2, NUREG/CR-0492, TREE-1322, February 1979.

A-2. P. G. Prassinos et al., Experiment Data Report for LOFT Power Ascension Experiment L2-3, NUREG/CR-0792, TREE-1326, July 1979.

A-3. E. L. Tolman and E. W. Coryell, Review of LOFT Cladding Temperature Response for L2-2 and L2-3: Recommendations for Improved LOFT Fuel Rod Measurements, EGG-LOFT-5244, October 1980.

A-4. R. C. Gottula, LOFT Transient (Blowdown) Critical Heat Flux Tests, TREE-NUREG-1240, April 1978.

A-5. A. M. Eaton et al., LOFT Cladding Surface Thermocouple Calibration Test Results for Zircaloy Clad Rod IH-802902, EG&G Idaho, Inc., Internal Report LTR 141-88, February 1979.

A-6. T. R. Yackle, M. Waterman, P. MacDonald, Loss-of-Coolant Accident Test Series - Test TC-1 Test Results Report, EGG-TFBP-5068, May 1980.

A-7. R. C. Gottula and J. A. Good, The Effect of Cladding Surface Thermocouples on the Quench Behavior of an Electrical Heater Rod, EG&G Idaho, Inc., Internal Report, LO-00-80-115, March 5, 1980.

A-8. C. S. Olsen, Zircaloy Cladding Collapse Under Off-Normal Temperature and Pressure Conditions, TREE-NUREG-1239, April 1978.

BLANK

APPENDIX B
LIMITATIONS OF ELECTRIC HEATER RODS TO SIMULATE NUCLEAR ROD QUENCH BEHAVIOR

BLANK

APPENDIX B
LIMITATIONS OF ELECTRIC HEATER RODS TO SIMULATE NUCLEAR ROD QUENCH BEHAVIOR

Section 3.2 in the main body of this report includes a discussion of the cooldown and quenching characteristics of a solid-type heater rod of the Semiscale design under high-pressure and rapid flooding conditions during experiments in the Loss-of-Fluid Test (LOFT) Test Support Facility (LTSF). Section 3.2 also discusses data from the Power Burst Facility (PBF) experiments that illustrate the short-term cooling characteristics of a nuclear fuel rod under transient hydraulic conditions intended to simulate the initial quenches observed in LOFT Loss-of-Coolant Experiments (LOCEs) L2-2 and L2-3. Comparison of the PBF and LTSF data indicates that a nuclear rod tends to cool down and quench more rapidly than a solid-type heater rod subjected to similar initial thermal-hydraulic boundary conditions. This observation is consistent with data from the LOFT large break nuclear LOCEs L2-2 and L2-3 (see Appendix A).

To better understand the reasons for the difference in responses of the electric and nuclear rods during rapid flooding events, a series of RELAP4/MOD6 computer code[B-1] calculations were undertaken. These computer code calculations centered on evaluating the response of a Semiscale heater rod and a nuclear fuel rod under typical LTSF test conditions. The principal results of this work are shown in Figure B-1.

In Figure B-1, a best estimate RELAP4/MOD6 calculation of electric rod temperature response is compared with the measured LTSF electric rod data. The difference between the calculated and measured electric rod quench characteristics is thought to be attributable to inaccurate modeling of the transition boiling regime by the code. Figure B-1 also illustrates the results of substituting a nuclear rod for a solid, internally heated electric rod and performing the same RELAP4/MOD6 calculation. Clearly, the calculations show the nuclear rod cladding temperature to cool more rapidly than for the electric rod. This discrepancy in rod behavior cannot be accounted for by making realistic changes in the electric rod input power.

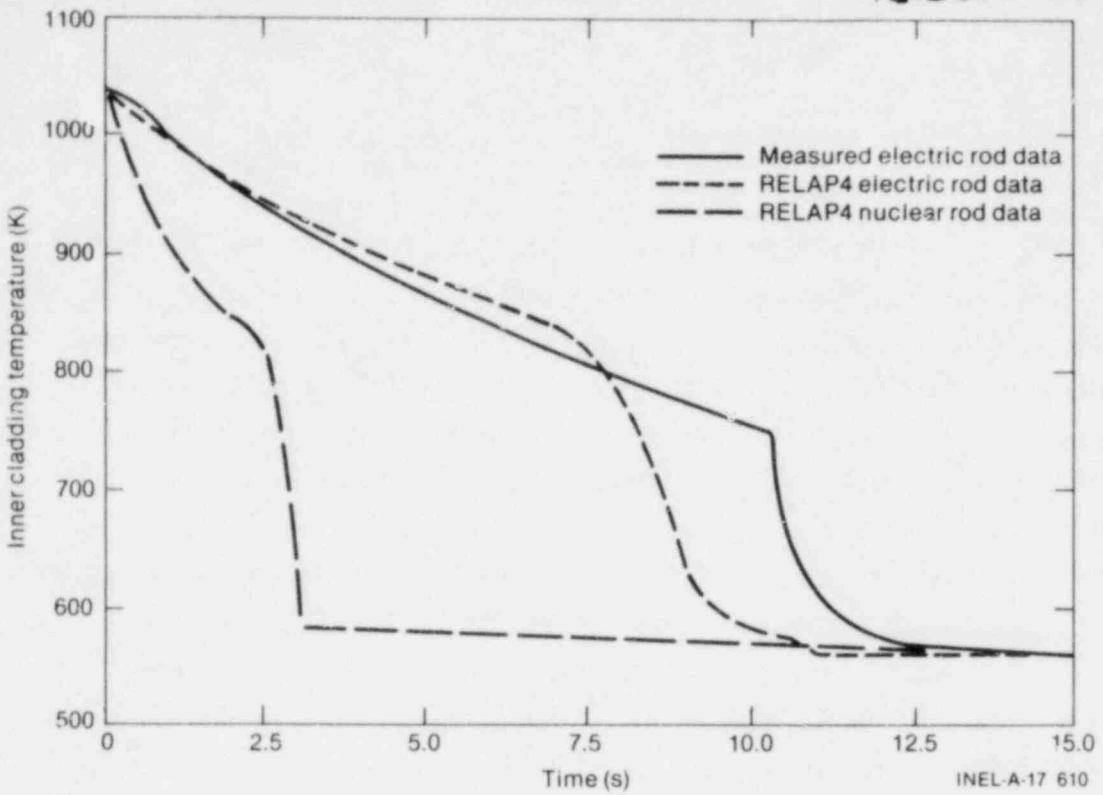

Figure B-1. Calculation results showing the capability of RELAP4/MOD6 to predict LTSF electric rod quench data and the difference between electric and nuclear rod thermal response for the LTSF hydraulic conditions.

An analysis was undertaken to determine the electric rod power required to duplicate the calculated nuclear rod response shown in Figure B-1. Figures B-2 and B-3 show the nuclear rod cladding temperature and surface heat flux with an expanded time base. These two boundary conditions must be maintained by the heater rod for adequate thermal simulation of the nuclear rod. In order to simulate the nuclear rod cladding temperature and heat fluxes, the electric rod power must be specified as shown in Figure B-4, which shows large negative powers are required to simulate the cladding quench. Obviously, negative powers cannot be achieved; therefore, the nuclear rod quench simulation cannot be achieved.

As a further example, Figure B-5 shows the calculated local electric rod power required to reproduce the measured surface cladding temperature and corresponding surface heat flux for a LOFT nuclear rod during LOCE L2-3 as represented by Figures B-6 and B-7, respectively. Again, as shown in Figure B-5, large negative powers are needed for the heater rod to reproduce

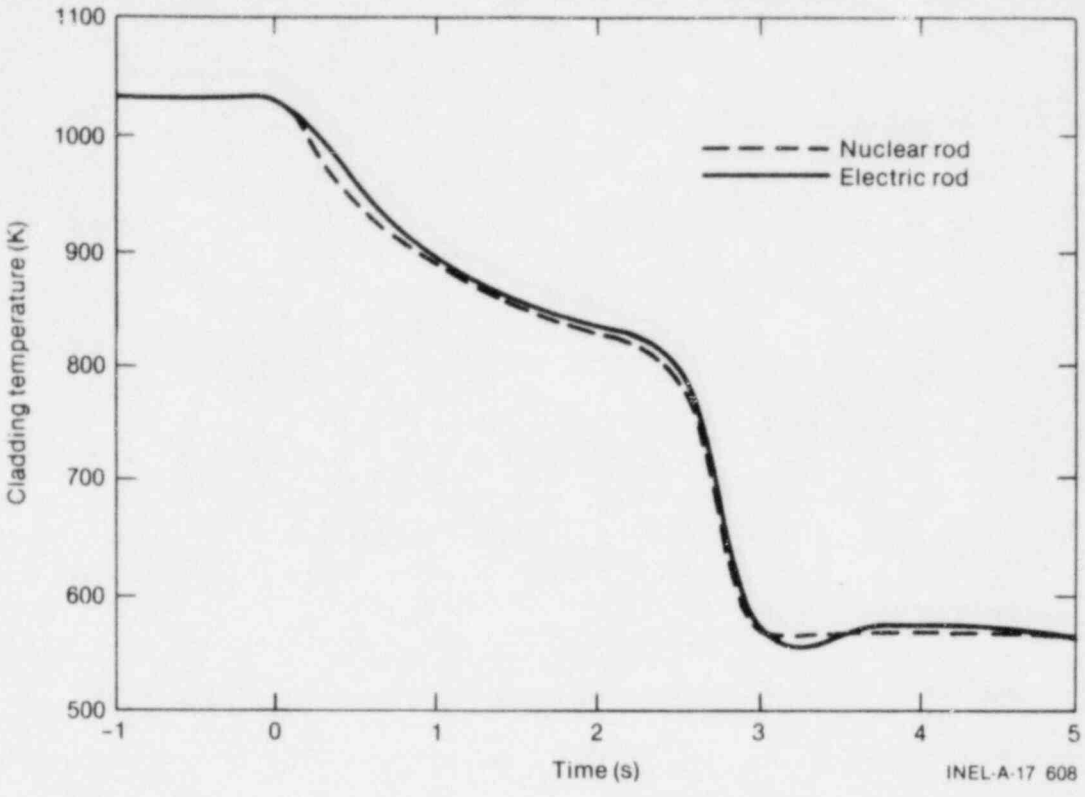

Figure B-2. Comparison of calculated electric and nuclear rod cladding temperatures using the electric rod power specified in Figure B-4.

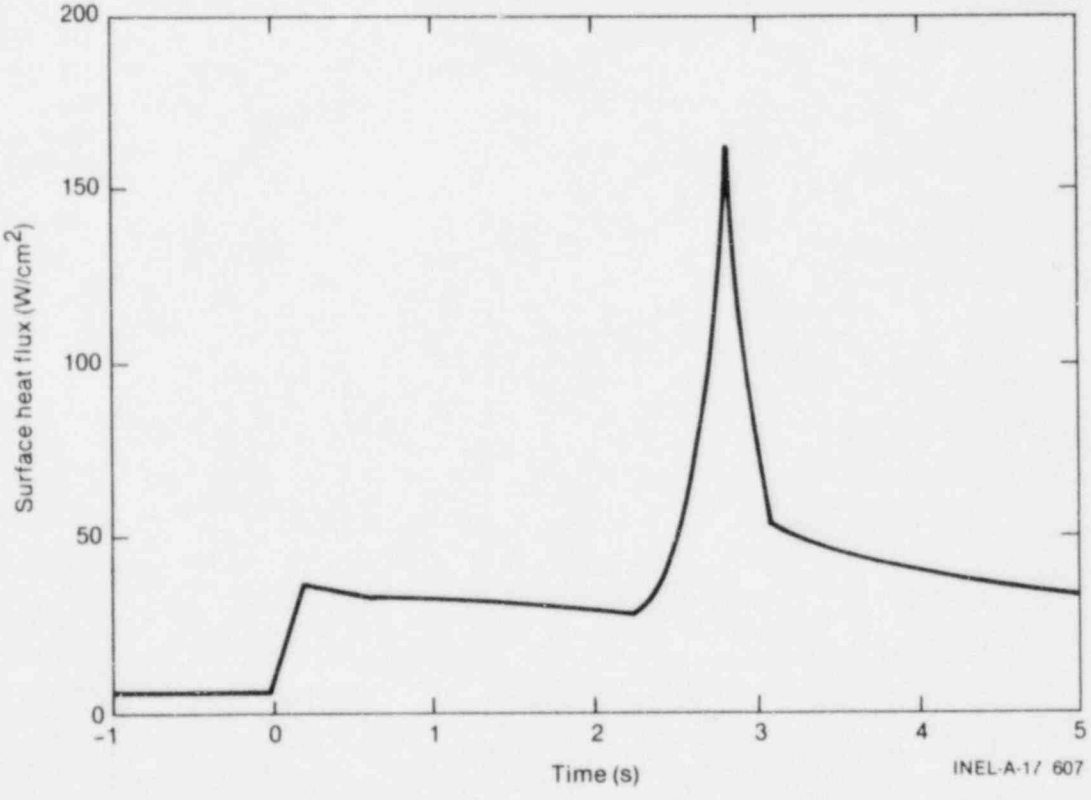

Figure B-3. Comparison of calculated nuclear and electric rod surface heat fluxes using the electric rod power specified in Figure B-4.

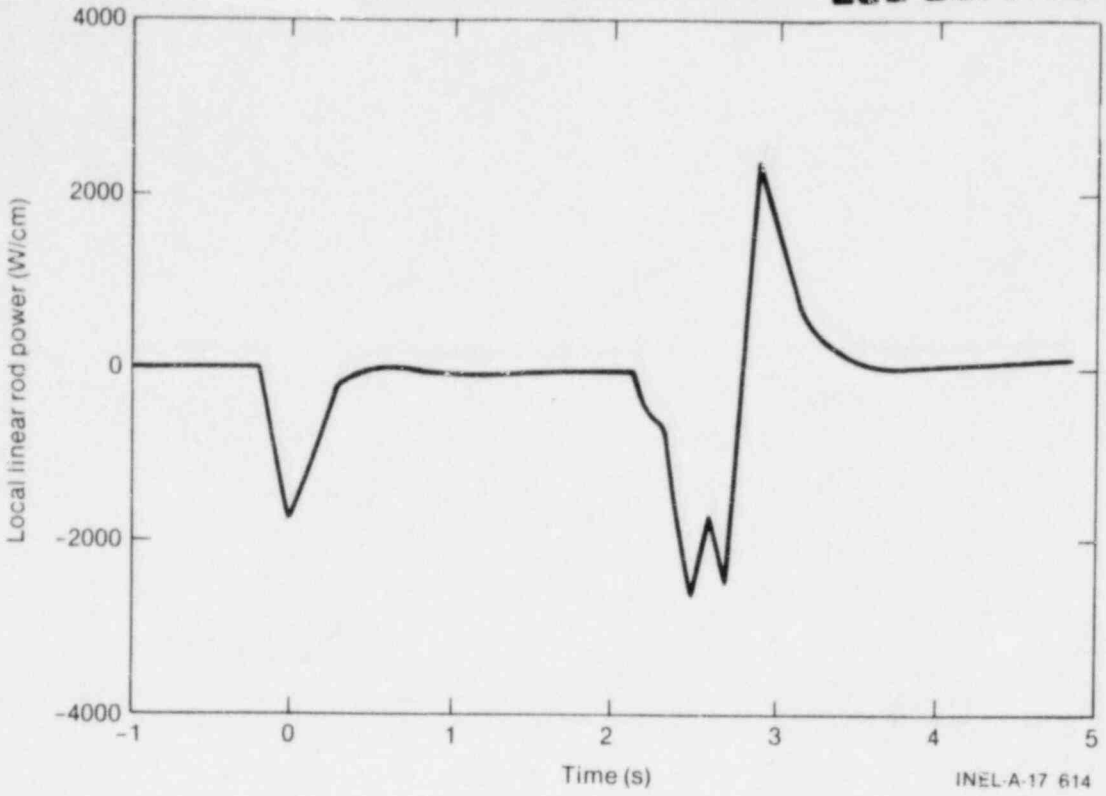

Figure B-4. Semiscale power necessary to achieve the nuclear rod cladding temperature and surface heat flux shown in Figures B-2 and B-3.

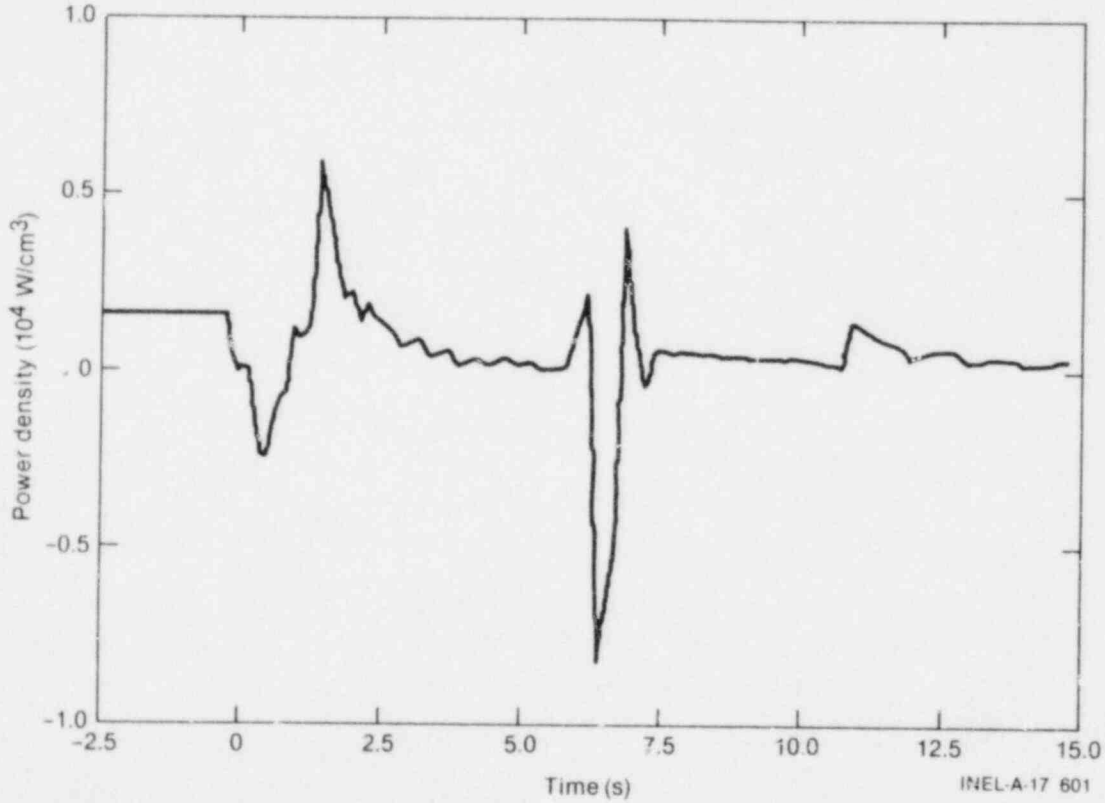

Figure B-5. Electric rod power needed to reproduce the LOFT LOCE L2-3 hot rod cladding temperature and heat flux.

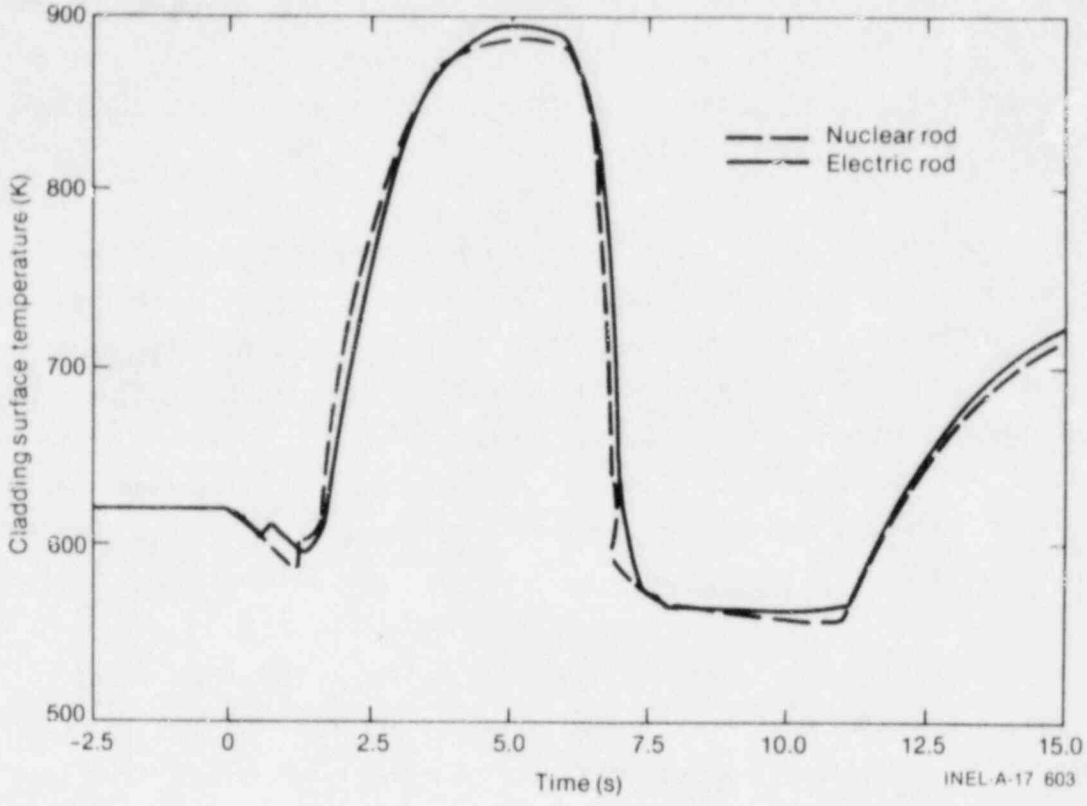

Figure B-6. Comparison of LOFT LOCE L2-3 hot rod and Semiscale electric rod temperature responses using the electric rod power specified in Figure B-5.

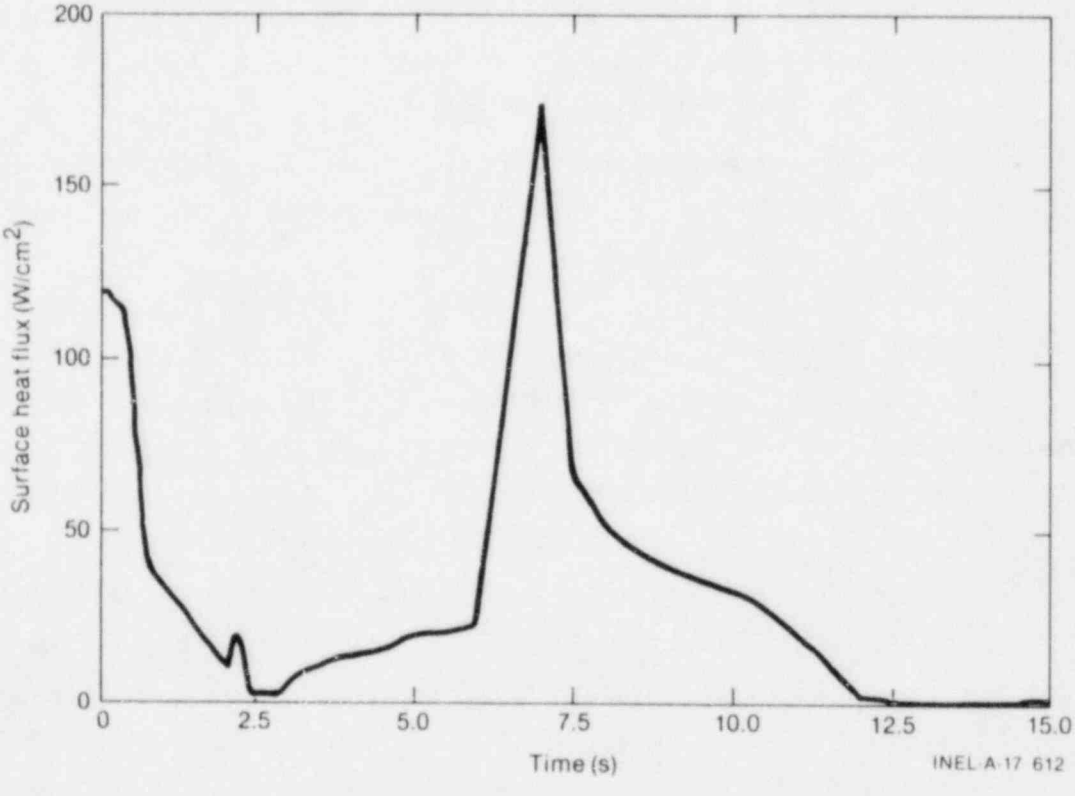

Figure B-7. Hot rod cladding heat flux for LOFT LOCE L2-3.

the nuclear rod response. Most prominent in Figure B-5 is the large negative power transient that begins slightly before and continues through the rapid nuclear rod cladding quench at 6.5 s.

The requirement of unrealistic negative powers in the ideal electric rod powering function indicates that the observed differences in the electric and nuclear rod responses, as shown in Figure B-1, are the result of inherent limitations in the electric rod design. Supporting analysis has shown that differences in the thermal conductivity of the boron nitride insulator and the UO_2 fuel pellet and the absence of a thermal-gas gap in the electric rod are the primary factors that cannot be simulated by the solid heater rod.

Because of the low thermal conductivity of UO_2, the presence of cracks in the fuel, and the existence of a gap between the fuel and the cladding, the cladding of a nuclear rod is thermally decoupled from the stored energy and heat generation within the UO_2 pellet during rapidly cooling transients. This is illustrated in Figure B-8 by comparing the steady state nuclear and electric rod radial temperature profiles at rod powers of 39 kW/m. The steepness of the nuclear rod temperature profile indicates a low coupling path between the cladding and the fuel. In contrast, the relatively flat distribution in the electric rod shows a high degree of coupling between the inner heat source and the cladding surface via the relatively low thermal resistance path provided by the boron nitride insulation.

During a rapid cooling transient such as the LOFT LOCEs L2-2 and L2-3 quenches, the energy in the fuel is decoupled from the cladding by the high thermal resistance of the UO_2 and the pellet-cladding gap. This decoupling limits the energy flow into the cladding as it begins to cool, and the cladding temperature can be effectively cooled by removing only the energy in the cladding. In contrast, for the electric rod, the rod internal energy is delivered very rapidly to the cladding as it begins to cool, and in order to cool the rod down so the coolant can rewet the rod, a large portion of the total rod energy must be removed.

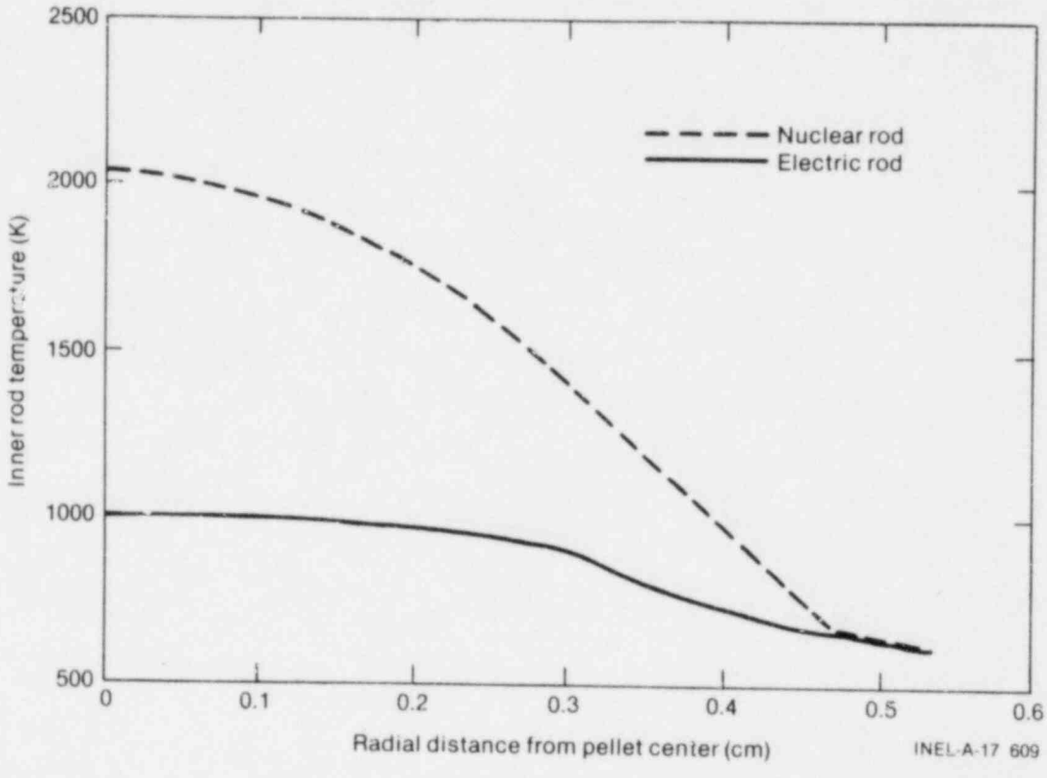

Figure B-8. Comparison of Semiscale electric and LOFT nuclear rod steady state radial temperatures for rod powers of 39.4 kW/m (12 kW/ft).

REFERENCE

B-1. EG&G Idaho, Inc., RELAP4/MOD6 - A Computer Program for Transient Thermal-Hydraulic Analysis of Nuclear Reactors and Related Systems - User's Manual, CDAP-TR-003, January 1978.

APPENDIX C
COMPARISON OF SYSTEM RESPONSE FOR LOFT EXPERIMENT L2-3 AND SEMISCALE TEST S-06-3

BLANK

APPENDIX C
COMPARISON OF SYSTEM RESPONSE FOR LOFT EXPERIMENT L2-3 AND SEMISCALE TEST S-06-3

One of the several nuclear test series designed for performance in the Loss-of-Fluid Test (LOFT) facility was Test Series L2.[C-1] These experiments were designed to provide integral system data related to the full-size double-ended cold leg break at ascending power levels. Prior to performance of the Test Series L2 experiments, a series of companion experiments, defined as Test Series 6, was performed in the Semiscale Mod-1 facility[C-2] as a counterpart to the LOFT experiments. One of the primary purposes of the Semiscale experiments was to assist in the planning of the Test Series L2 experiments, which were the first nuclear experiments in LOFT.

Both LOFT and Semiscale Mod-1 are scaled models of a pressurized water reactor (PWR) power plant with overall volumetric scaling ratios of approximately 1/40 and 1/1500, respectively. The Semiscale-to-LOFT volumetric scaling ratio is 0.0285. Both facilities are equipped with a pressure vessel; an intact loop with pump, steam generator, and a pressurizer; and a broken loop with a simulated pump and a simulated steam generator. The intact loop in each facility is essentially three times the size of the broken loop, thus simulating three intact loops and one broken loop in a four-loop PWR. A significant difference between the test facilities is that electrically heated rods are used in Semiscale.

To date, Loss-of-Coolant Experiments (LOCEs) L2-2 and L2-3 from LOFT Test Series L2 have been performed. These two experiments were similar in that both were initiated from a system temperature and pressure typical of a PWR operating at comparable peak power densities. LOCE L2-3, however, was initiated from a greater peak linear power, 39.47 kW/m versus 26.35 kW/m for LOCE L2-2, and resulted in higher cladding temperatures than experienced for LOCE L2-2. Therefore, LOFT LOCE L2-3[C-3] and its counterpart Semiscale test, Test S-06-3,[C-4] were chosen for this comparison. The initial conditions for these two experiments are provided in Table C-1.

Differences in nuclear and electrically heated rod design and the resulting differences in the thermal response characteristics are summarized

TABLE C-1. INITIAL CONDITIONS FOR LOFT EXPERIMENT L2-3 AND ITS COUNTERPART SEMISCALE TEST S-06-3

Parameter	LOFT	Semiscale
System pressure (MPa)	15.06	15.77
Broken loop hot leg temperature (K)	565.5	591.0
Broken loop cold leg temperature (K)	554.3	562.0
Saturation temperature (K)	615.6	619.3
Intact loop hot leg temperature (K)	592.9	597.1
Intact loop cold leg temperature (K)	560.7	563.0
System volume (m^3)	7.896	0.221
Intact loop mass flow (kg/s)	200.0	5.0

in Section 3.1 in the main body of this report and are discussed in detail in Appendix B. It is noted from Appendix B that the Semiscale heater rod cannot duplicate the rapid quench behavior of a nuclear fuel rod. However, before attributing the differences between LOFT and Semiscale response to differences in rod thermal behavior, the hydraulic response of the two systems must be shown to be identical. This analysis includes comparisons of rod cladding temperatures, core coolant mass flows, system pressure and temperature responses, and coolant mass flow in the intact and broken loops.

1. ROD CLADDING TEMPERATURE

The cladding surface temperatures measured at the hottest rod during the LOFT and Semiscale experiments are compared in Figure C-1. These data clearly show that the thermal response for the nuclear and electric rods were not the same. The most significant difference is that the LOFT nuclear rod experienced a large and rapid reduction in cladding temperature (quench) at about 6.5 s, while the electrically heated rod did not. Causes for this different response can be hypothesized as:

1. Different rod design characteristics, for example, different materials and geometry, resulting in a different thermal response

2. Different hydraulic responses between the two systems such that the nuclear rod received more cooling than the electric rod

3. A combination of the above.

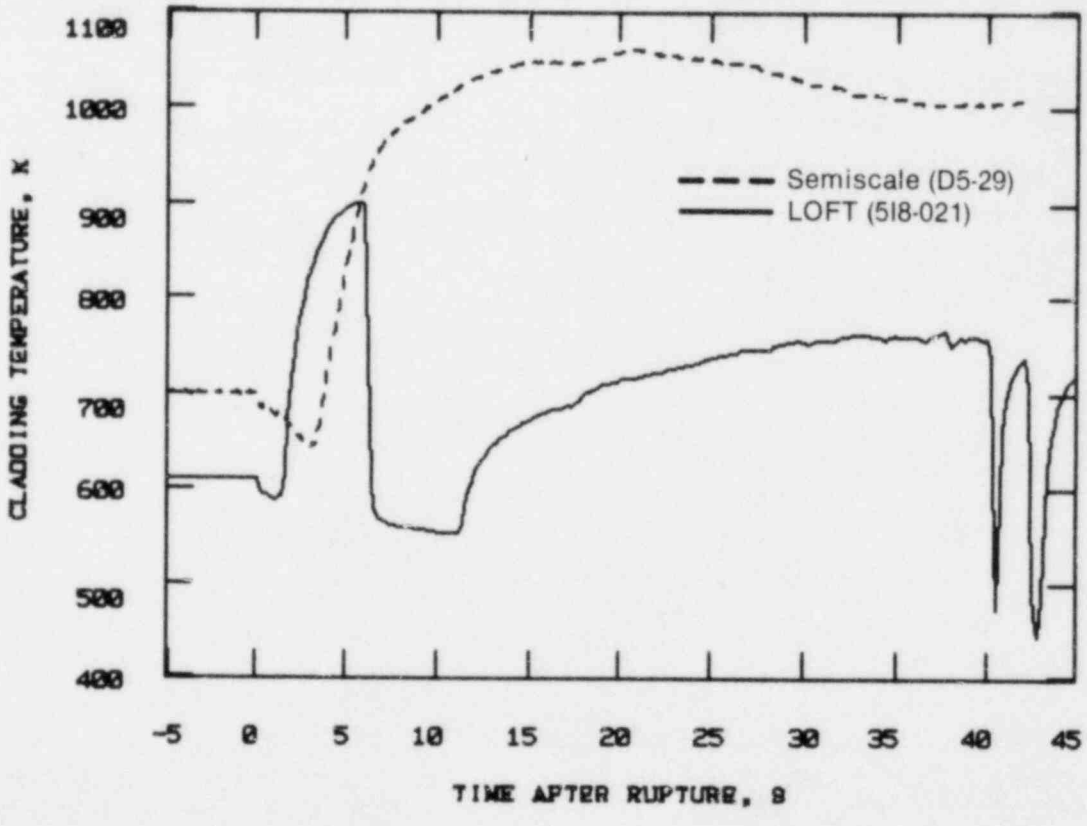

Figure C-1. Cladding temperature measured at core hot spot for LOFT LOCE L2-3 and Semiscale counterpart Test S-06-3.

Since the major differences in cladding temperature between LOFT and Semiscale occurred during the blowdown phase (0 to 15 s after blowdown initiation), the hydraulic comparisons are limited to that part of the experiments

The LOFT cladding temperature response in Figure C-1 indicates that a significant mass of coolant passed through the LOFT core, causing the quench (see Appendix A for details of the LOFT core measurement). A review of the LOFT cladding temperature data in Figure C-2 shows that the sequence of the cladding quench occurred from the bottom to the top of the core, thus indicating the coolant flow causing the quench entered the core from the bottom. A similar review of Semiscale temperature data in Figure C-3 shows no evidence of increased cooling occurring during the transient at the time of the LOFT quench. Therefore, the same relative core flows may not have occurred in Semiscale that occurred in LOFT. The Semiscale coolant flow data[a], shown in Figure C-4, indicate a small positive coolant flow at the inlet to the Semiscale core in the 6.5- to 9-s time interval, which is coincident with the LOFT quench. The elevation of the lowest temperature measurement in Semiscale is about 23 cm above the bottom of the active core, and as shown in Figure C-3, no significant rod cooling was experienced during the 6.5- to 9-s time interval. It is concluded, therefore, that either the coolant flow was not sufficient to cause significant cooling or its penetration into the core was less than 23 cm.

---

a. Mass flow data considered here are actually a composite of momentum flux and density data which may be found in the respective experiment data reports.[C-3,C-4] These data contain no error analysis, and no modifications or other corrections have been made.

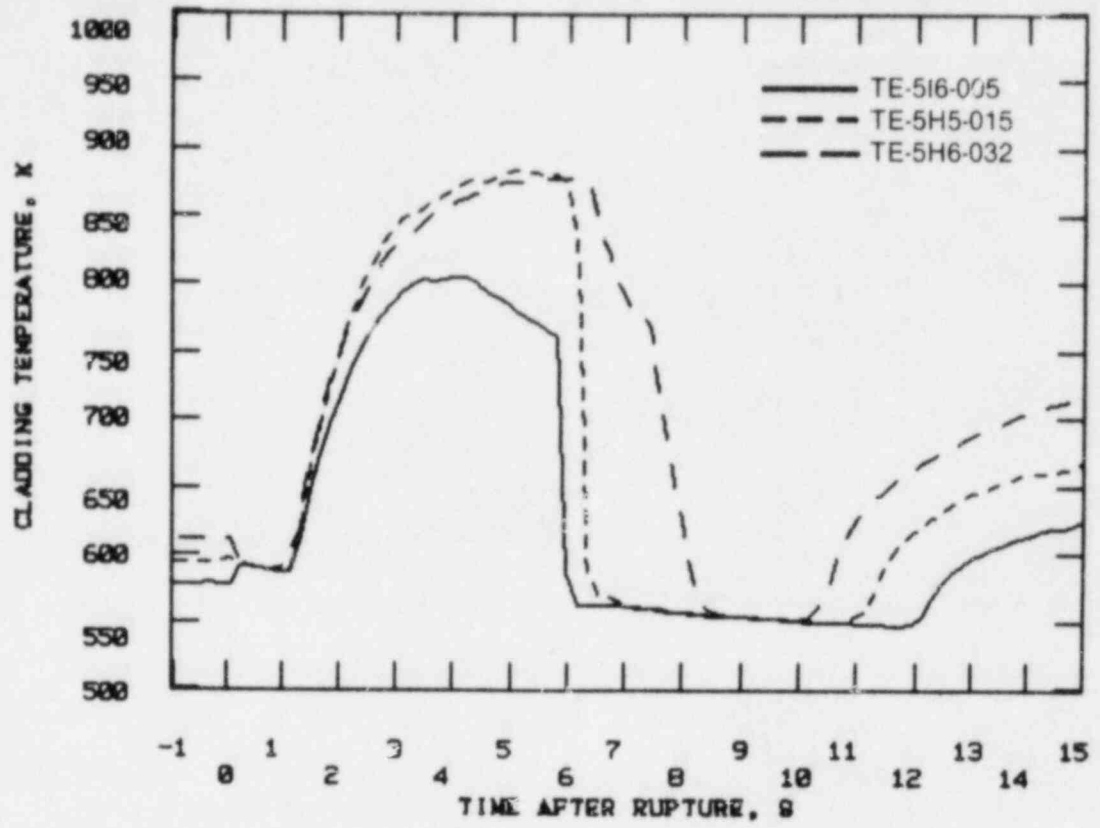

Figure C-2. Cladding temperatures for LOFT LOCE L2-3 showing quench front propagation from bottom to top of core.

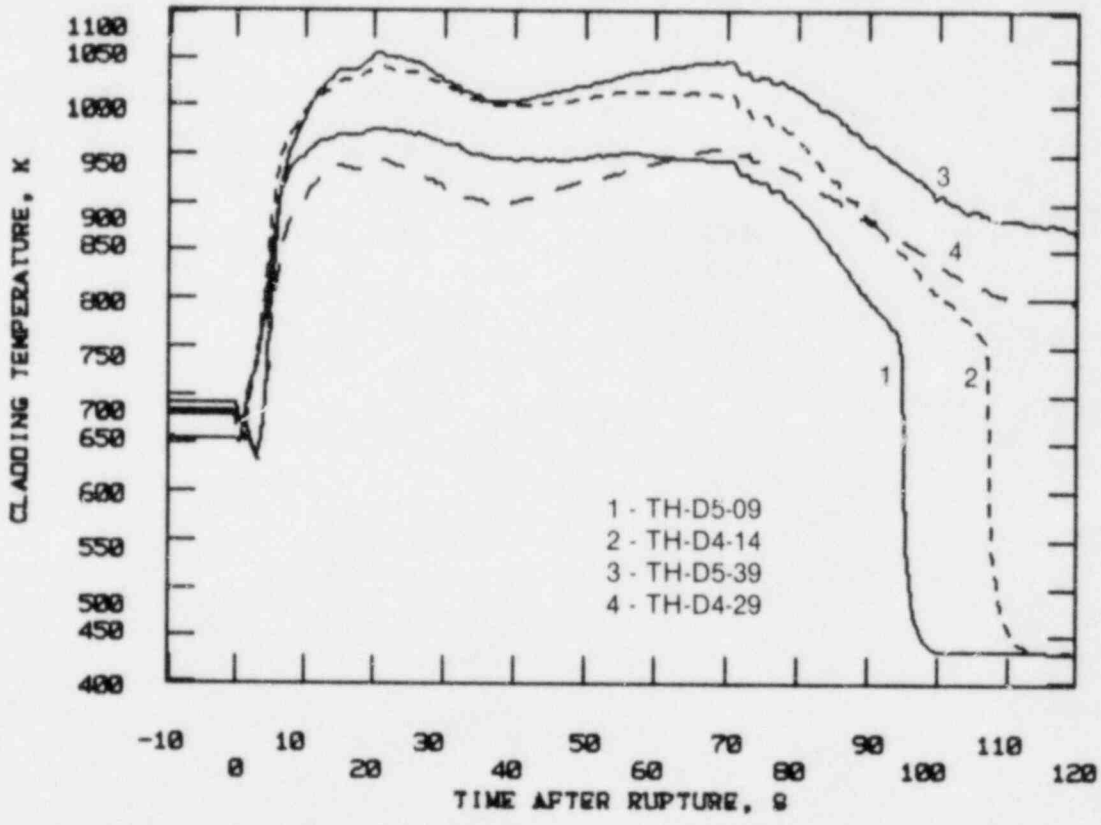

Figure C-3. Cladding temperatures for Semiscale Test S-06-3 showing no early quench.

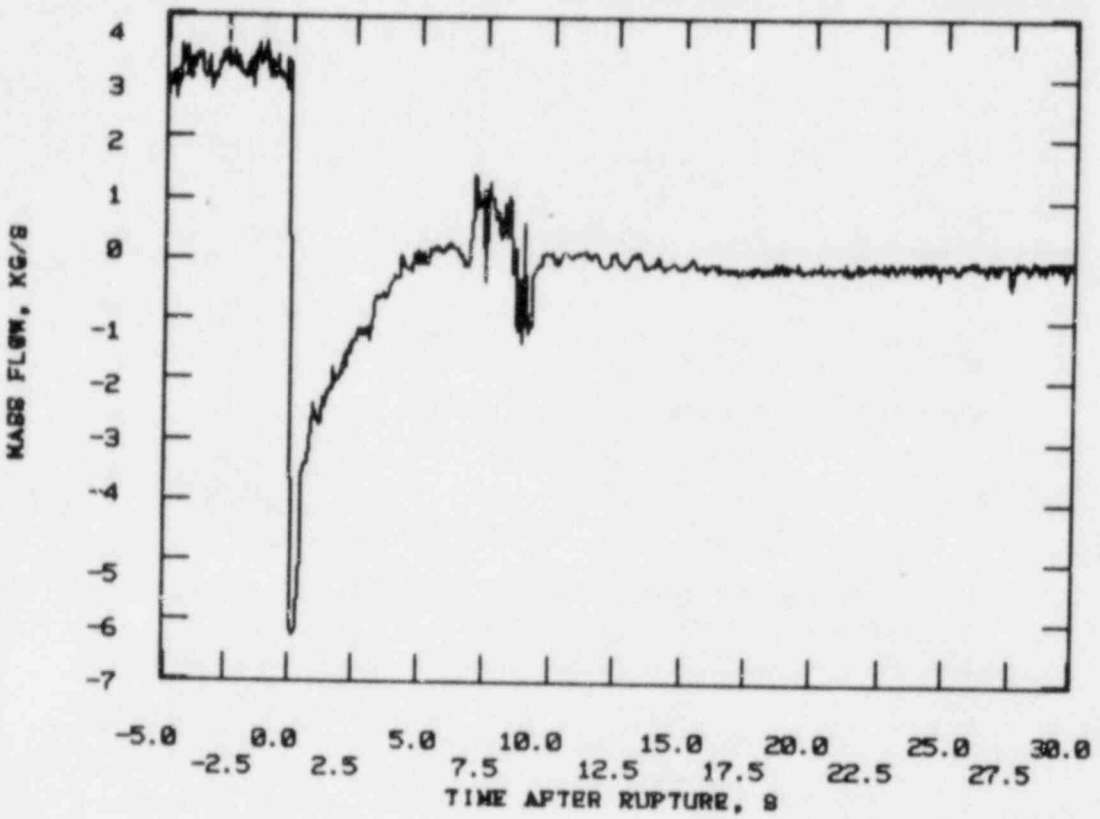

Figure C-4. Mass flow measured at inlet to Semiscale core during Test S-06-3.

2. CORE COOLANT MASS FLOW

Measurements of mass flow at the inlet to the LOFT core are not available; consequently, direct comparisons cannot be made. Posttest analyses[C-5] for LOFT LOCE L2-3 using the RELAP4/MOD6 computer program,[C-6] however, were in good agreement with experiment results. For example, the data in Figure C-5 show the calculated and measured mass flow through the hot leg of the broken loop have essentially the same response. In particular, it is noted that the calculated and measured data show an increase in the flow at about 3 s. Assuming that the core flow calculated for LOFT is representative of the actual flow, it is compared with the measured Semiscale core flow in Figure C-6. This data comparison indicates that positive core flow was reestablished earlier in LOFT, reached a slightly greater value, and extended over a longer time interval than the corresponding flow in Semiscale.

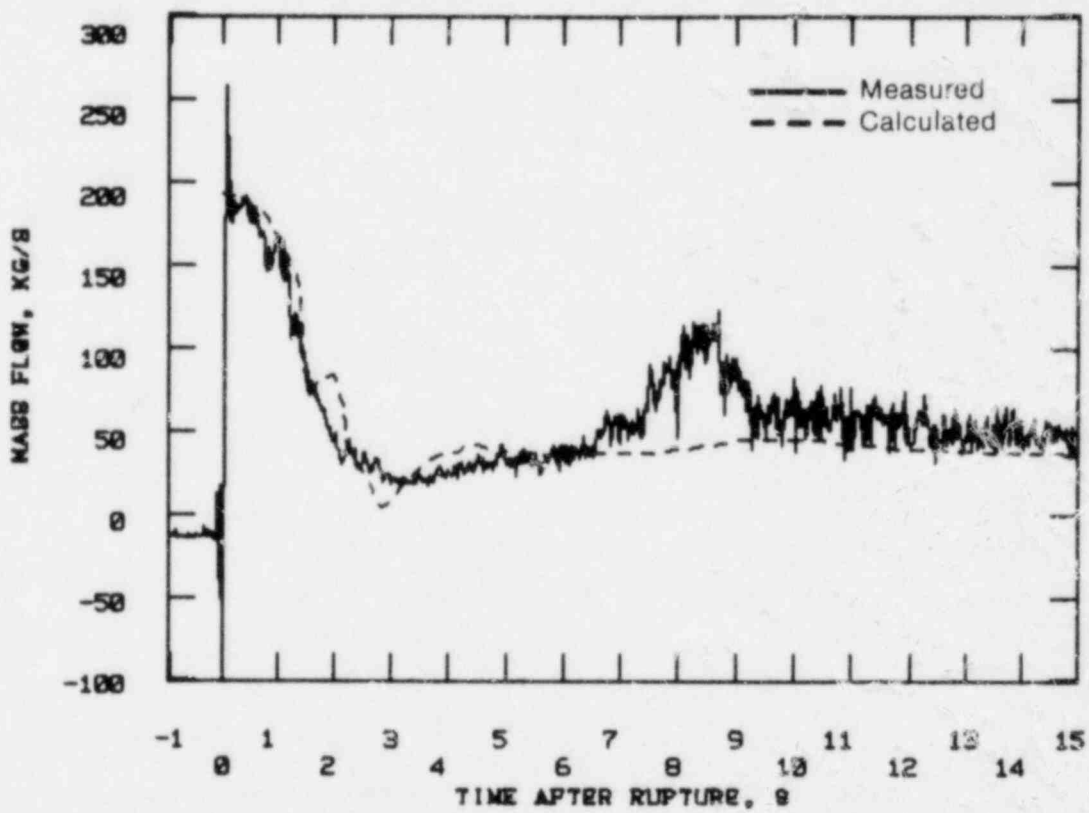

Figure C-5. Comparison of calculated and measured mass flows through the broken loop hot leg for LOFT LOCE L2-3.

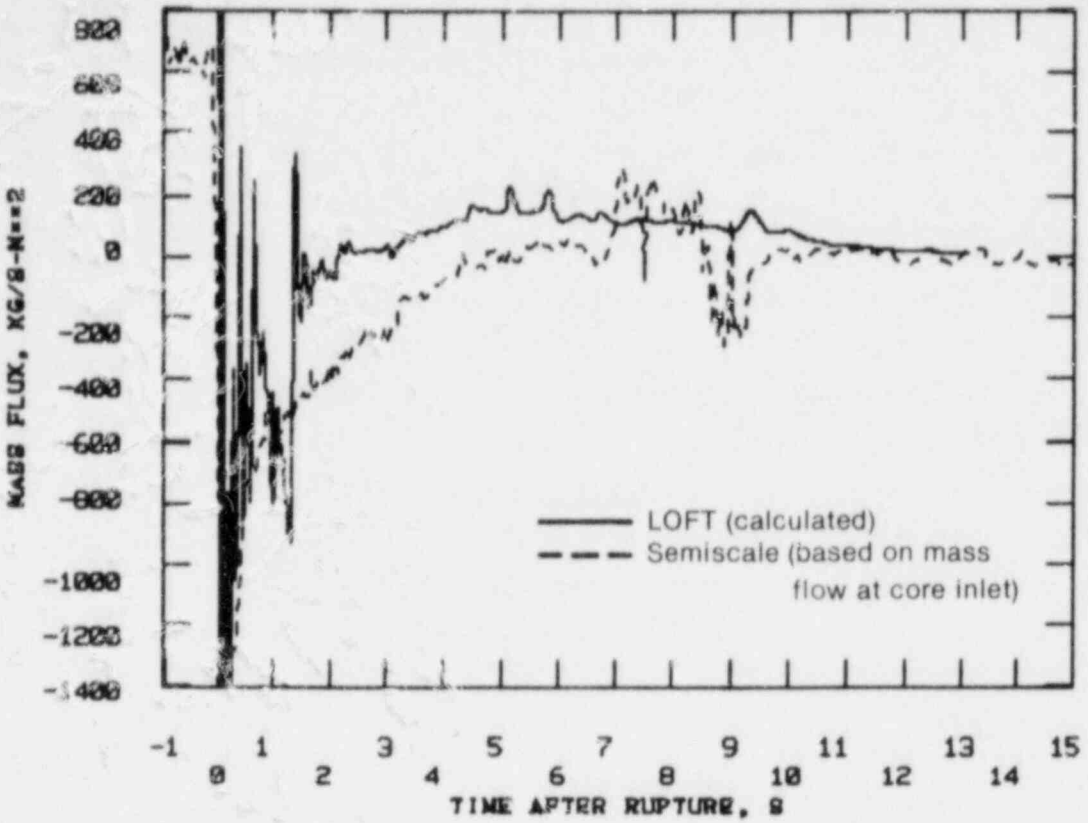

Figure C-6. Comparison of mass fluxes near core inlet as calculated for LOFT and measured for Semiscale (Semiscale data based on mass flow measured at core inlet)

Another indication of the relative mass flow through the respective cores can be obtained by reviewing the hot leg mass flow. These mass flow data are shown in Figures C-7 and C-8 for the LOFT and Semiscale experiments, respectively. The flow through the hot leg of the broken loop in LOCE L2-3 is observed to reach a minimum at about 3 s, then to continually increase until about 8.5 s. The flow through the hot leg of the intact loop, however, remains positive, that is, also flowing out of the upper plenum, until approximatey 7 s. These relative hot leg mass flow rates, therefore, are indicative of a positive core flow during the 3- to 7-s interval. The corresponding data for Semiscale Test S-06-3 are shown in Figure C-8. Although the hot leg mass flow response for both systems are similar, the relative magnitudes are significantly different. For example, mass flow through the intact loop hot legs of both systems shows a large initial drop between 0 to 0.5 s, which recovers rapidly, and attains a maximum value at about 1.5 s, before declining again. The maximum recovered value for Semiscale, however, is almost 100% of the preblowdown value;

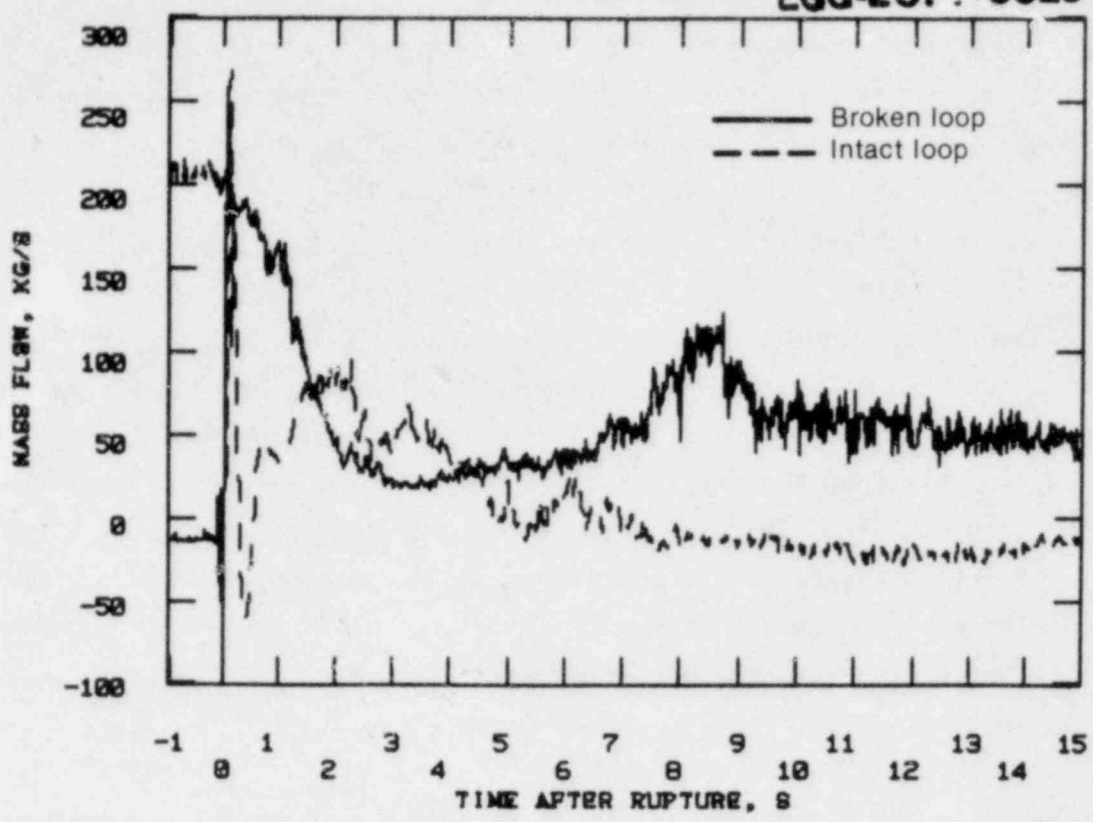

Figure C-7. Comparison of mass flows measured in LOFT intact and broken loop hot legs for LOCE L2-3.

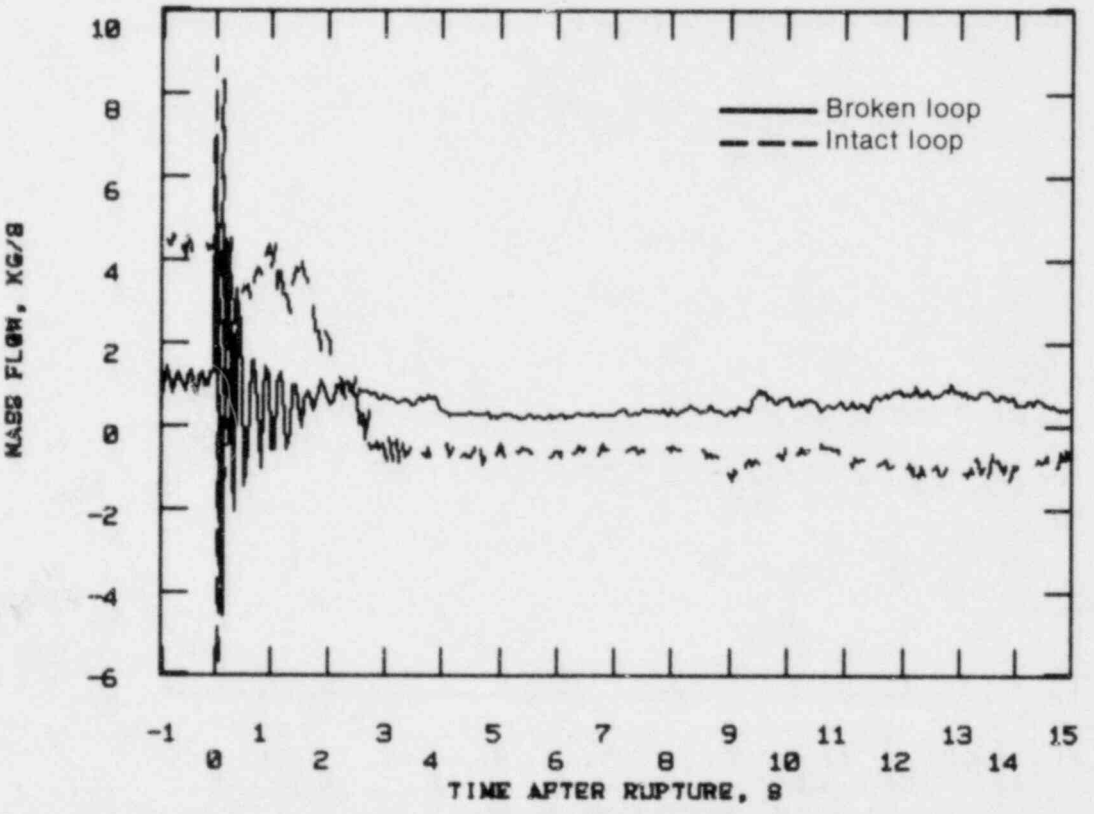

Figure C-8. Comparison of mass flows measured in Semiscale intact and broken loop hot legs for Test S-06-3.

whereas, the corresponding maximum is less than 50% for LOFT. In addition, the decline in the mass flow occurring after the recovered maximum is more rapid in Semiscale, resulting in flow stagnation and reversal at approximately 2.5 s. The flow reversal continues past 15 s, as shown in Figure C-8, and indicates coolant is entering the upper plenum directly from the intact loop. As indicated previously, the same phenomenon does not occur in LOFT until about 7 s. Thus after 2.5 s, a portion of the flow out of the Semiscale upper plenum through the broken loop hot leg may originate from the intact loop. Based on the data in Figure C-8, the mass flow into the upper plenum directly from the intact loop is greater than the flow out of the broken loop hot leg. This seems to indicate that after about 4 s, the Semiscale core flow may have been negative. The corresponding LOFT data in Figure C-7, however, show the mass flow out of the upper plenum for the first 15 s to be greater than the mass flow into the plenum directly from the intact loop and is, therefore, indicative of a positive core flow.

Based on the comparison of the Semiscale core flow with the corresponding data calculated for LOFT (Figure C-6) and the relative mass flow through the hot legs of both facilities (Figures C-7 and C-8), it is concluded that the relative flow through the LOFT core during the LOFT quench was probably significantly greater than that through the Semiscale core.

3. SYSTEM PRESSURE AND TEMPERATURE RESPONSES

In an effort to determine the cause for the apparent differences in the core hydraulic responses of Semiscale and LOFT, the system pressure responses are compared in Figure C-9. Except for the Semiscale system pressure being 1 to 0.5 MPa higher than the LOFT system pressure during the first 25 s of the blowdown, the pressure responses are actually quite similar. The higher Semiscale pressure is the result of the slightly higher initial temperature in the Semiscale broken loop (refer to Table C-1). The similar shape of the pressure curves indicate that the rate of blowdown (mass flow leaving the system on a volumetric basis) is about the same for both systems. Also, the mass flow per unit volume in the cold leg of the broken loop for both systems is essentially the same, as shown in Figure C-10. The relative mass flow through the hot leg of the broken loop, shown in Figures C-11 and C-12, are, however, significantly different. Figure C-12, which has an expanded time scale to provide more detail shows the relative mass flow through the Semiscale hot leg is initially less than for LOFT. Based on the data in Figure C-13, which overlays the Semiscale saturation temperature with the coolant temperature at the hot and cold legs of the broken loop, saturated conditions are reached almost immediately in the hot leg. As the data in Figure C-12 show, the initial relative flow in the LOFT broken loop hot leg is greater than that in Semiscale and decreases slowly until about 1.1 s, when it begins a rapid decline. This rapid decline corresponds to the development of two-phase flow, as indicated by the coolant temperature data for LOFT shown in Figure C-14. The decline in the flow through the LOFT hot leg continues until about 3 s, when it begins a slow increase. This increase in flow occurs at about the same time that two-phase flow is being developed in the cold leg, as observed by the temperature data in Figure C-14. It is possible, therefore, that the flow reduction in the cold leg flow caused by the developing two-phase flow, is directed up through the core, into the upper plenum, and out the hot leg. Although two-phase flow conditions occur in the Semiscale cold leg at about the same time, as indicated by Figure C-13, there is no indication by the relative mass flow data in Figure C-14, that this resulted in an increase in flow through the hot leg. It could be concluded, therefore, that the flow through the LOFT broken loop hot leg is more sensitive to changing conditions in the cold leg than is the corresponding flow for Semiscale.

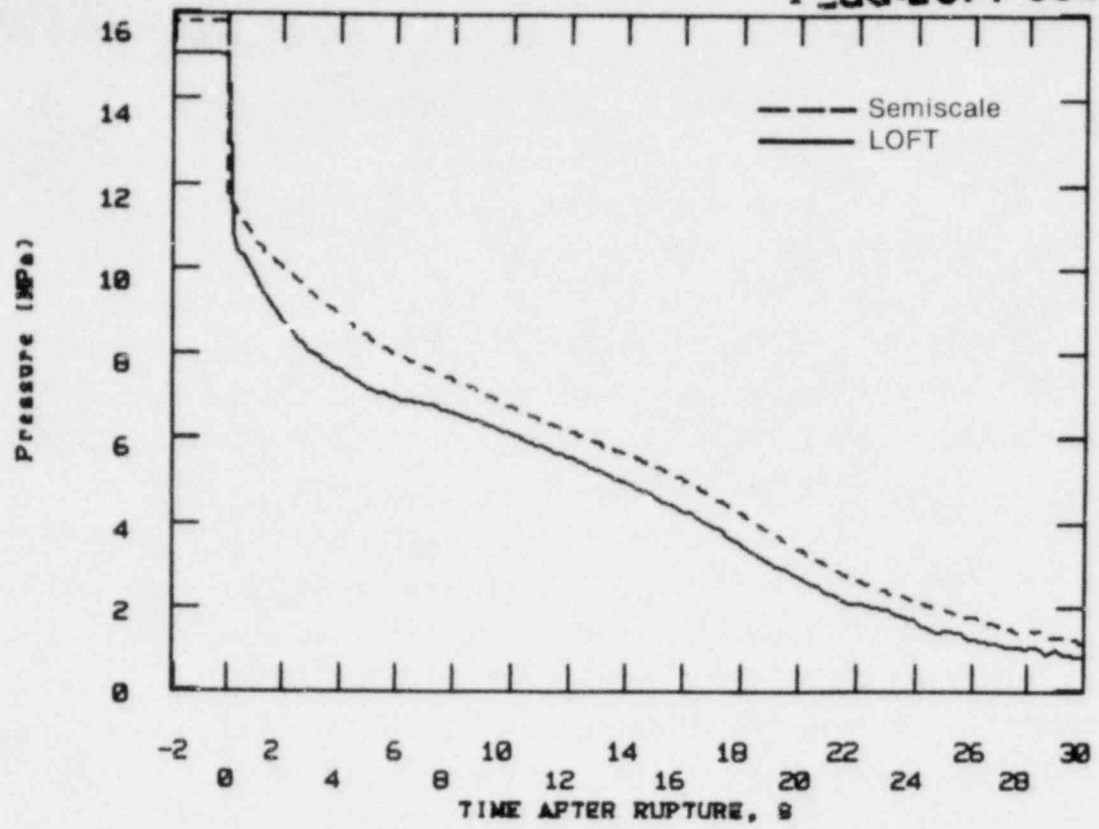

Figure C-9. Comparison of system pressure measured for LOFT and Semiscale for LOCE L2-3 and Test S-06-3, respectively.

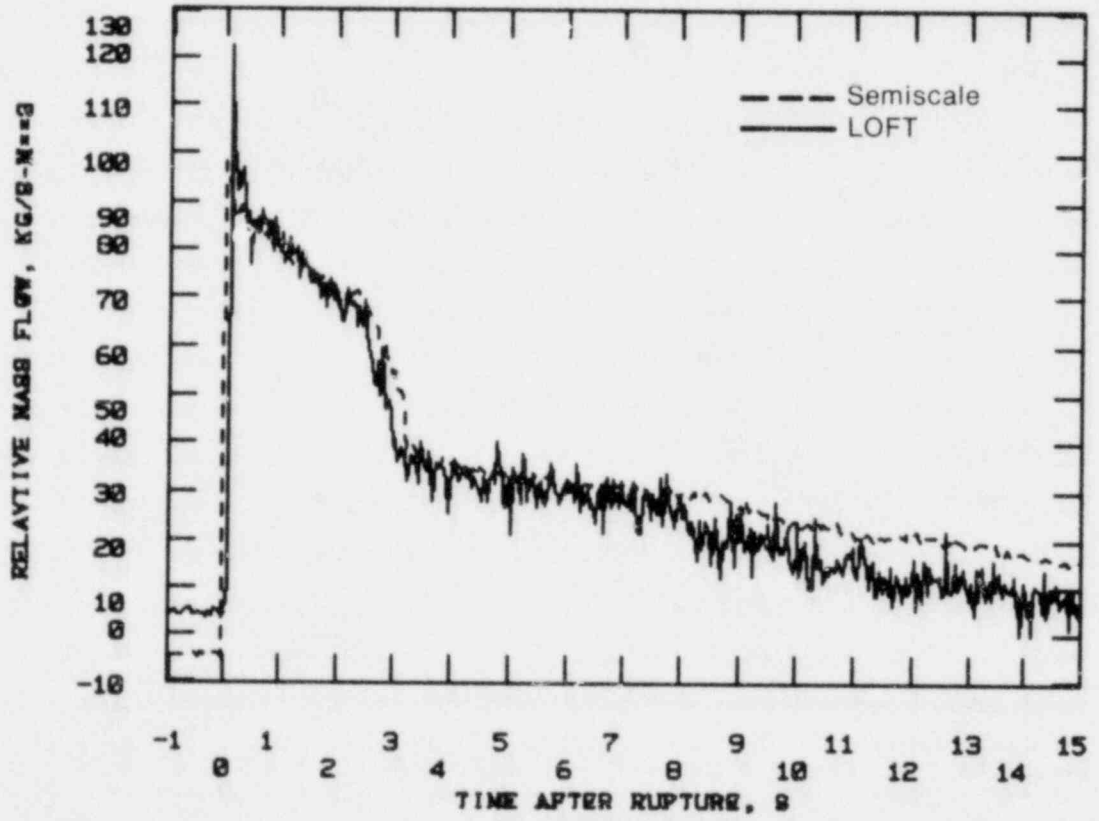

Figure C-10. Comparison of volumetrically scaled mass flows in LOFT and Semiscale broken loop cold legs for LOCE L2-3 and Test S-06-3, respectively.

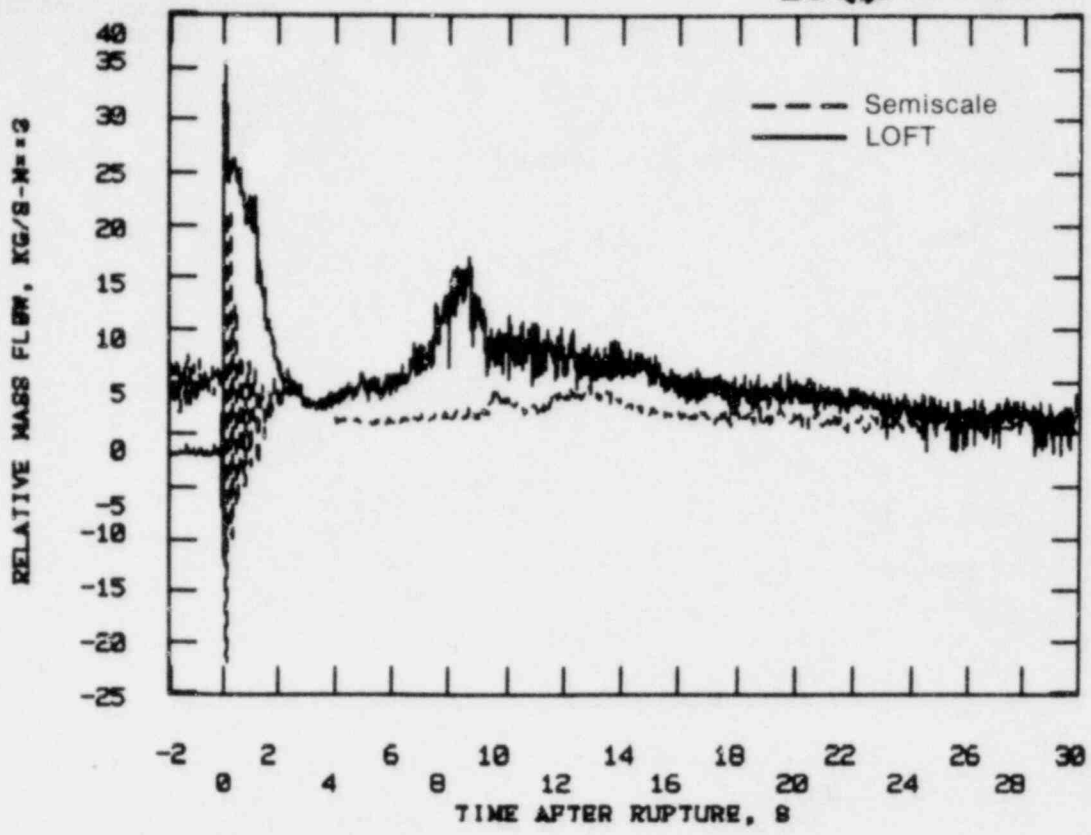

Figure C-11. Comparison of volumetrically scaled mass flows through LOFT and Semiscale broken loop hot legs for LOCE L2-3 and Test S-06-3, respectively.

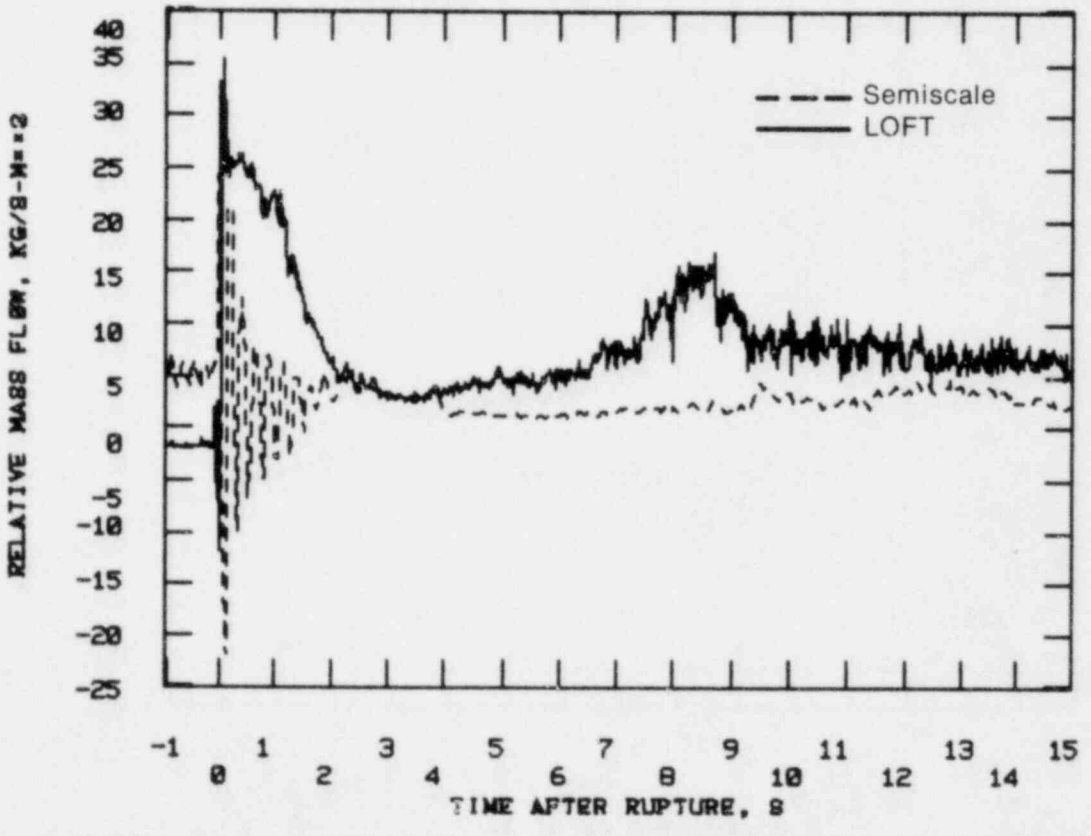

Figure C-12. Comparison of volumetrically scaled mass flows through LOFT and Semiscale broken loop hot legs for LOCE L2-3 and Test S-06-3, respectively (expanded time scale).

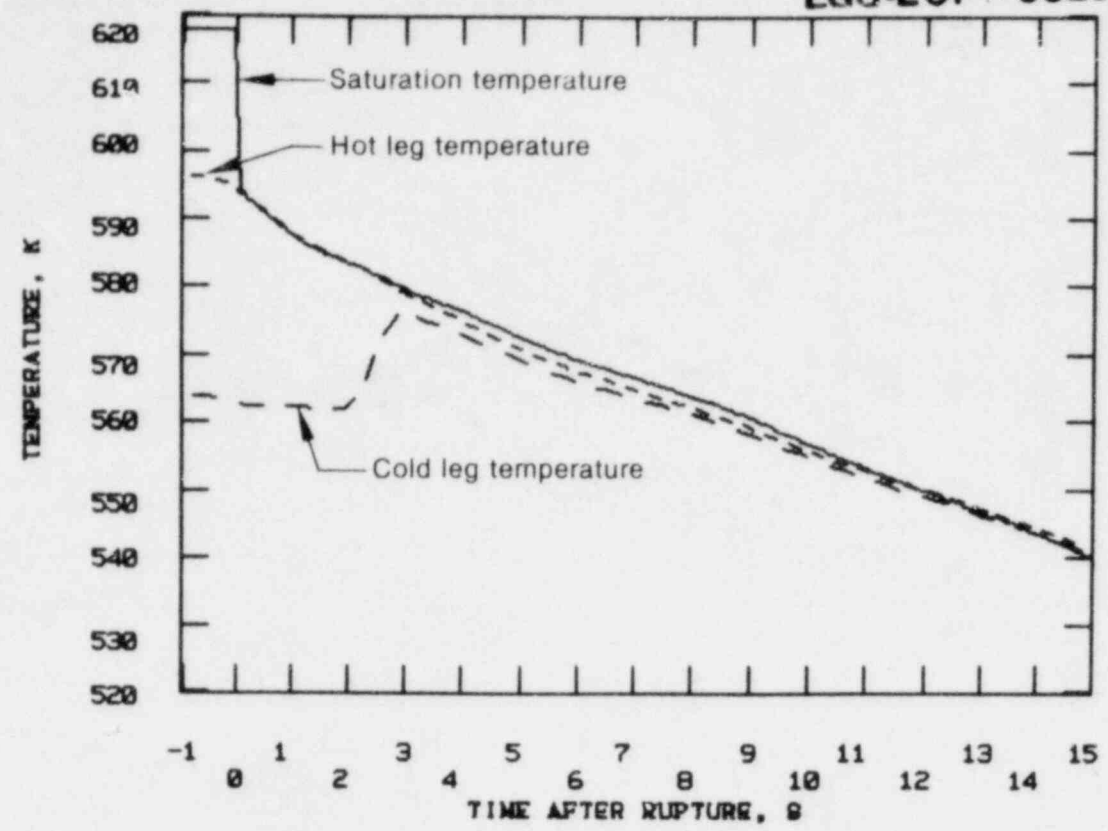

Figure C-13. Comparison of saturation temperature and hot and cold leg temperatures in Semiscale broken loop for Test S-06-3.

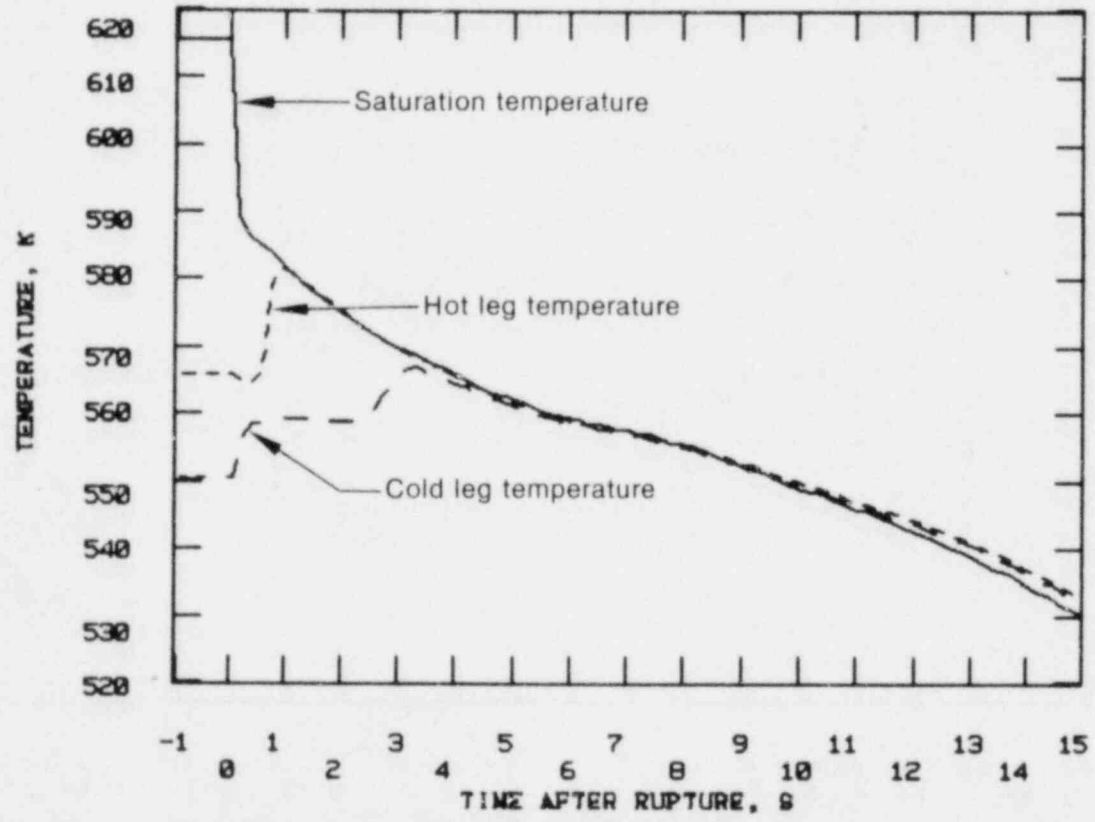

Figure C-14. Comparison of saturation temperature and hot and cold leg temperatures in LOFT broken loop for LOCE L2-3.

4. COOLANT MASS FLOW IN INTACT AND BROKEN LOOPS

Relative mass flows for LOFT and Semiscale are compared in Figures C-15 and C-16 for the respective hot and cold legs of the intact loop. The data in Figure C-15 show the flow in the Semiscale hot leg to stagnate and reverse at approximately 2.5 s. The same phenomena does not occur in LOFT until 5 to 7 s. This indicates that the relative amount of coolant available for pumping into the lower plenum and possibly through the core may not have been as great in Semiscale as it was in the LOFT system. One reason that flow stagnation and reversal can occur at different times for these two facilities is because of different pump characteristics. As the data in Figure C-17 show, the smaller Semiscale pump degrades faster than the LOFT pumps, when the void fraction becomes greater than approximately 13%. The data in Figure C-16 show, however, that at the time of core quench in LOFT, the relative mass flow into the Semiscale pressure vessel is greater than it is in LOFT. It appears, therefore, that the different pump characteristics may have had little affect on the different core hydraulic responses observed at the time of the LOFT core quench.

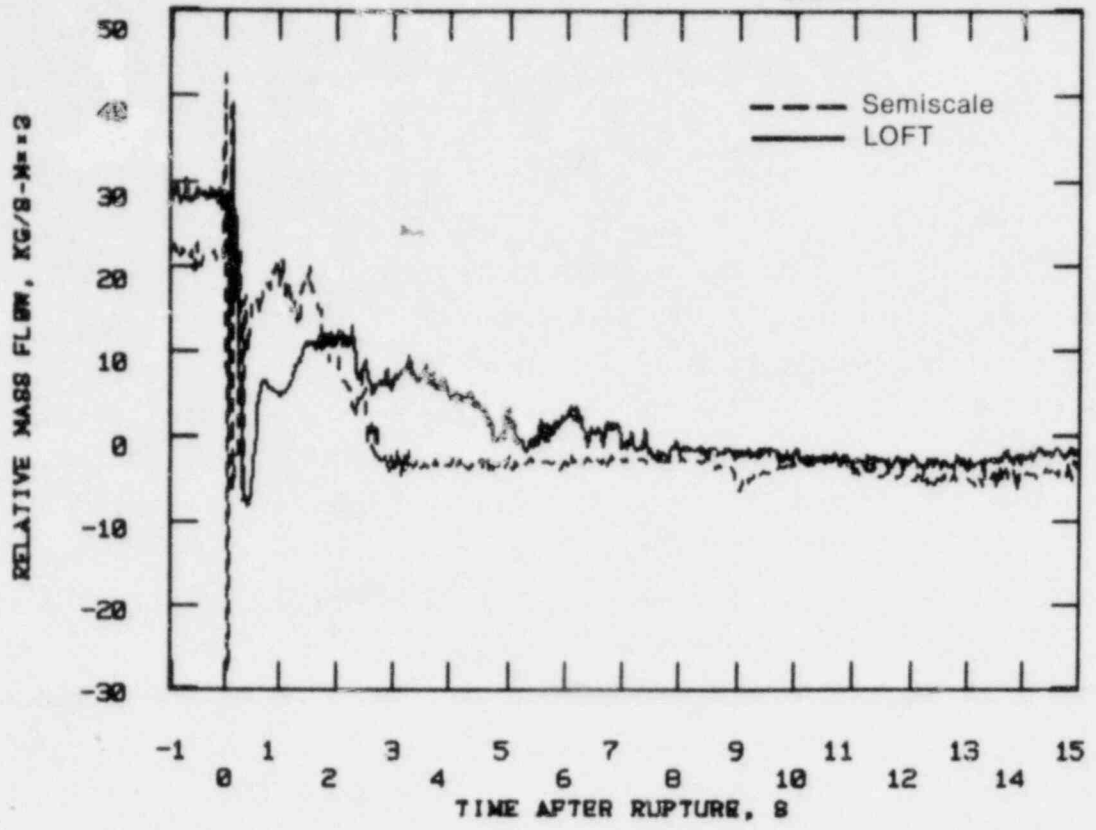

Figure C-15. Comparison of volumetrically scaled mass flows through LOFT and Semiscale intact loop hot legs for LOCE L2-3 and Test S-06-3, respectively.

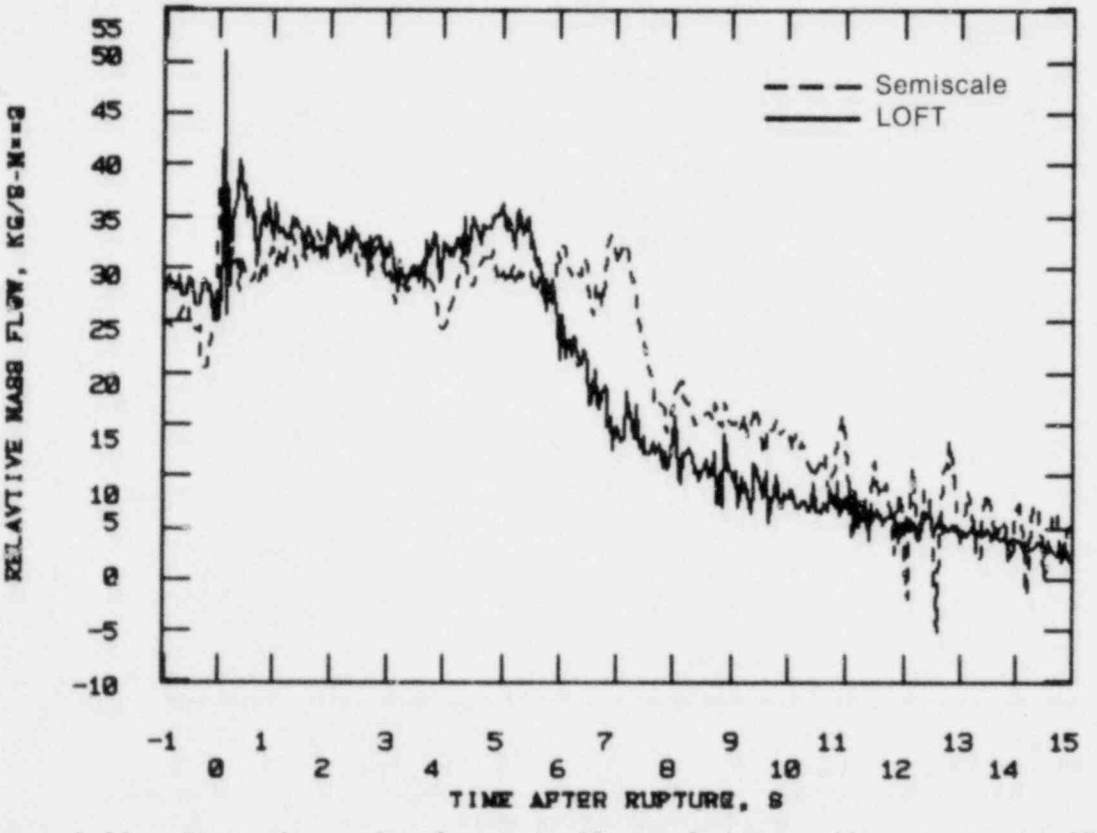

Figure C-16. Comparison of volumetrically scaled mass flows through LOFT and Semiscale intact loop cold legs for LOCE L2-3 and Test S-06-3, respectively.

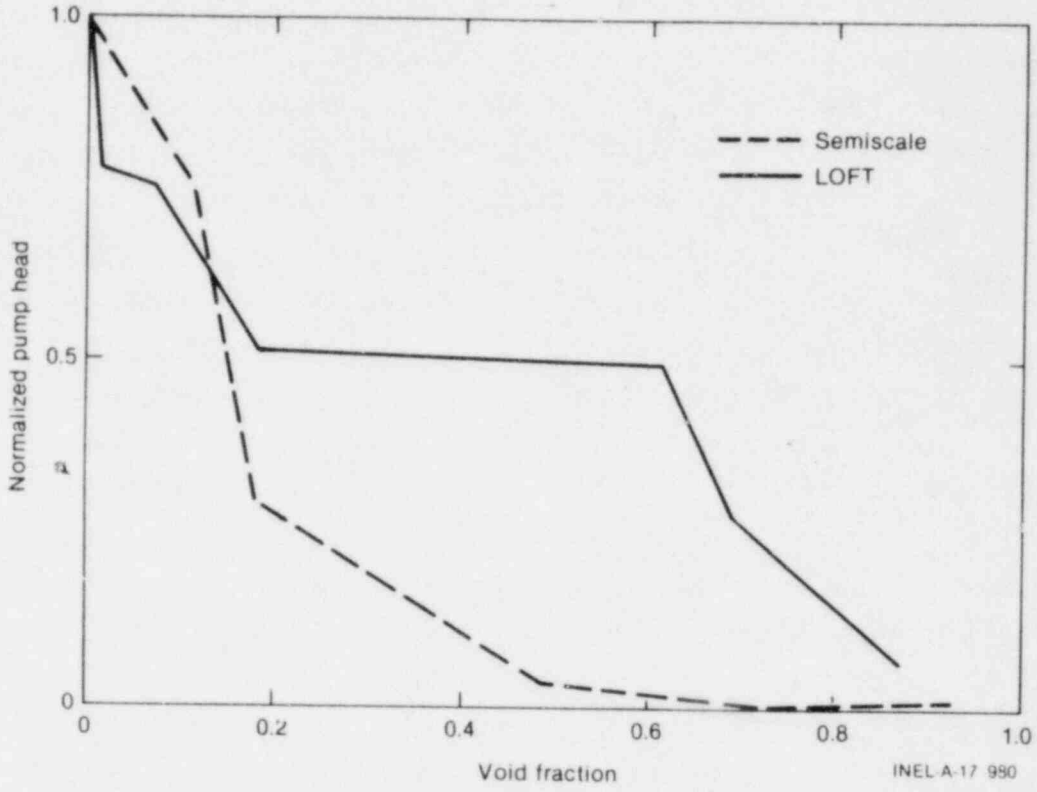

Figure C-17. Normalized pump head versus the void fraction at pump suction for Semiscale Mod-1 and LOFT facilities.

5. OBSERVATIONS AND CONCLUSIONS

As shown by the data in Figure C-4, there was a small amount of positive coolant flow measured at the inlet of the Semiscale core at about the time the quench occurred in LOFT. The Semiscale electrically heated rods have a relatively larger thermal diffusivity than the nuclear rods because of the cladding-boron nitride contact (no gap resistance) and the relatively high thermal conductivity of the boron nitride compared to the UO_2 nuclear rods. The coolant entering the Semiscale core, therefore, may have been quickly vaporized and/or superheated, resulting in a rapidly expanding gaseous coolant or pressure source near the core inlet, thus preventing additional coolant from entering the core. It could be concluded, therefore, that different design characteristics between the LOFT nuclear rod and the electrically heated Semiscale rod resulted in a relatively stronger thermal-hydraulic coupling in the Semiscale system which altered the core hydraulic response.

Based on the experimental data obtained from LOFT LOCE L2-3 and its Semiscale counterpart Test S-06-3, it is concluded that the fuel rod quench occurring in LOFT at about 6.5 s after initiation of blowdown resulted from a positive flow (up flow) of coolant through the core. Although the Semiscale data show a positive flow at the core inlet that was coincident with the LOFT core quench, it is concluded that the flow for Semiscale occurred over a shorter period of time and was probably of a smaller magnitude. Comparison of data obtained from both experiments indicate that the difference in the core flow may have resulted from either (a) different blowdown hydraulic responses occurring in the hot leg of the broken loop, or (b) different thermal response between the nuclear and electrically heated rod. Some combination of both is also possible; perhaps insight to which is the real cause and/or the relative magnitude can be obtained from calculations of thermal-hydraulic responses using the present computer codes. Calculations are underway to investigate the sensitivity of these parameters on the core flows.

6. REFERENCES

C-1. D. L. Reeder, LOFT System and Test Description (5.5-ft Nuclear Core 1 LOCEs), NUREG/CR-0247, TREE-1208, July 1978.

C-2. L. J. Ball et al., Semiscale Program Description, NUREG/CR-0172, TREE-1210, May 1978.

C-3. P. G. Prassinos et al., Experiment Data Report for LOFT Power Ascension Experiment L2-3, NUREG/CR-0792, TREE-1326, July 1979.

C-4. B. L. Collins et al., Experiment Data Report for Semiscale Mod-1 Test S-06-3 (LOFT Counterpart Test), NUREG/CR-0251, TREE-1123, July 1978.

C-5. J. Lin, Posttest Analysis of LOFT Loss-of-Coolant Experiment L2-3, EGG-LOFT-5075, March 1980.

C-6. EG&G Idaho, Inc., RELAP4/MOD6 - A Computer Program for Transient Thermal-Hydraulic Analysis of Nuclear Reactors and Related Systems - User's Manual, CDAP-TR-003, January 1978.

BLANK

APPENDIX D
POWER BURST FACILITY NUCLEAR ROD QUENCH EXPERIMENTS TC-1 AND TC-3

BLANK

APPENDIX D
POWER BURST FACILITY NUCLEAR ROD QUENCH EXPERIMENTS TC-1 AND TC-3

Several loss-of-coolant accidents (LOCAs) have been conducted in the Power Burst Facility (PBF) to evaluate the cooling effects of surface thermocouples during blowdown and reflood conditions. For each of these experiments, four individually shrouded test rods were used, as shown in Figure D-1. Two of the rods were instrumented with surface thermocouples similar to the type used in the Loss-of-Fluid Test (LOFT) facility, while the other two rods contained no thermocouples on the cladding outer surface. All rods were instrumented with internal fuel rod thermocouples, either in the fuel pellet near the outer surface, or directly attached to the cladding inner surface, as shown in Figure D-2.

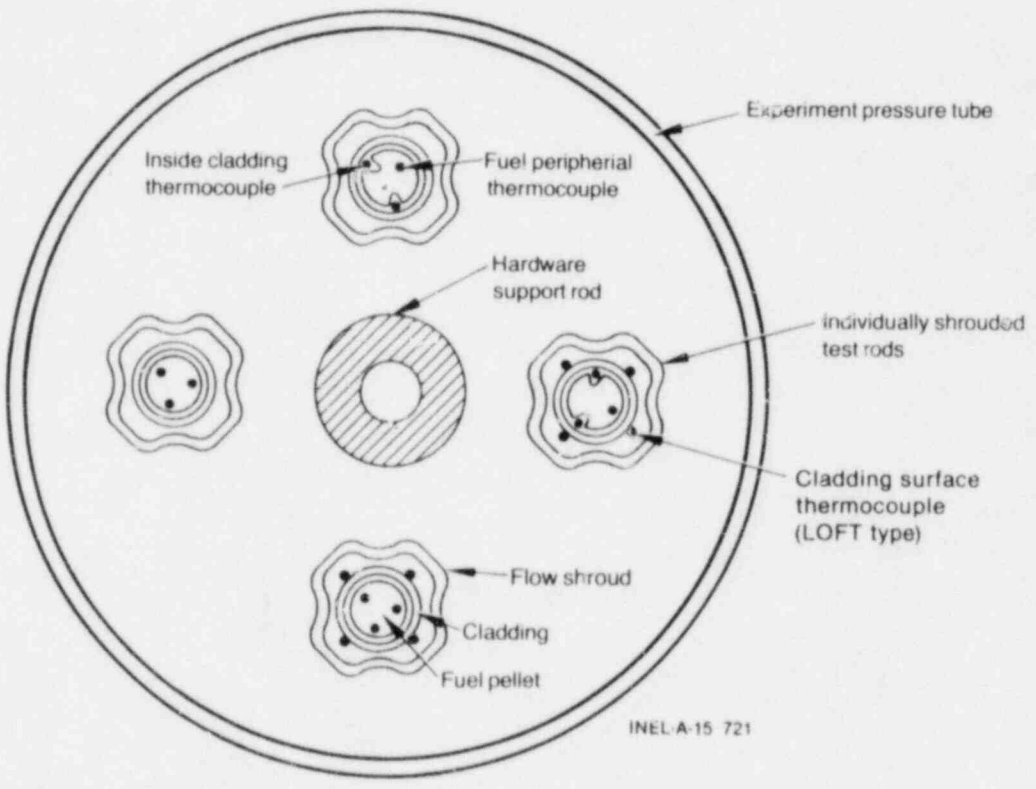

Figure D-1. PBF test fuel rod configuration for Experiment Series TC-1.

The primary objective of the PBF LOCA experiments was to simulate fuel rod response during the rapid cooling conditions observed early in LOFT

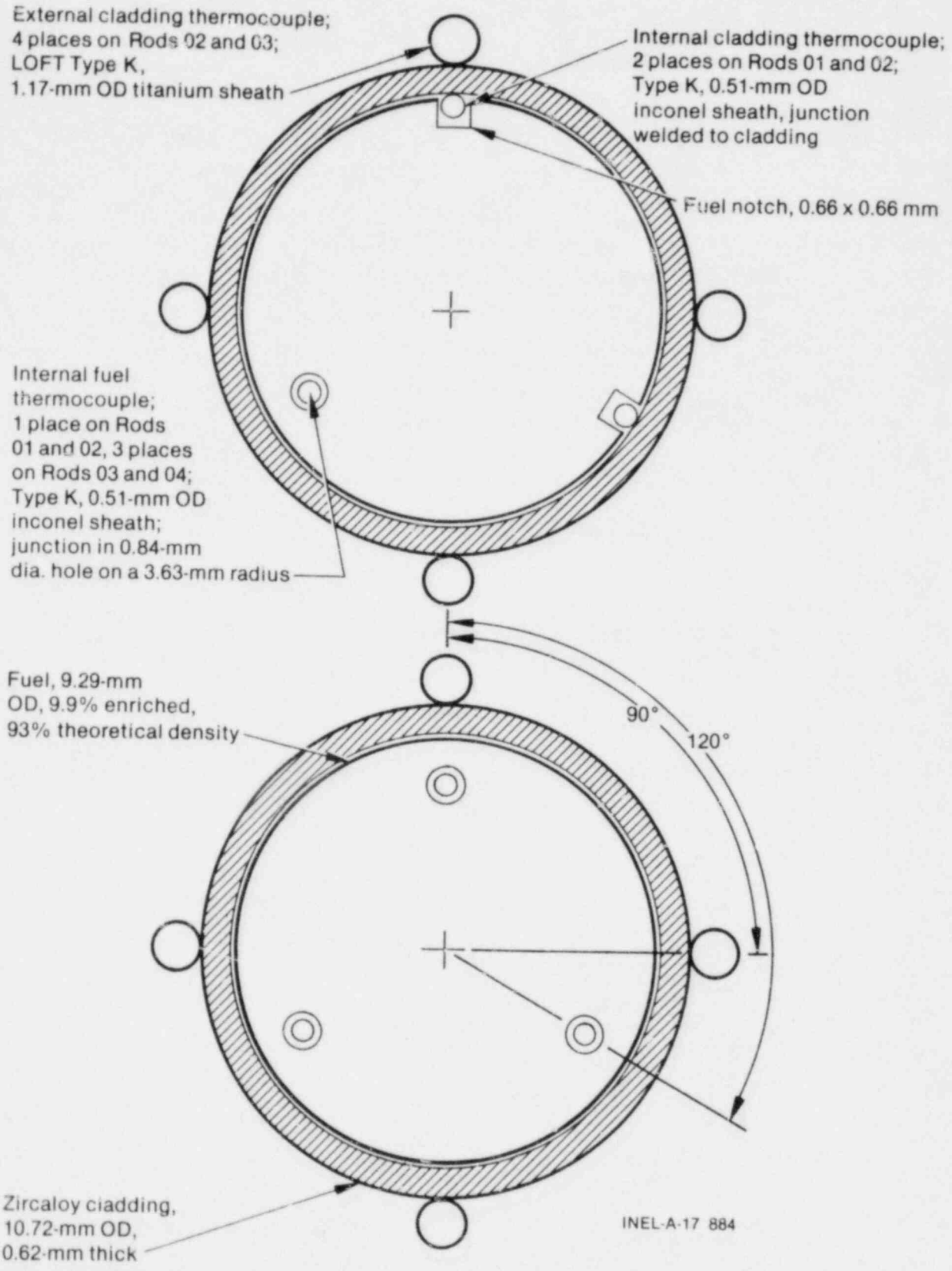

Figure D-2. PBF test fuel rod dimensions for Experiment Series TC-1.

large break Loss-of-Coolant Experiments (LOCEs) L2-2 and L2-3. The rapid, low quality flooding of the test section was to be achieved by cycling the blowdown loop isolation valves and/or the hot leg and cold leg blowdown valves several seconds after test initiation to produce a rapid, low quality flow in the test section. After cycling the blowdown valves and completion of the blowdown, the rods were powered for approximately 100 s to increase the cladding temperature to approximately 1200 K. The test section was then reflooded at a rate similar to the LOFT core final reflood rates during LOCEs L2-2 and L2-3 ($\sim$10 cm/s).

1. TC-1 EXPERIMENTS[D-1]

Four successive LOCA transients were initially conducted in the PBF TC-1 experiment series. For these experiments, the LOFT quench conditions were simulated by cycling only the hot and cold leg blowdown valves. The blowdown valve cycling times and rod transient power were slightly different for each experiment which resulted in slightly different peak cladding temperatures. The test section coolant flow, resulting from cycling only the blowdown valves, was predominantly steam and did not simulate the rapid cladding quench observed in the LOFT large break experiments. For example, a maximum steam cooling of ~20 K/s was measured during the quench simulation period by both the cladding surface and internal thermocouples, compared to a 200- to 300-K/s cooling rate measured during the LOFT core quenches. The cladding temperature response for one of these experiments (Experiment TC-1B) is shown in Figure D-3.

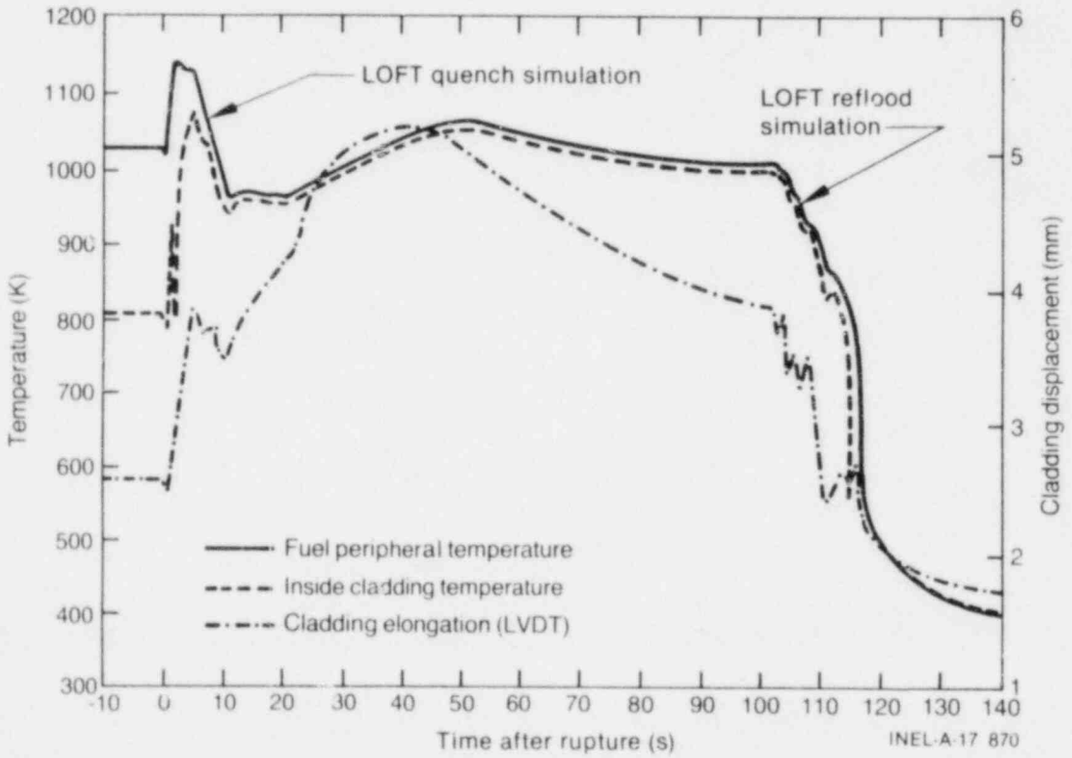

Figure D-3. General cladding temperature response for PBF Experiment TC-1B.

The TC-1 experiments showed a time-to-departure from nucleate boiling (DNB) delay on rods with surface thermocouples, although care must be taken in quantifying the time delay because of the nonuniform flow between the

individual test rod shrouds. The experiments provided data to characterize the effect of time-to-DNB on the peak cladding temperature, since different time-to-DNB and peak cladding temperatures were observed on each test rod. Figure D-4 presents the time-to-DNB versus peak cladding temperature data from the TC-1 experiments; by comparing the data from rods with and without surface thermocouples, the cooling influence of the surface thermocouples on the peak cladding temperature is estimated to be approximately 50 K.

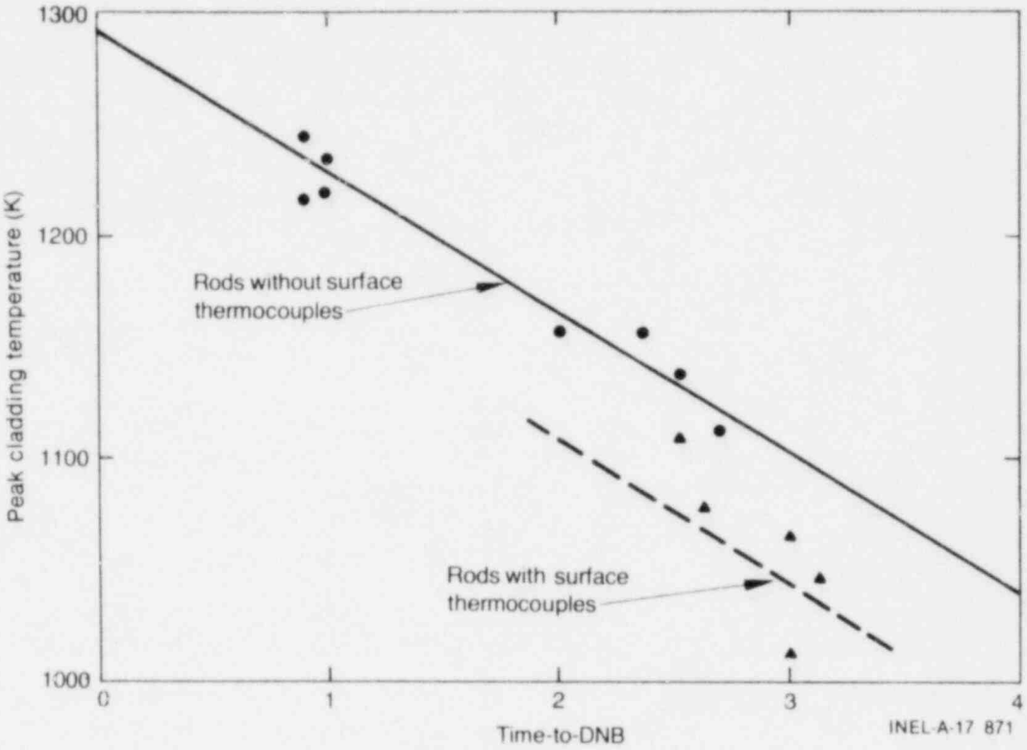

Figure D-4. Time-to-DNB versus peak cladding temperature for PBF TC-1 experiments.

All four TC-1 experiments very clearly showed the cooling influence of the surface thermocouples during the final reflood cooling (~10 cm/s reflood rate). Figure D-5 shows the internal rod thermocouple responses during reflood for Experiment TC-1B, which is representative of the response from all four experiments; notice that the rods with surface thermocouples quenched 5 to 10 s earlier and from higher cladding temperatures than did the bare rods. However, the cooling rates of all rods prior to quenching were nearly the same. Figure D-6 compares surface thermocouple and internal rod thermocouple responses during reflood and indicates that the cladding

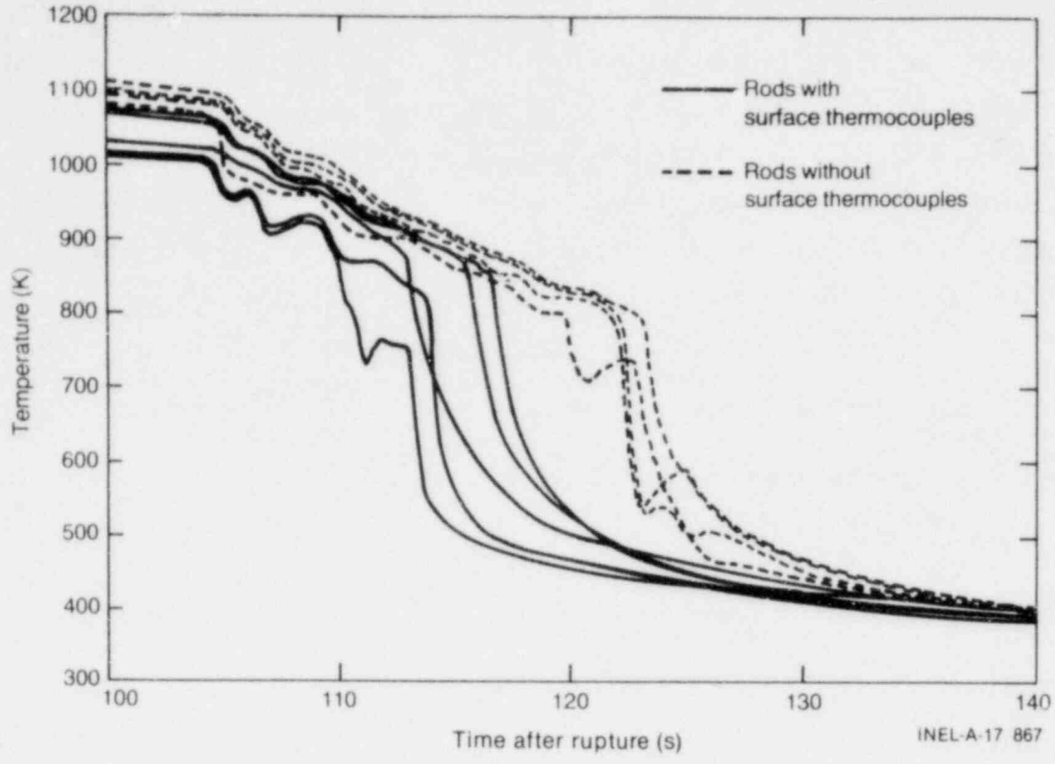

Figure D-5. Comparison of temperatures from all internal rod thermocouples during reflood for PBF Experiment TC-1B showing the influence of surface thermocouples.

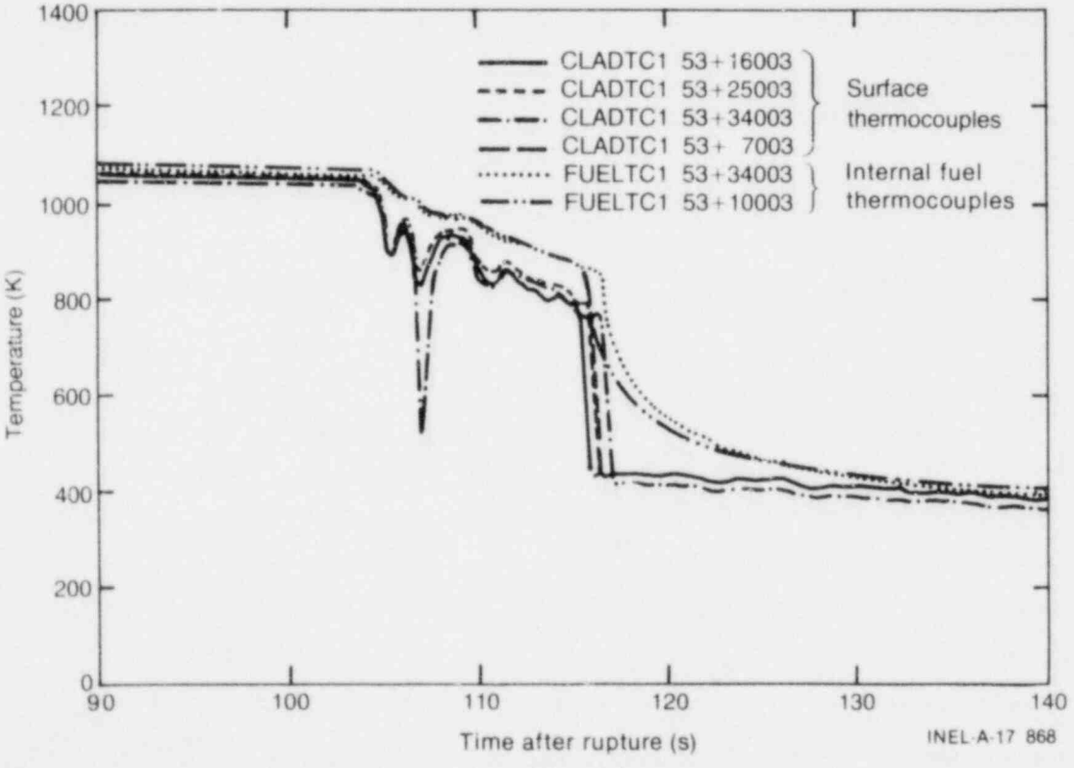

Figure D-6. Comparison of temperatures from cladding internal and surface thermocouples during reflood for PBF Experiment TC-1B.

surface thermocouples quenched at nearly the same time as the internal cladding and fuel thermocouples. These results suggest that during reflood, the cladding surface thermocouples did not appreciably affect cladding cooling rates, but enabled the cladding to quench at higher (50 to 100 K) temperatures.

2. TC-3 EXPERIMENT[D-2]

The TC-1 experiments did not produce the rapid quenches observed in the LOFT large break experiments; therefore, for the PBF TC-3 experiment, the valve sequencing was adjusted by first opening the blowdown system isolation valves (for approximately 150 to 200 ms) prior to cycling the hot and cold leg blowdown valves. This valve sequence resulted in low quality fluid through the test section and a rapid cooling of the test rods.

Plot (a) on Figure D-7 shows the measured fuel rod temperatures and Plot (b) shows the coolant velocity past the rods and the axial cladding elongation measurement during the TC-3 experiment. Notice that the flow velocity rapidly fell to near zero after blowdown initiation as a result of the check valve at the top of the flow shroud. As the low quality fluid was drawn through the test section between 5 and 10 s after blowdown initiation, the upper flow turbine indicated a flow increase. Notice that the rapid cooling of the nuclear rod exactly coincided with the valve cycling and increased test section flow. The initial cooling rates of the nuclear rod ranged from 250 to 350 K/s on the external cladding thermocouple to 40 to 100 K/s on the internal fuel thermocouples. The low quality flow did not last longer than about 1.5 s, since at 6.5 s the fuel cladding temperatures (including surface thermocouple) showed a critical heat flux (CHF) condition on the rod. The cladding elongation measurement is also shown in Plot (b) and indicates that the entire cladding axial length was rapidly cooled, although the hot spot may not have been quenched as indicated by the decreasing elongation measurement at the time of secondary CHF (6.5 s).

The rods without external thermocouples responded similar to those with external thermocouples, as shown in Figures D-8 and D-7, respectively. Table D-1 summarizes the measured fuel rod cooling rates during the simulated LOFT core quench, and it is clear that (a) the fuel rod cooled rapidly as a result of low quality flow, which lasted for less than 1.5 s, and (b) rods with and without LOFT-type surface thermocouples cooled at about the same rates as measured by the internal thermocouples.

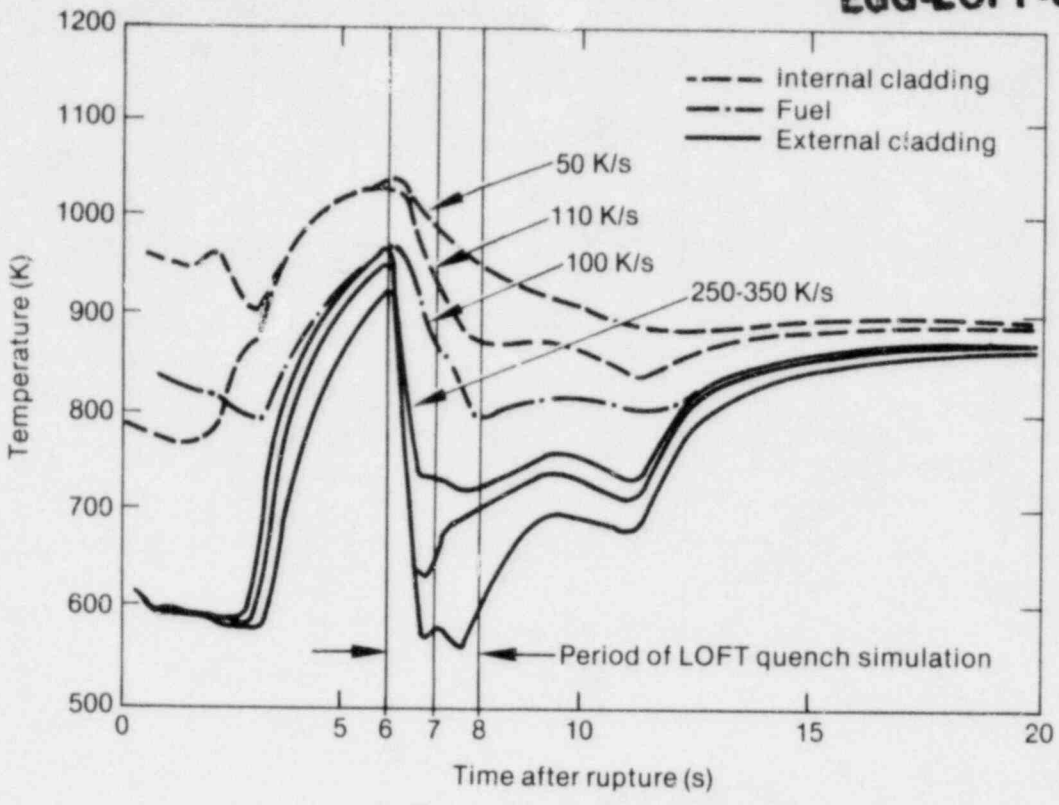

a. Fuel rod internal temperatures

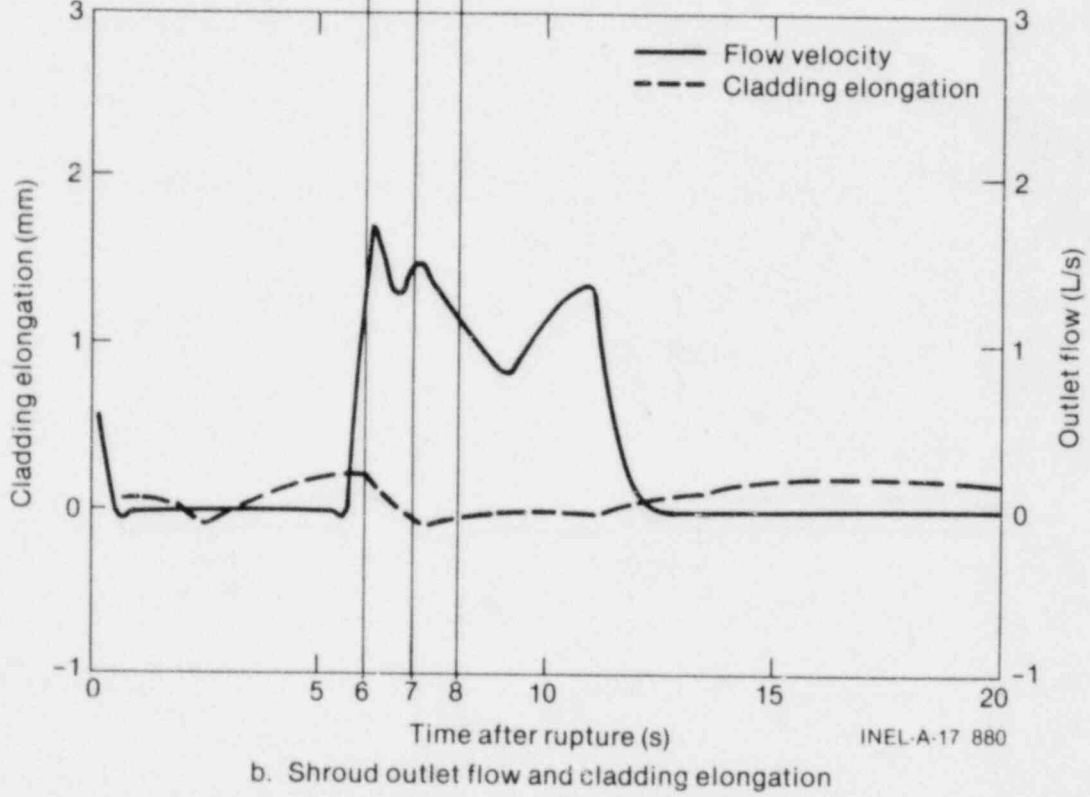

b. Shroud outlet flow and cladding elongation

Figure D-7. Fuel rod internal temperature, shroud outlet flow, and cladding elongation responses for Rod 3 with external thermocouples for PBF Experiment TC-3.

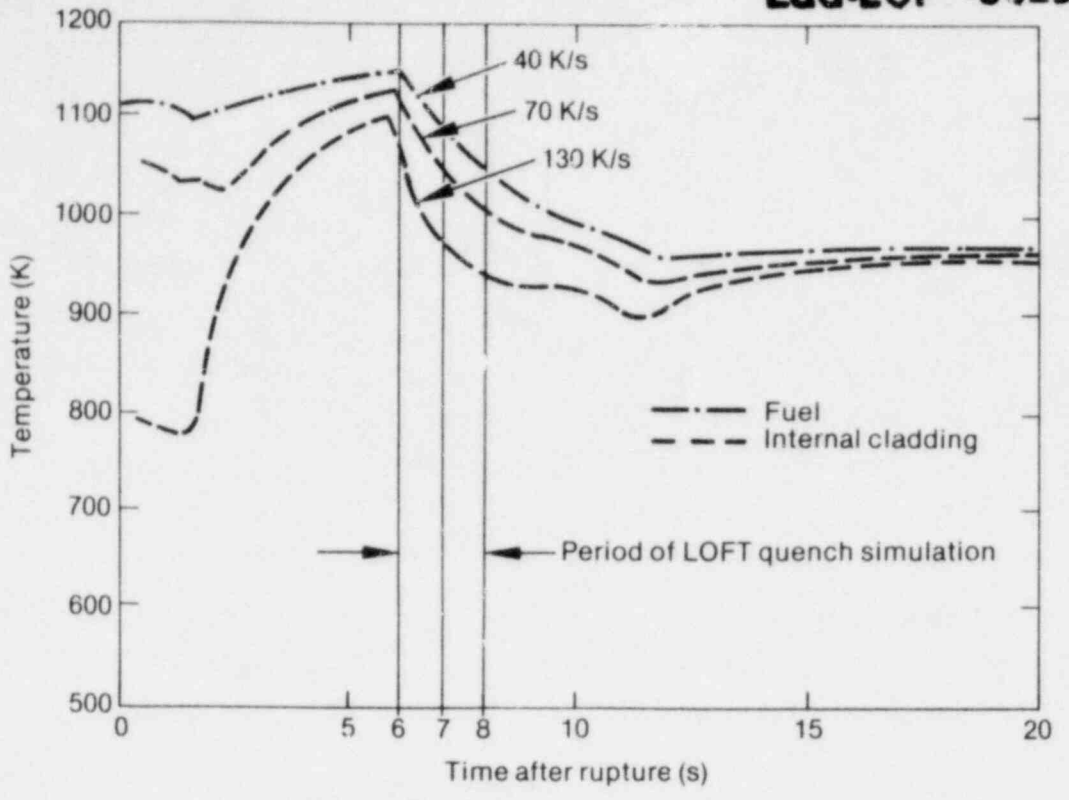

a. Fuel rod internal temperatures

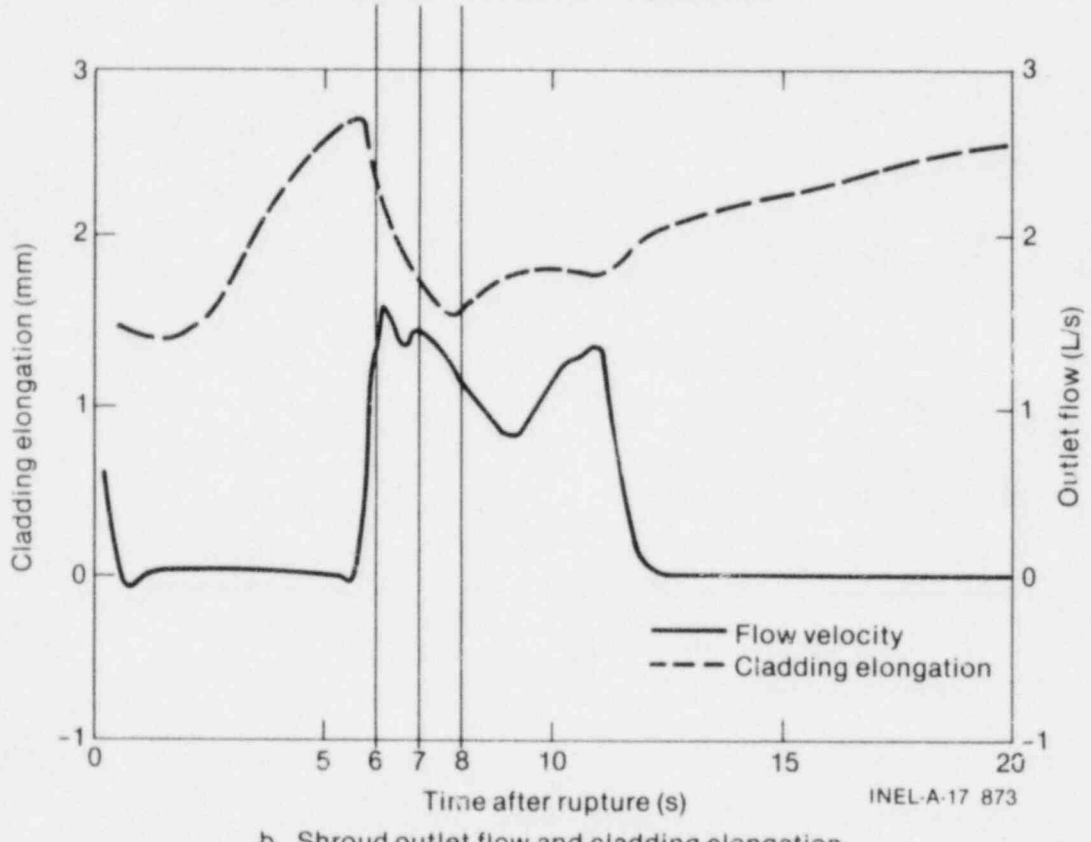

b. Shroud outlet flow and cladding elongation

Figure D-8. Fuel rod internal temperature, shroud outlet flow, and cladding elongation responses for Rod 1 without external thermocouples for PBF Experiment TC-3.

TABLE D-1. SUMMARY OF INITIAL COOLING RATES FOR EXPERIMENT TC-3 RODS DURING RAPID QUENCH

Rod	Cooling Rate (K/s)		
	Fuel Thermocouple	Internal Cladding Thermocouple	Surface Cladding Thermocouple
1	40	70 - 130	NA[a]
2[b]	--[c]	--[c]	--[c]
3[b]	100	50 - 110	250 - 350
4	65	90 - 115	NA

a. NA - not applicable.

b. With LOFT-type thermocouples.

c. Rod failed during experiment.

The reflood response during the TC-3 experiment is shown in Figure D-9 and is similar to that shown in Figure D-6 for the TC-18 experiment. Figure D-9 shows rods with the surface thermocouples quenched several seconds earlier and from higher temperatures than did the bare rods.

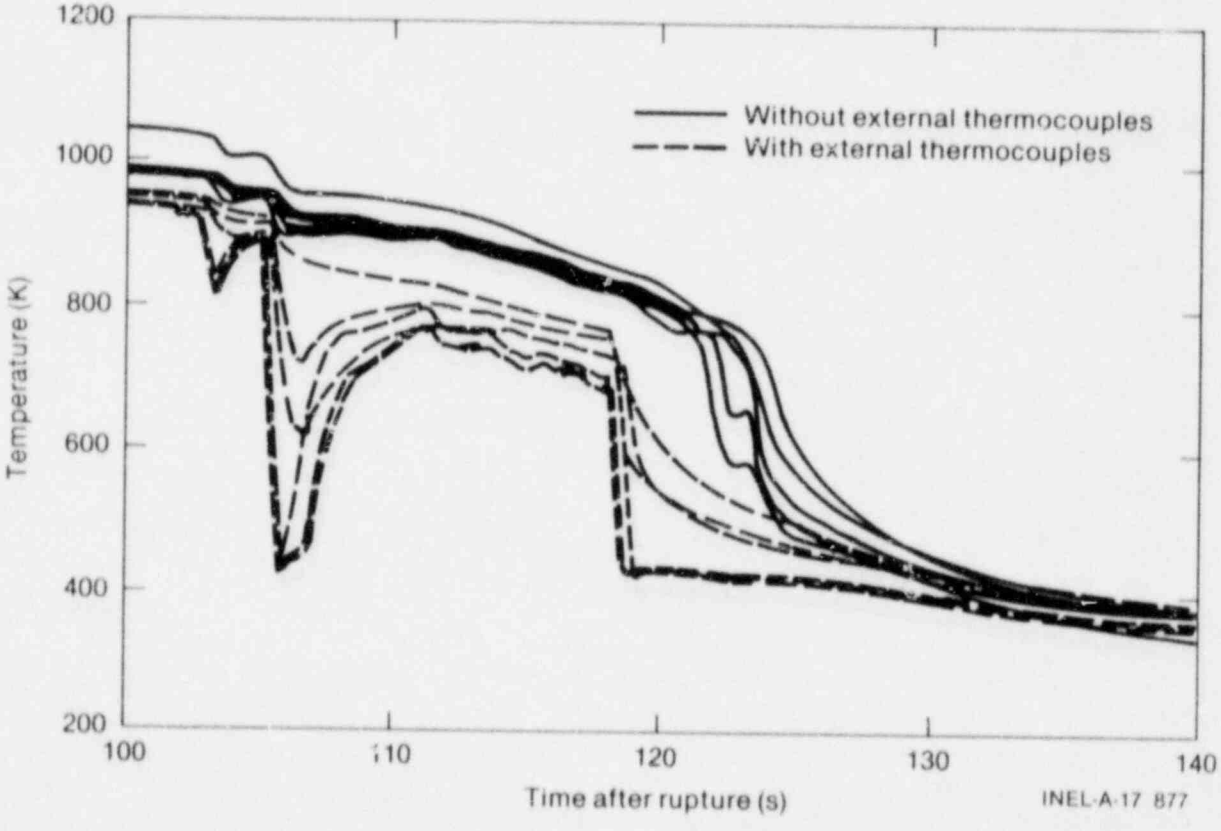

Figure D-9. Reflood response indicated by internal fuel temperatures from rods with and without LOFT-type surface thermocouples.

3. CONCLUSIONS

The initial TC-1 experiment series did not simulate the LOFT initial quench (blowdown period) but showed that the LOFT thermocouples provided additional cooling during reflood.

The TC-3 experiment showed that for rapid (4 m/s), low quality fluid past the fuel rods. the cladding temperatures were rapidly cooled. The cooling influence was not sustained for more than 1.5 s, and this time may not have been sufficient to quench the entire rod. Additional experiments will be conducted with an embedded thermocouple on the inside surface of the cladding and over a range of cooling conditions to better simulate the LOFT quench.

4. REFERENCES

D-1. T. Yackle et al., Loss-of-Coolant Accident Test Series--Test TC-1 Test Results Report, EGG-TFBP-5068, May 1980.

D-2. T. Yackle, "An Assessment of the Influence of Surface Thermocouples on the Behavior of Nuclear Fuel Rods During Large Break LOCE," Eighth U.S. NRC Water Reactor Safety Research Information Meeting, Gaithersburg, Maryland, October 27-30, 1980.

BLANK

APPENDIX E
SUMMARY OF THE HALDEN NUCLEAR AND ELECTRIC ROD REFLOODING EXPERIMENTS

BLANK

APPENDIX E
SUMMARY OF THE HALDEN NUCLEAR AND ELECTRIC ROD REFLOODING EXPERIMENTS

The majority of experiments performed to understand the core thermal and hydraulic and fuel rod response during the heatup and reflood phases of a large break loss-of-coolant accident (LOCA) have been performed using electric heater rods instrumented with both surface and internal cladding thermocouples. However, the applicability of these data have been subject to question because of uncertainty regarding the ability of electric heater rods to simulate the thermal response of nuclear fuel rods. Experiments in Experiment Series IFA-511[E-1] performed in the Halden research reactor in Norway have exposed nuclear and electric heater rods to identical thermal and hydraulic heatup and reflood conditions to resolve this uncertainty. The test rods were instrumented with both surface and internal cladding thermocouples to determine if surface thermocouples provide an accurate measurement of cladding temperatures.

The experiments from Halden Experiment Series IFA-511 are described in Section 2, and results from the nuclear and electric rod experiments are discussed and compared in Section 3. Conclusions are presented in Section 4.

1. EXPERIMENT DESCRIPTION

The IFA-511 experiments included a series of experiments with nuclear rods (IFA-511.2)[E-2] and a series of experiments with Semiscale solid-type electric heater rods (IFA-511.3).[E-3] The experiments are listed in Table E-1. The test rod bundles, the experiment conditions, and a nuclear rod experiment selected as a base case are described in the following sections.

1.1 Experiment Design and Performance

Each experiment was performed with a seven-rod bundle consisting of six peripheral rods symmetrically surrounding the center rod, see Figure E-1. The heated length was 1.5 m. Five of the rods were instrumented with internal cladding thermocouples. The cladding thermocouples were positioned at various azimuthal orientations and at five different axial elevations as shown in Figure E-1.

Parameters varied during each experiment series were rod power, peak cladding temperature prior to reflood initiation, and reflood rate. The average linear heat generation rate ranged from about 1.0 to 3.0 kW/m. Measured peak cladding temperatures ranged from 580 to 1100 K, and the reflood rate was systematically varied from approximately 2 to 10 cm/s. The experiment conditions for the IFA-511.2 and -511.3 experiment series are summarized in Table E-1.

The experiments were performed by depressurizing the pressure flask containing the test bundle and then allowing the rods to heat to the desired temperature at constant power. The range of desired peak cladding temperature was obtained by controlling the time to reflood. Reflood was initiated by rapidly refilling the reflood pipes and pressure flask lower plenum. The bundle reflood then proceeded at a preselected flooding rate. The IFA-511.3 experiment series was prematurely terminated because of three failed heater rods. The test bundle will be rebuilt and the experiment series repeated.

TABLE E-1. EXPERIMENTS IFA-511.2 AND IFA-511.3 TEST MATRIX

Run	Average Linear Heat Generation Rate (kW/m)	Reflood Rate (g/s)	Time to Reflood (s)
IFA-511.2 (Nuclear Fuel Rod)			
4693	1.05	61	58
4694	1.07	59	58
4695	1.06	61	58
4696	1.99	60	58
4697	1.93	54	58
4698	1.95	14/54	58
4719	2.82	66	58
4712	2.88	66	44
4714	2.92	64	44
5236	1.87	55	58
5237	1.91	55	58
5238	1.91	43	58
5239	1.90	33	58
5240	1.89	12	58
5241	1.89	43	82
5242	1.89	42	92
5243	1.90	42	92
5244	1.89	43	103
5245	1.92	42	113
5246	1.92	41	113
5247	1.92	42	113
IFA-511.3 (Semiscale Electric Heater Rod)			
5257	1.85	53	58
5258	1.87	55	58
5259	1.91	55	58
5260	1.91	40	58
5261	1.90	34	58
5262	1.89	12/30	58
5263	1.92	44	113
5264	1.92	44	113
5265	1.92	44	113
5266	2.0	12	11
5267	3.0	14	58

TC#	Elevation from rod bottom (m)
TOC1	0.15
TOC2	0.90
TOC3	1.35
TOC4	0.60
TIC3	0.60
TIC4	0.15
TIC5	0.40
TIC6	0.60
TIC10	0.60
TIC11	0.40
TIC12	0.15
TIC13	1.35
TIC14	0.73
TIC15	0.90
TIC16	0.60
TIC20	0.73
TIC21	1.35
TIC26	0.73
TIC27	0.90

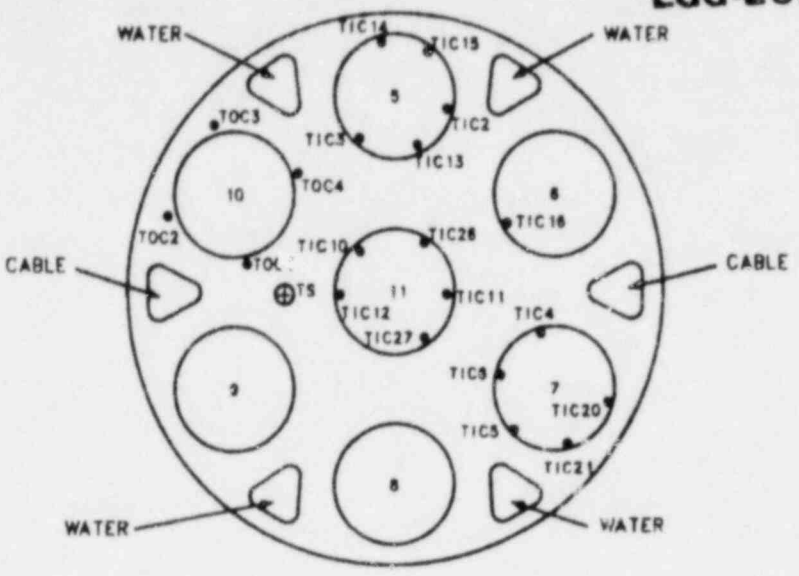

a. Nuclear rod test bundle

SXX-281-2

TC#	Elevation above rod bottom (m)
TOC1	0.13
TOC2	0.88
TOC3	1.33
TOC4	0.58
TIC4	0.13
TIC5	0.38
TIC6	0.60
TIC7	0.15
TIC8	0.40
TIC9	0.60
TIC20	0.72
TIC21	1.34
TIC24	0.90

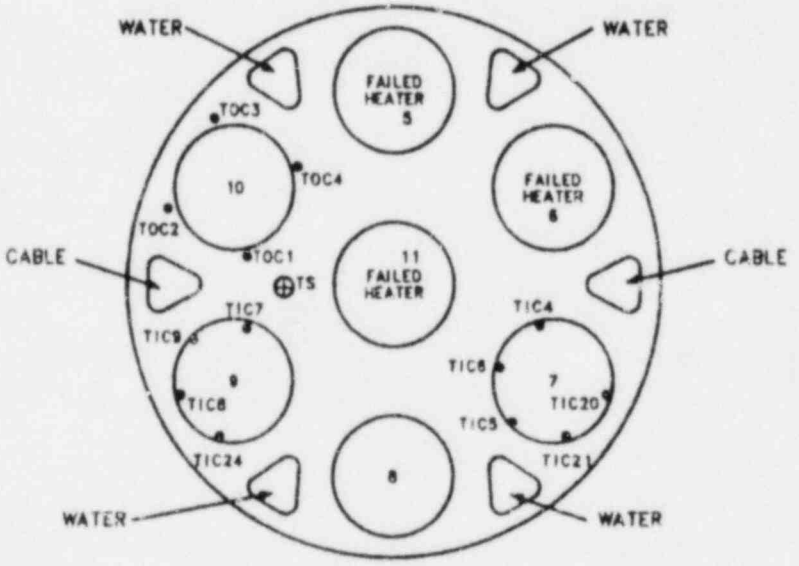

b. Electric rod test bundle

SXX-281-1

Figure E-1. Schematics of electric and nuclear rod test bundles for Halden IFA-511 experiments.

1.2 Base Case Experiment Description

The thermal response of the center nuclear rod during the highest temperature experiment, Run 5246 in Table E-1, is shown in Figure E-2. The measured cladding surface temperatures at four elevations between 0.15 and

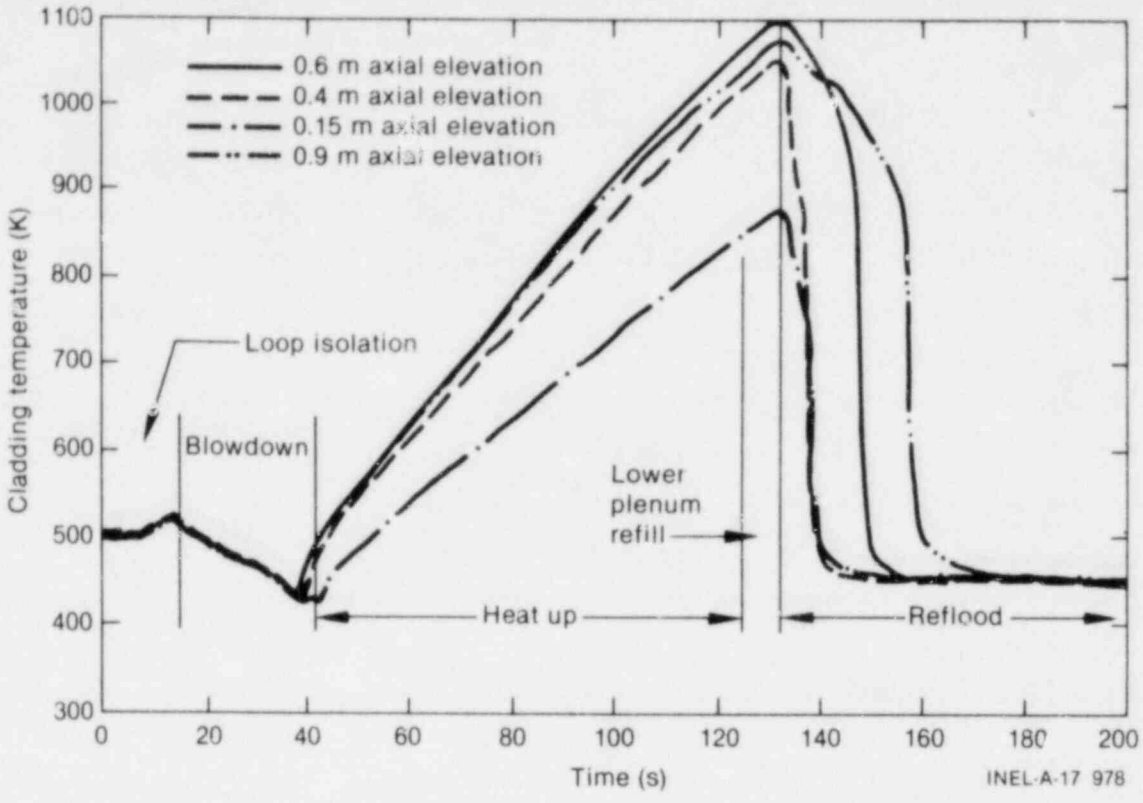

Figure E-2. Thermal response of center rod cladding internal thermocouples for Halden nuclear rod experiment during highest temperature Run 5246.

0.90 m from the bottom of the fuel column are shown as a function of time after initiation of the transient. Isolation of the steady state cooling system from the blowdown system was initiated at 0 s and required approximately 13.5 s to complete. Loop blowdown was then initiated at 14.5 s and completed after approximately 30 s. The system pressure then remained constant at about 0.15 MPa. Cladding temperatures were initially at about 500 K and did not change until completion of loop isolation. The cladding temperatures increased approximately 25 K as the coolant flow stagnated after about 12 s and then measured the coolant saturation temperature during blowdown. Dryout occurred within the rod bundle, starting at the top at about 40 s. The cladding temperatures then increased nearly linearly at approximately 12 K/s, which is about 95% of the calculated adiabatic heatup rate. At 134 s, the measured peak cladding temperature was 1103 K at the 0.60-m elevation. At 128 s, reflood was initiated at a high rate to fill the reflood piping system and test train lower plenum.

When the reflood coolant entered the system, steam was generated via heat transfer from the piping, pressure flask, and test train structure and was rapidly expelled through the test bundle. This saturated two-phase mixture (from liquid entrainment) significantly increased the rod surface heat transfer and for all experiments, nuclear or electric, rapidly terminated the cladding heatup.

The reflood rate after 134 s was almost 7 cm/s and a significant delay in time to quench was expected. However, cladding quench at the lower thermocouples, 0.15- and 0.40-m elevations, occurred within 6 s. The cladding quench then rapidly progressed up the fuel rod, and the thermocouple at the 0.90-m elevation indicated quench at about 162 s and the fuel centerline thermocouple at the 1.35-m elevation indicated quench at about 170 s. There was, in general, no well defined "quench temperature" which was indicated by a knee or inflection point in the time-temperature plot from the IFA-511.2 experiments. Instead, the cladding cooldown rate continually increased after initiation of reflood, until the rod quenched.

Circumferential temperature differences in the range of 20 to 40 K on the peripheral test rods was caused by radiation heat transfer to the cold wall of the pressure flask. This was determined by comparing measured cladding temperatures at the same elevation, but on the rod inner surface facing the center rod and on the rod outer surface facing the pressure flask, and increased with higher cladding temperatures.

The ability of the system to repeat exact experiment conditions is important if direct comparisons between nuclear and electric rods are to be made. To verify system repeatability, three experiments were performed with identical nominal initial conditions and experiment sequencing, as for Run 5246 (base case). The response of the cladding internal and surface thermocouples at the 0.60-m elevation for one center and one peripheral rod (Rods 10 and 11) for these repeat nuclear rod experiments are shown in Figure E-3. For the blowdown and heatup portions of the experiments, the three traces for each thermocouple nearly overlay. The heatup rate and measured peak cladding temperature of the internal thermocouple was slightly greater than the surface thermocouple. This was caused because (a) of a variation in the response of internal and surface thermocouples and (b) the center

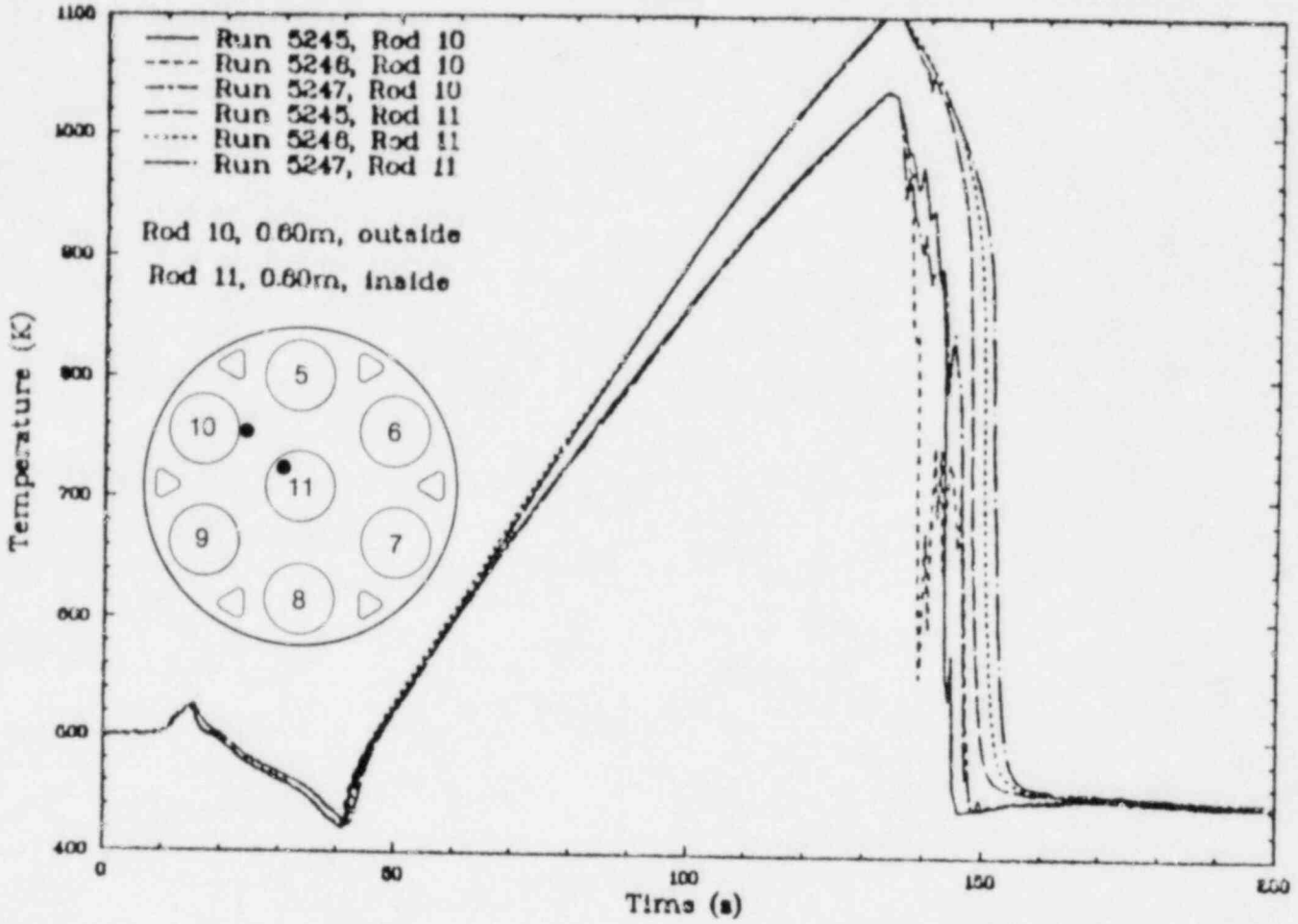

Figure E-3. Comparison of measured cladding internal and surface temperatures for Halden repeat nuclear rod experiments with identical experiment conditions.

rod was at a slightly greater power because of incorrect enrichment. During quench there were slight variations in the thermal response of the fuel rods, but these are considered insignificant, as the general trend was nearly identical and the difference in quench time was only about 5 s.

2. RESULTS

Results from the nuclear and electric rod experiments from Experiment Series IFA-511.2 and IFA-511.3, respectively, are discussed and compared in the following sections.

2.1 Comparison of Cladding Internal and Surface Thermocouples During Nuclear Rod Experiments

The comparative behavior of cladding internal and surface thermocouples on the nuclear rods during the experiment, Run 5236, and the base case at the highest temperature, Run 5246, is shown in Figures E-4 and E-5, respectively. For both cases through blowdown and heatup until temperatures exceeded 700 K, the responses of the surface and internal thermocouples were nearly identical. However, after about 700 K, the temperature measured by the surface thermocouple was less than was measured by the internal thermocouple, and the difference increased with increasing cladding temperatures. The measured peak cladding temperature was 24 to 40 K less than the internal temperature. The increased heat transfer within the bundle from flowing steam during the lower plenum refill terminated the temperature increase indicated by the surface thermocouples 5 to 10 s earlier than was indicated by the internal thermocouples. Throughout reflood, the indicated temperature of the surface thermocouple was at least 50 K less than that indicated by the internal thermocouples and the surface thermocouples indicated quench 5 to 20 s earlier than did the internal thermocouples.

2.2 Effect of Rod Power, Peak Cladding Temperature, and Reflood Rate

Experiments were performed in the IFA-511.2 experiment series in which the peak rod power was increased from ∿1 to ∿3 kW/m for both low and high cladding temperature (580 to 1100 K) at the initiation of reflood. It was anticipated that the increased power and temperature would significantly delay the temperature turnaround and time to quench after initiation of reflood. This was not the case. Evidently, the thermal resistance across the fuel-cladding gap and the UO_2 fuel pellet effectively decouples the cladding thermal response from the fuel and permits the cladding to cool relatively fast, compared to solid electrical rods.

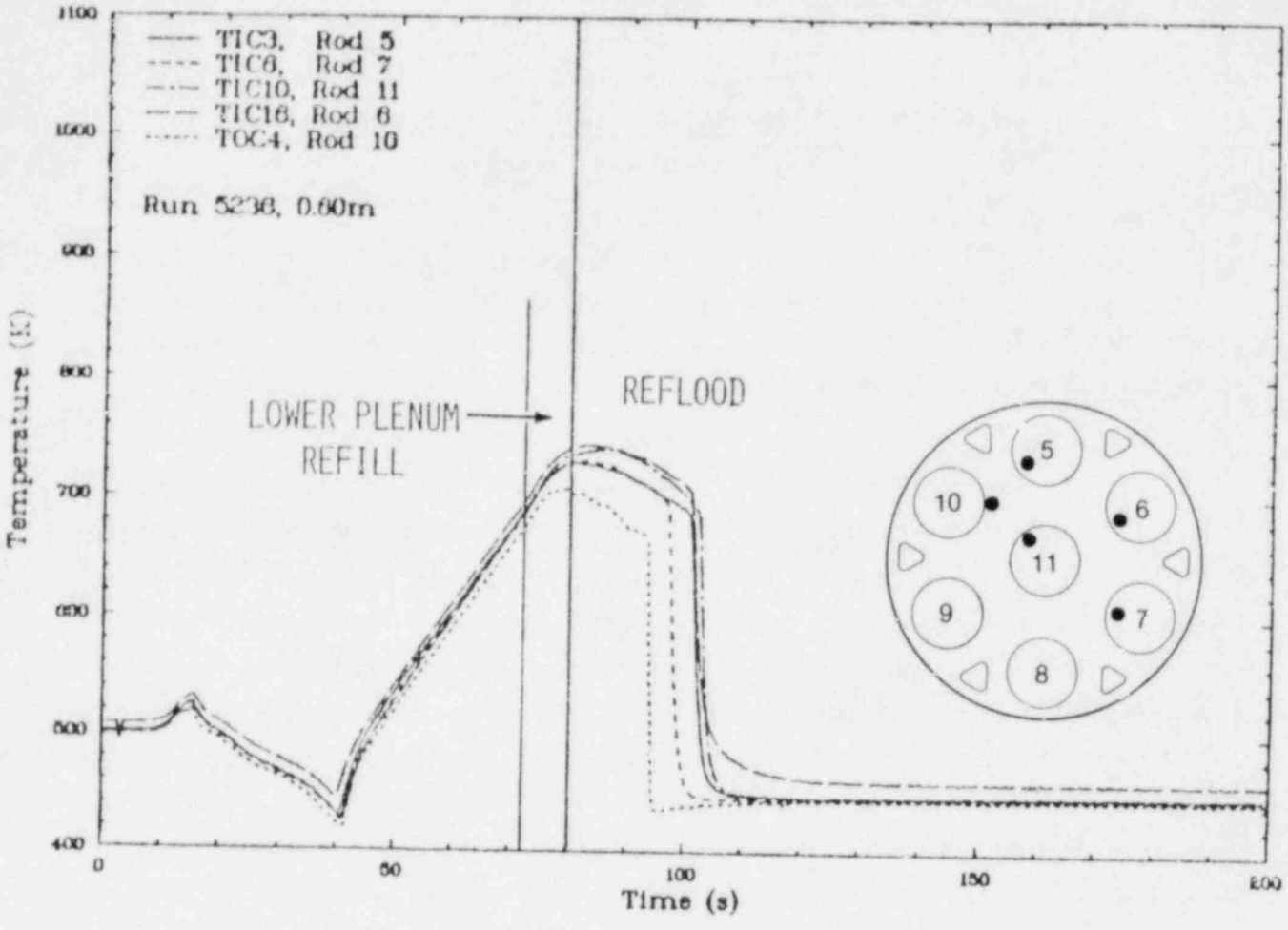

Figure E-4. Comparison of temperatures from cladding internal and surface thermocouples for Halden nuclear rod experiment during lowest temperature Run 5236.

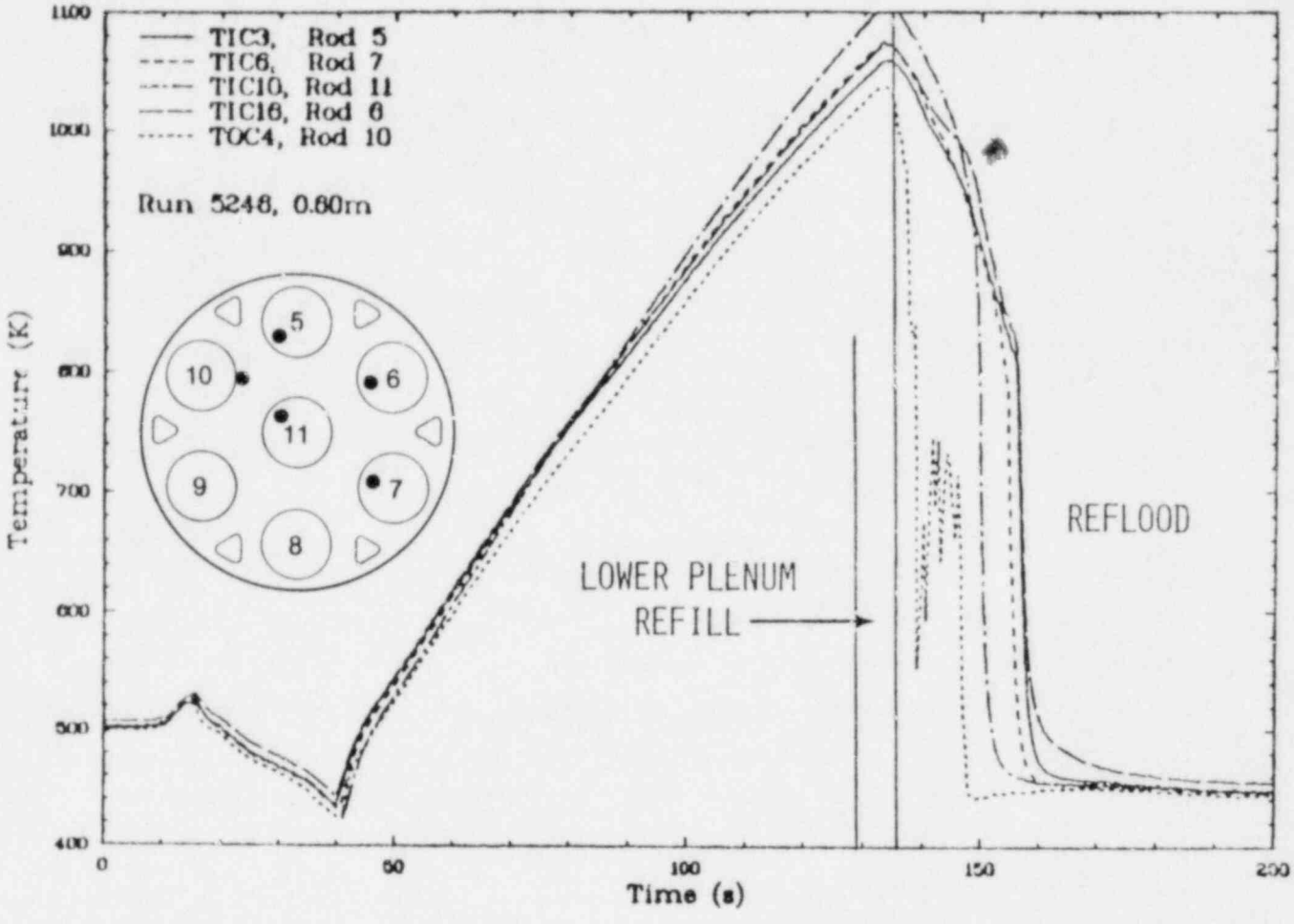

Figure E-5. Comparison of temperatures from cladding internal and surface thermocouples for Halden nuclear rod experiment during highest temperature Run 5246.

The reflood rate was also an experiment parameter and was varied from approximately 2 to 8 cm/s (12 to 55 g/s). The observed tendency was to cause higher cladding temperatures and to delay quench with decreasing reflood rate. This general trend is consistent with previous results from out-of-pile electric heater rod heatup and reflood experiments.[E-4--E-7]

2.3 Comparison of Nuclear and Electric Rod Behavior

The IFA-511.3 experiment series was essentially intended as a duplication of the IFA-511.2 nuclear rod experiment series, except the experiments were performed with solid-type Semiscale electric heater rods. Unfortunately, three of the seven rods (Rods 5, 6, and 11) were failed at the start of the series. Eleven experiments were performed, as summarized in Table E-1, and these selected experiment results are compared in this section with similar results from the nuclear rod experiment series, IFA-511.2.

The measured cladding temperatures (internal thermocouple) at the 0.60-m elevation for three electric rod experiments that were run under the same boundary conditions as the nuclear rod base case experiment (discussed in Section 2.2) are overlayed with the nuclear base case cladding temperature in Figure E-6. These temperatures are from Rod 7, a peripheral rod, and the thermocouple was located on the side of the fuel rod facing the failed center rod. The observed cladding thermal response during blowdown and heatup was basically the same, as discussed previously. The measured peak cladding temperatures for the electric rod ranged from about 1060 to 1080 K, but they did not occur until approximately 10 s after initiation of bundle reflood. After the cladding temperatures turned around at 145 s, they gradually decreased to about 790 K when the rod quenched between 240 and 252 s. The experiment repeatability was excellent, as for the nuclear rod experiments.

During blowdown and heatup, the response of the nuclear and electric heater rods essentially overlayed. However, the cladding temperature rise was terminated on the nuclear rod about 5 s after the initiation of system reflood at 128 s. This was about 12 s earlier than for the electric rod. The indicated quench of the nuclear rod was only 20 s after initiation of test rod bundle reflood, compared with about 110 s for the electric heater

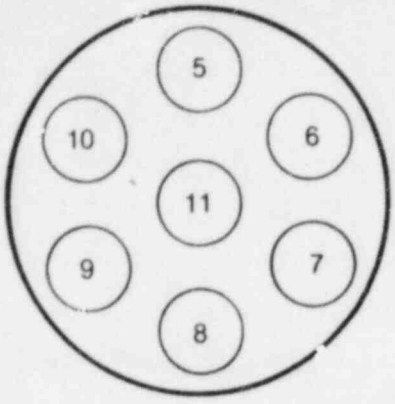

IFA-511 test
rod configuration

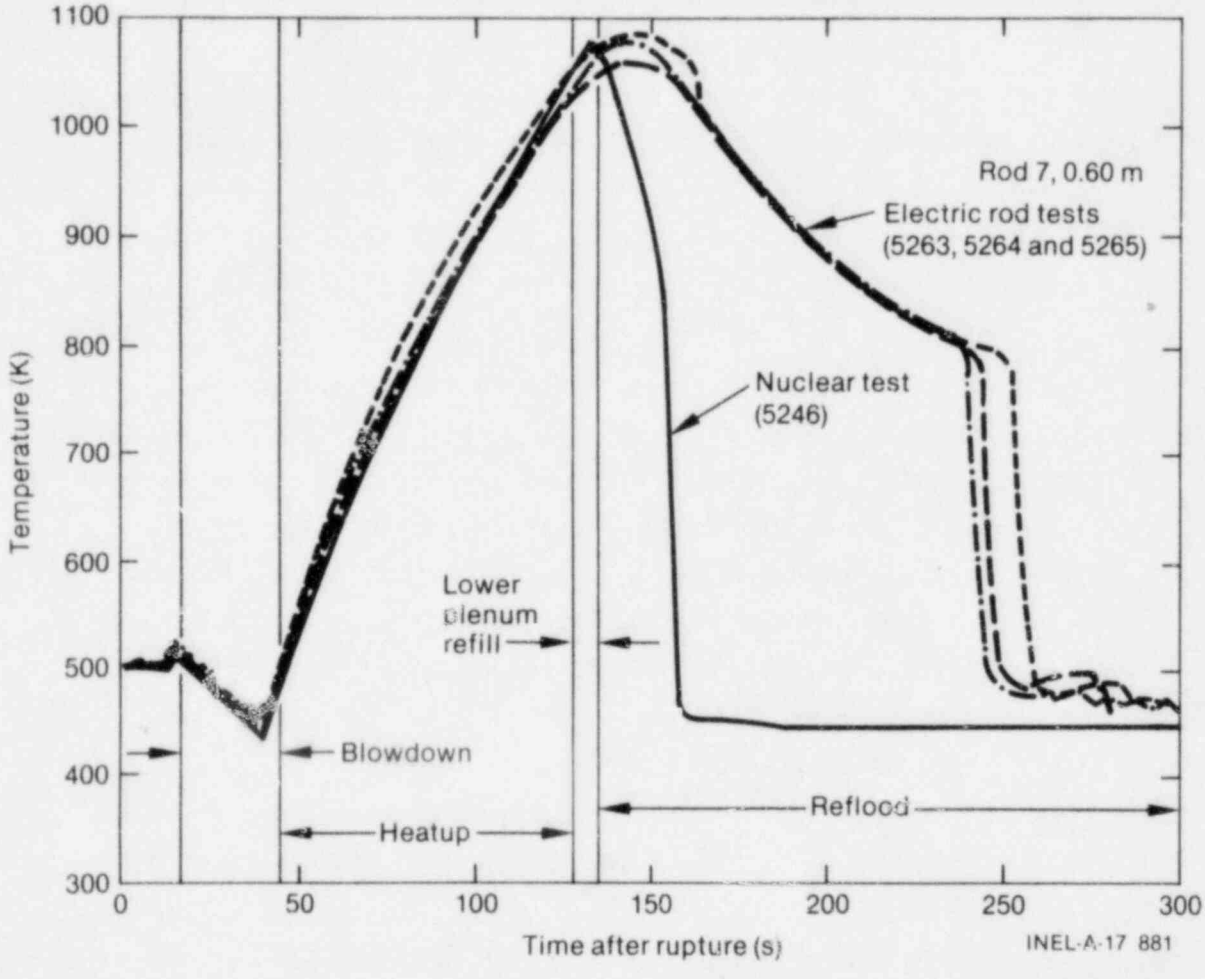

Figure E-6. Comparison of nuclear and electric rod temperature responses for similar Halden reflood experiments.

rod. A similar comparison was made between the temperatures measured by the external thermocouples, and similar differences in behavior were observed; however, the difference in time to quench from the surface thermocouples on electric and nuclear rods was only about 50 s.

The three failed test rods introduced several complicating factors into the test rod bundle thermal-hydraulic behavior that could have adversely affected the comparison presented in the preceding paragraph. The relatively cool, unheated flow channels could have caused local variations in the coolant conditions. The reduced heat input to the coolant during reflood resulted in a significant reduction in steam generation, approximately 43%, compared with the similar nuclear rod experiment. This should have resulted in less liquid entrainment and, thus, reduced heat transfer above the quench front and a faster rise rate of the liquid level within the test rod bundle.

Temperature responses from an electric rod experiment and the base case nuclear rod experiment with approximately the same steam rates are compared on Figure E-7. Again, the data are from peripheral Rod 7 and the thermocouple at the 0.60-m elevation. The reflood rate within the electric heater rod bundle was approximately 8.5 cm/s compared with 5.2 cm/s for the nuclear rod experiment. The higher reflood rate into the electric heater rod bundle should have resulted in an increased liquid level rise rate within the bundle of about 66%, compared with the nuclear rod case. Thus, with the increased flooding rate in the electric rod bundle, the rod surface area covered with reflooding water which produces steam is the same as for the electric rod experiment in which all the rods are powered, but with the nominal reflood rate. For the electric heater rod experiments, the peak cladding temperature was about 825 K at 102 s, after which cladding temperatures decreased to about 770 K when the rod quenched between 170 and 180 s. For comparison, as shown in Figure E-7, the peak temperature for the nuclear rod was about 755 K at 90 s and the rod quenched from 735 K at approximately 100 s. There was a significant difference in time to peak cladding temperature ($\sim$12 s), peak cladding temperature ($\sim$55 K), and time to quench ($\sim$75 s) between the electric heater rod and nuclear rod, even though the reflood rates were higher and producing steam at rates similar to those expected for a bundle with no failed rods.

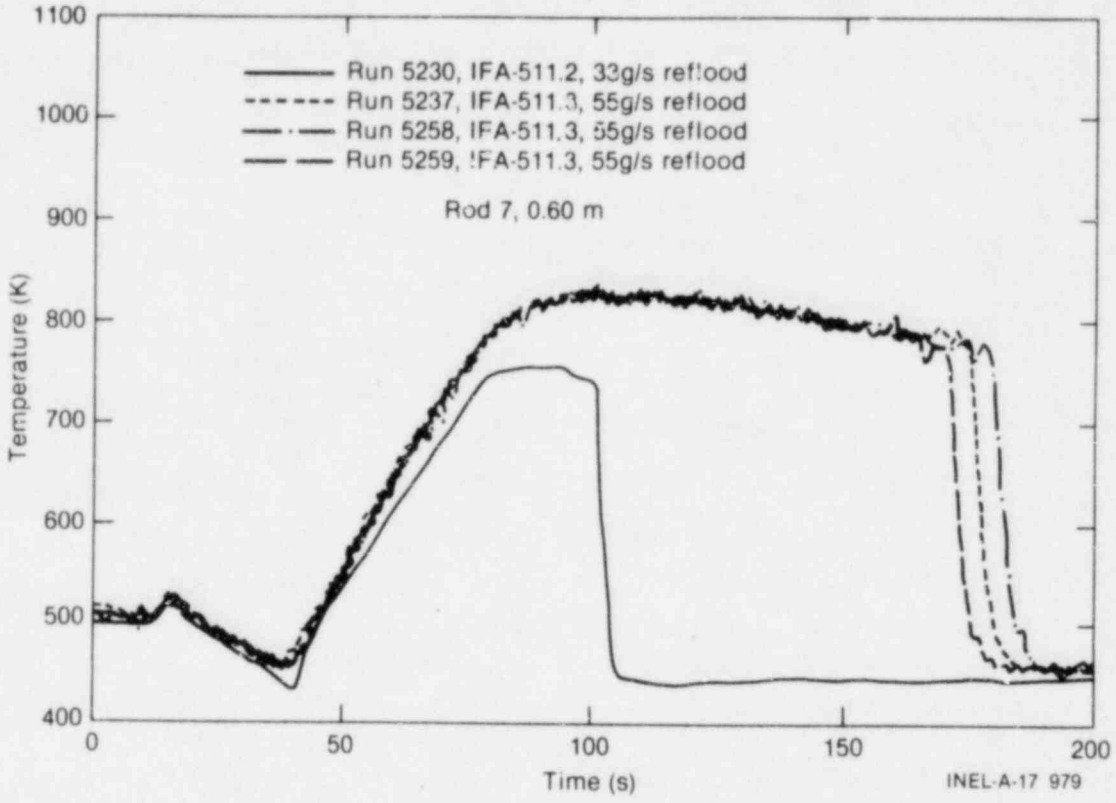

Figure E-7. Comparison of electric and nuclear rod temperature responses from internal thermocouples for runs with nearly identical rod powers and steaming rates during reflood.

3. CONCLUSIONS

Based on the preceding discussion, the following conclusions are presented:

1. The reliability and repeatability of the IFA-511 test system and test rod response were excellent, showing that comparison experiments between electric and nuclear experiments are possible.

2. The response of the cladding surface thermocouples was significantly different than that of the comparative cladding internal thermocouples during the reflood conditions tested.

3. Increasing the fuel rod power and peak cladding temperature did not significantly affect the thermal behavior of the nuclear rods during reflood as was expected from previous out-of-pile experiments. Increasing the time to reflood resulted in rod behavior that was qualitatively similar to that observed in previous out-of-pile experiments.

4. For the relatively limited experiment conditions against which the response of the nuclear and electric rods can be compared, there was a significant difference between their behavior during reflood and quench. Because of the failed heater rods in the IFA-511.3 experiments, the test bundle will be rebuilt and the experiment series repeated. The IFA-511.4 experiment series will be performed with REBEKA cartridge-type heaters and is scheduled for performance during 1981.

4. REFERENCES

E-1. R. A. Cushman et al., Proposed Test Specifications for Halden Instrumented Fuel Assembly IFA-511 Light Water Flow Starvation Test Series, TFBP-TR-316, Revision 1, December 1979.

E-2. C. Vitanza et al., Results of Blowdown/Reflood Tests with Nuclear Heated Rods (IFA-511.2), HPR-2A8, May 1980.

E-3. R. A. Cushman, private communication, EG&G Idaho, Inc.

E-4. F. F. Cadek et al., PWR-FLECHT Final Report Supplement, WCAP-7931, October 1972.

E-5. J. A. Blaisdell et al., PWR FLECHT-SET Phase A Report, WCAP-8238, December 1973.

E-6. A. C. Peterson et al., Thermal and Hydraulic Response of the Semiscale MOD-1 Core During Forced Feed Reflood Tests, TREE-NUREG-1001, October 1976.

E-7. G. E. McCreery et al., Thermal-Hydraulic Analysis of Semiscale MOD-1 Reflood Test Series (Gravity Feed Tests), TREE-NUREG-1010, January 1977.